DESIGNING FOR UPPER SEAM STABILITY IN MULTI-SEAM MINING

By

Yingxin Zhou

Dissertation submitted to the Faculty of the
Virginia Polytechnic Institute and State University
In Partial fulfillment of the requirements for the degree of

DOCTOR OF PHILOSOPHY

in

Mining and Minerals Engineering

APPROVED:

C. Haycocks, Chairman

M. Karmis, Department Head

J. R. Lucas

G. J. Faulkner

T. Kuppusamy

May 1988
Blacksburg, Virginia

DESIGNING FOR UPPER SEAM STABILITY IN MULTI-SEAM MINING

By

Yingxin Zhou

Committee Chairman: Christopher Haycocks
Mining and Minerals Engineering

(ABSTRACT)

The problem of interaction resulting from mining seams above a previously mined seam has been thoroughly investigated in order to develop and evaluate methods of improving upper seam ground conditions when mining through either active or passive subsidence waves. Design criteria have been developed based on results from case studies, statistical analyses, geological characterizations, numerical studies and physical modelling. These include identification of critical factors, prediction of the location and magnitude of potential interaction areas, and remedial options.

Complete design procedures have been devised which include five essential steps: data collection and mapping, classification of mining conditions, characterization of strata, preliminary evaluations, and stability analyses.

The methods developed for interaction analysis are classified into two categories: qualitative and quantitative. Qualitative methods can be used for a preliminary evaluation using rules of thumb and empirical formulas developed from statistical analyses. Quantitative methods involve more detailed stress and strain computations based on quantified interaction mechanisms. These mechanisms include trough subsidence, load transfer, pressure arch, large-scale caving and fracturing, and interseam failure. Finally, in order to expedite the transfer of research findings to the field for application, an interactive and comprehensive computer program has been developed which incorporates all possible interaction mechanisms and aspects of the design and evaluation process for multi-seam mining.

ACKNOWLEDGEMENTS

The author is deeply indebted to Dr. Christopher Haycocks, his major advisor, for his guidance and invaluable advice throughout the course of this research, whose undying support and encouragement have made the writing of this dissertation possible. The author would also like to express his sincere gratitude to the other members of his advisory committee, Dr. M. Karmis, Dr. J. R. Lucas, Dr. G. J. Faulkner, and Dr. T. Kuppusamy, for their advice and many constructive suggestions and comments.

To the other members of the Department of Mining and Minerals Engineering the author expresses his thanks for their generous help in many ways. A special note of thanks is given to for the final editing of this dissertation. Thanks also go to his fellow students, especially Dr. W. Wu and , for the many helpful discussions.

This work was made possible, in part, by the United States Bureau of Mines Grant No. G1125151. The author sincerely thanks the Li Foundation, Inc. for the fellowship which initiated his graduate studies in the United States.

Finally, the author is forever indebted to his mother and father, without whose limitless love and support none of this would have been possible.

TABLE OF CONTENTS

LIST OF FIGURES

LIST OF TABLES

I. INTRODUCTION

1.1 Statement of Problem

When seams are being mined over a previously-mined seam, ground control problems may occur due to interactions resulting from the mining of the lower seam. These interaction effects may create major ground control problems, including floor, roof, and pillar failures which result in lost reserves, production delays, and major safety problems. Initial failure of lower seam structures usually commences with caving and fracturing of the overlying strata. Pressure arches can be formed which create destressed zones and highly stressed zones due to load transfer. Seams lying in close vertical proximity to the lower seam can be directly affected by large-scale caving and fracturing. As the opening width increases and the pressure arch is no longer capable of obtaining support from the solid coal, trough subsidence is initiated under most geologic conditions. Subsidence creates tension zones in the upper seam at the trough edges. Major interactive ground control problems are frequently encountered in such tension zones because coal measure rocks have inherently low tensile strengths and the rock mass dilates. These interaction effects present major obstacles to mine safety and produc-

tivity if they are not dealt with through proper ground control practices.

1.2 Background and Justification

Ideally, multi-seam mining should proceed in a descending order, starting with the uppermost seam, with extraction of each seam being completed before the next adjacent seam is mined. In practice, however, the choice is often determined by many factors other than ground control considerations. Traditionally, the selection of mining sequence has been based upon ownership, economy and accessibility without due consideration of ground control practices in subsequent mining. In many cases, the lower seam has been the more attractive, owing to its greater thickness, superior quality or easier accessibility. Today with the depletion of some reserves and increased demand for coal, many operators are increasingly finding themselves mining above existing or abandoned mines. This is especially true in the Appalachian coal fields where the majority of the coal seams occur in multiple horizons. In addition, improvement in equipment and technology have helped to make even the thinner and sometimes laminated upper seams economically attractive.

Many attempts have been made to predict interactions in multiple seam mining, which is also proof of the ever-

increasing concern of the coal industry with seam interaction. Simple statistical models and rules of thumb have been developed based on case study data and experience. However, these models and rules of thumb are usually site-specific and often descriptive concerning mine design. Design techniques and methods for stabilizing openings where interactive problems exist due to subsidence or arching are inevitable remains to be addressed. Development of quantitative rational design criteria for the upper seam that would alleviate damage due to negative interaction effects would contribute substantially to the safety and productivity of many mining operations.

1.3 Objectives and Methodology

The primary objective of this research is to develop and evaluate methods of improving ground control conditions in upper seams when mining through either active or passive subsidence waves. These methods concentrate on improved ground control practices for the upper seam, rather than reducing the amount of subsidence in the upper seam by improved practices in the lower seam. These include development of design criteria and eventually of a computer model that can predict potential interactions for given geological settings and mining conditions, and can provide design guidelines and options for improving upper seam con-

ditions.

The rationale is based upon the conclusions and results that can be derived from the considerable number of field studies available on upper seam interaction. The complexities of the geological and mining conditions dictate a comprehensive approach which incorporates results from case studies, statistical analysis, numerical and physical modelling as well as geological characterizations. In order to concentrate on the most important aspects of the investigation during the time span of this research, only two horizontal seams lying in close proximity have been investigated for the Appalachian coal region. The mining method is confined to the room-and-pillar method as the majority of the coal seams in the U.S. are extracted using this method. For application purposes, super-critical conditions are assumed. These assumptions are made without losing generality because such conditions are the most common in Appalachian multi-seam coal mines.

II. LITERATURE REVIEW

The problem of interaction in multiple-seam mining has attracted the attention of many researchers. Although work has been done as early as the early 1900's, more vigorous and systematic research into the mechanisms of interaction is relatively recent. This chapter reviews major studies performed to date and covers the various aspects of multi-seam mining and other related areas.

2.1 Interaction Phenomena in Multi-Seam Mining

2.1.1 Interaction Mechanisms

In mining operations where more than one seam is involved, the sequence of mining the various seams is often used for the classification of multi-seam mining. Hladysz (1985) calculated 168 possible sequences of mining for four seams, based on combinations and permutations. However, if geological and mining conditions are imposed, the number of possible sequences is quickly reduced to a much smaller number. Generally, there are four basic sequences in which multi-seam mines can be worked (Haycocks and Karmis, 1984; King et al., 1972; Hladysz, 1985). These are defined as(Figure 2.1):

1) where the lower seam is mined out prior to the mining of the superimcumbent seams.

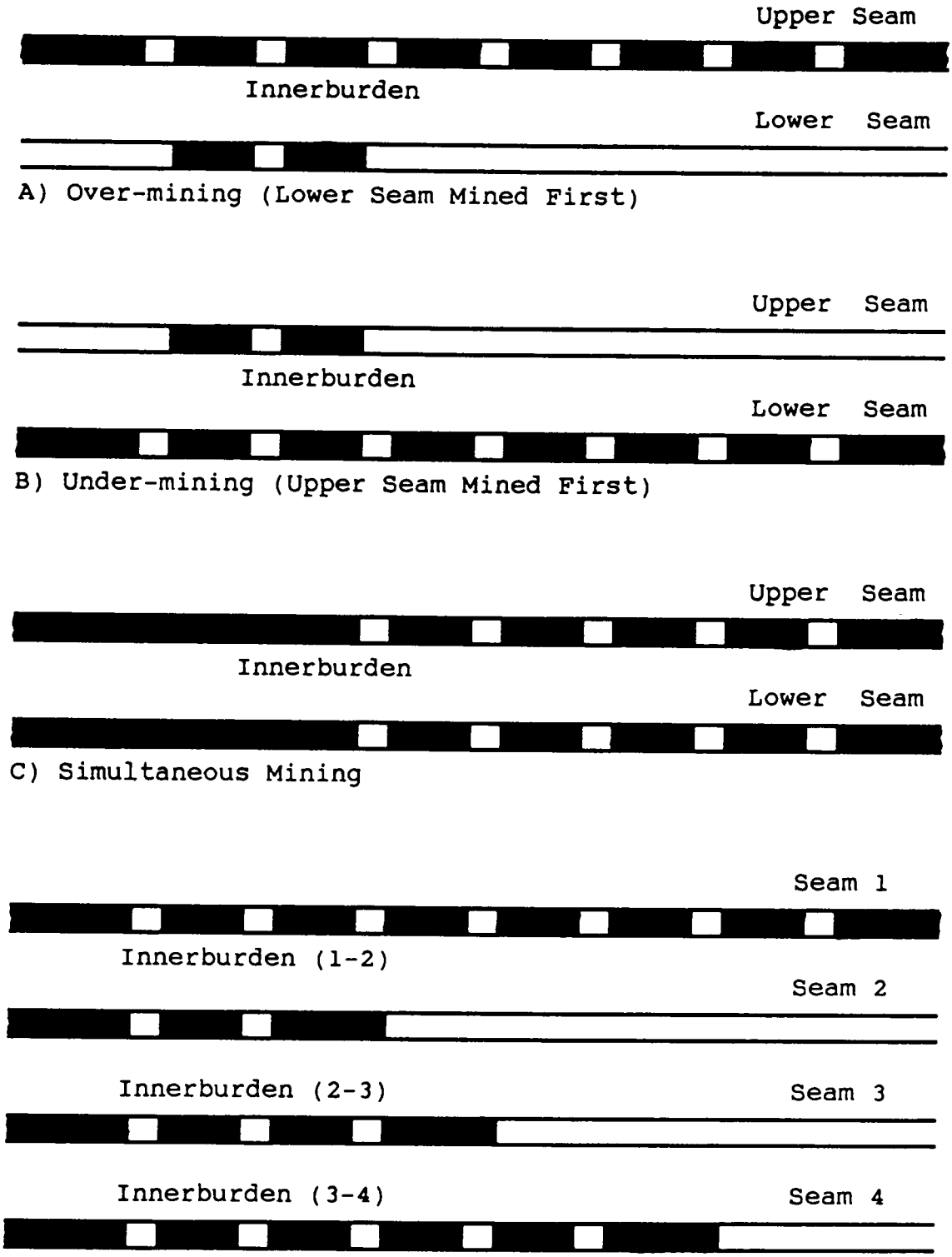

Figure 2.1 Basic Sequences of Mining Multiple Seams

2) where simultaneous mining of upper and lower seams occurs.

3) where the upper seam is mined out prior to the mining of the lower seam.

4) combinations of the above.

Different interaction mechanisms are activated as a result of the mining sequence, resulting in a variety of ground control failures.

In the case of the lower seam being mined out before the extraction of the upper bed, or overmining, Hasler (1951) observed two basic types of problem in the upper seam:

1) unavoidable damage as a result of prior removal of all of the coal from a lower seam without provision for adequate support for the overlying seam. Such damage includes varying degrees of subsidence, fracture, and parting of the overlying strata and beds of coal.

2) avoidable damage due to large and extensive pillars of coal left in the lower, worked-out seam. The effects observed in the upper seam are bumps in the floor, crushing of the coal in the upper bed, and fractures in the coal.

In one of the most exhaustive early investigations into the problem of interaction, Stemple (1956) examined 15 cases of overmining operations. He reported bed separa-

tions of up to several inches in the upper seam, causing the coal seam to drop out of the roof or the floor strata to drop out of the coal. He also described several cases of severe roof problems where mining in the upper seam took place in areas above the edge of solid coal (Figure 2.2)

Various causes of innerburden failure have also been identified by Hedley (1974) in the analysis of multi-seam mining of the Elliot Lake uranium mines, such as buckling due to high horizontal forces, tensile failure at the center of the roof in the lower bed, and shear or tensile failure in the interseam.

Another mechanism is the interseam shearing failure caused by removal of underlying pillars. In 38 case studies in the Appalachian coalfields reported by Holland (1951), about 75% had a shear or shear tensile failure after an underlying bed had been mined. In extreme cases, such failure can extend through to the surface, as demonstrated in Figure 2.3.

Pillars of substantial size left in the lower seam can create shearing and high stress concentrations in the upper seam due to continued subsidence of the strata on the two sides of the pillar and the support provided by the pillar (Lazer, 1965). Arching and caving create high stress concentrations as well as zones of relieved stress, which can also affect the upper seam if the height of the arching or caving extends to the upper seam level.

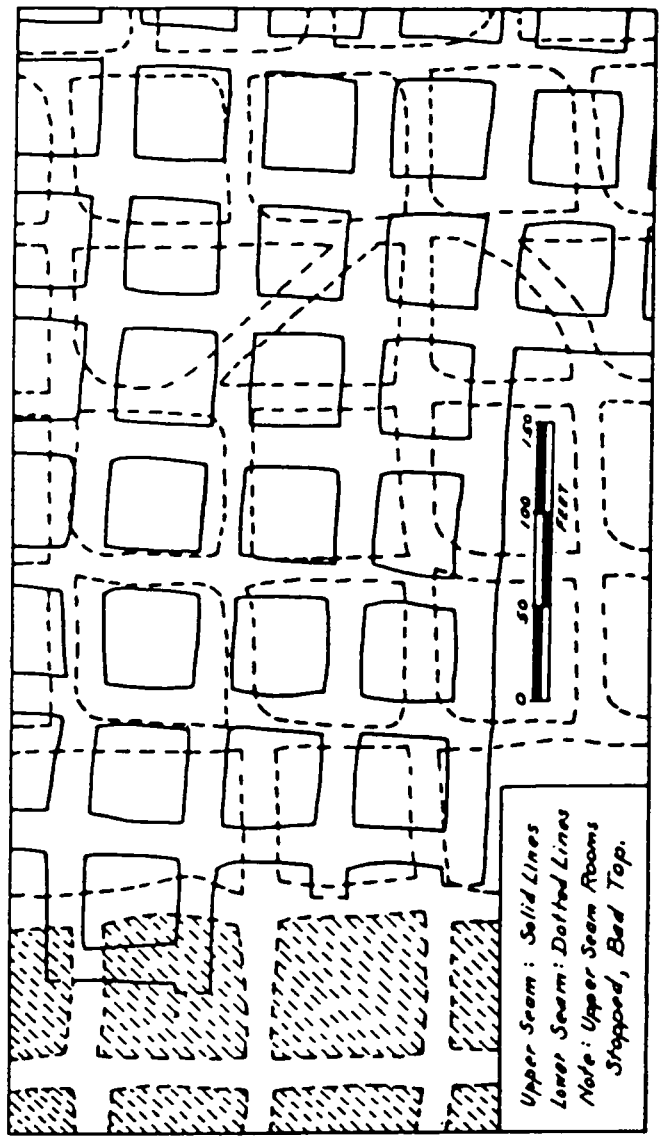

Figure 2.2 Area of Disturbance in a Superjacent Seam above the Line Between Solid Coal and Gob of an Underlying Seam. Monongalia County, West Virginia (Stemple, 1956)

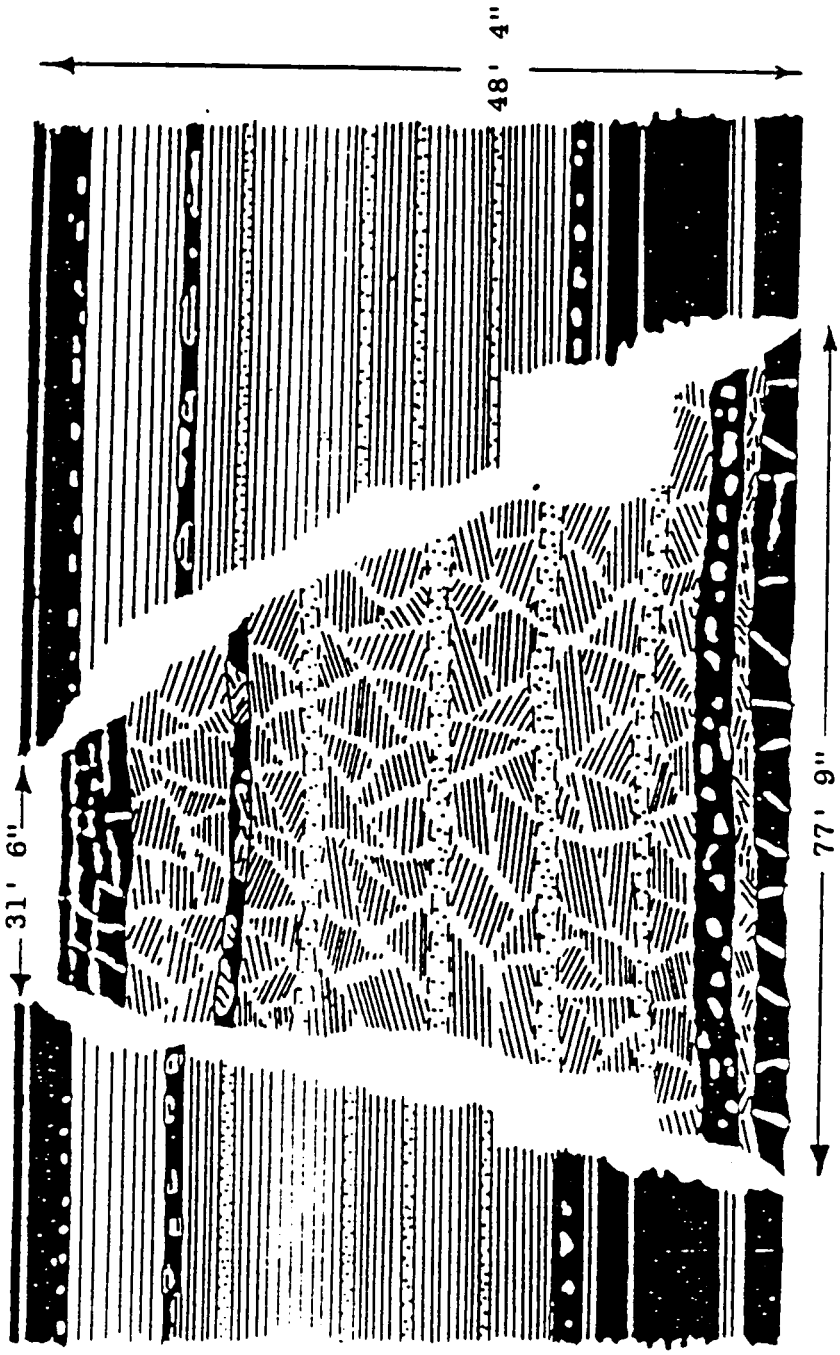

Figure 2.3 Massive Interseam Failure Caused by Removal of the Pillars in the Pittsburgh or Big Vein Seam, Georges Creek Region, Maryland (Holland, 1951)

In summary, subsidence is responsible for most of the interaction effects on the overlying seam; therefore, if general principles determining the effects produced are to be investigated, it is necessary to inquire into subsidence, force distribution as induced by mining, and factors that affect these interactions (Holland, 1951). In association with the subsidence process are three basic types of mechanisms, based on studies by Haycocks et al. (1983): 1) dilation (tension/compression) due to trough subsidence; 2) high stress concentration due to load transfer by remnant pillars and arching effects; and 3) block shearing failure due to inadequate lower seam support such as irregularly robbed pillars.

2.1.2 Factors Affecting Overmining Interactions

Factors that affect the amplitude and propagation of subsidence, and thus interactions, are usually divided into geological (uncontrollable) factors and mining (controllable) factors (Table 2.1). The following is a discussion of some of the more important these factors.

Effects of Mining Methods The method of mining employed has been considered as one of the controlling factors in the various aspects of the subsidence process. It affects not only the magnitude of subsidence, but also the subsidence pattern. In general, longwall mining causes a gradual bending of the superimcumbent strata, allowing them to

Table 2.1 Variables Affecting Multi-Seam Mining

Uncontrollable Variables:

- overburden structure and thickness
- innerburden structure and thickness
- seam height
- immediate roof and floor
- mechanical properties
- geological discontinuities
- ground water

Controllable Variables:

- methods of extraction
- excavation height
- entry orientation and geometry
- type of support
- percent recovery
- elapsed time between operations

settle slowly as the face is being advanced.

In room-and-pillar mining, where complete extraction is practiced, pillars are extracted in such a manner as to form a long extraction line, as is desired in order to relieve pillars of as much load as possible. The tendency is to create subsidence closely approaching the nature of subsidence induced by longwall mining.

Partial extraction is used where surface subsidence prevention is required or where surface conditions are such that pillar extraction would result in roof support problems. In this case, as Stemple (1956) pointed out, the rock forming the roof of a room or entry may fail because of overstress or weakness caused by chemical or physical action. The subsidence thus induced will consist of a fall of this failed rock along the room or entry to a height ranging from a few inches to several tens of feet. This type of subsidence, therefore, would have little effect upon the overlying coal seam unless it lay within the scope of strata reached by the fall. Where a pillar is left in a mined-out area of complete extraction mining, or where a large competent pillar is surrounded by numeraous relatively smaller pillars which are incapable of supporting the superimcumbent strata in partial extraction, the strata may shear at the edges of the pillar described and subside about this pillar, and definite difficulties will result in attempting to mine the overlying seam in this area.

Effects of Width-to-Depth Ratio In considering the effects of mining geometry, the width of excavation divided by the depth of mining, or the width/depth ratio, is often used. Studies have shown that for maximum subsidence to occur, the width/depth ratio of the extraction must exceed a certain minimum or critical value in both plan dimensions. Maximum subsidence increases as the width/depth ratio increases until a certain point at which the subsidence no longer increases. This is called the critical width/depth ratio. After this value, increased width-to-depth ratios will result in a more uniform subsided strata and less interaction problems in the overlying seam.

In other aspects, the inflection point, the angle of draw, and ribside subsidence are all considered to be functions of the width/depth ratio (Karmis, 1986). The shape of the subsidence trough also varies with the width/depth ratio, as has been shown by an analysis of a large number of field observations (NCB, 1975).

Effects of Geology The effects of geology on subsidence can be readily seen in the fact that maximum subsidence in British coal mines can be as much as 90 percent of extraction height while in the U.S. 70 percent is usually the upper limit (Gray and Bruhn, 1984; Webster et al., 1984). Stemple (1956), siting Briggs (1929), stated that the angle of draw is usually less in a hard rock such as sandstone

than in a soft rock such as shale.

In considering the effects of geology, the present practice in subsidence control is to incorporate the percent of hardrock in subsidence factor calculation (Karmis et al., 1984) or interaction prediction (Webster et al., 1984). Subsidence patterns are also greatly influenced by the large scale or regional lithologic, topographic, tectonic and structural trends of the particular coal region (O'Rourke and Turner, 1979), which determine the trough width, width of the tension zone and magnitude of strain created at the upper seam.

Effects of Time The effects of time are perhaps the most difficult factors to determine in precalculation of subsidence (Brauner, 1973). A subsidence trough is not initiated until after a certain minimum area has been extracted and this then evolves from the subcritical through critical to supercritical stage, as the extraction area is increased. The time factor is usually represented by the advance rate and the time after cessation of mining activity. The former determines the time taken for full subsidence to occur with regard to a surface point. As for the latter, which expresses the after-effects, studies have shown that over 90 percent of final subsidence occurs at the time of complete critical extraction (NCB, 1975; Gray and Bruhn, 1984). These two factors together determine if

the interaction is a purely active, an active/passive, or a passive condition.

2.2 Subsidence Control

2.2.1 Basic Parameters in Subsidence

To date, the majority of work on the subject of subsidence has been done with regard to the surface because of the damage and environmental impact that subsidence can create. The damage attributed to this phenomenon is seen in both rural and urban areas and includes land settlement and fracturing, structural damage to surface buildings, and disruption or contamination of ground water supplies (Karmis et al., 1985).

The meaning of subsidence in a broader sense embraces the whole process of ground movement due to mining of an underground seam. The surface manifestation of this process usually entails five distinct, basic types of surface movement, which can affect or damage surface structures, facilities and renewable resources (Karmis et al., 1985). These parameters are:

- Vertical displacement; this movement occurs in all portions of the subsidence trough, but achieves maximum values above the center portions of the extraction area.
- Horizontal displacement.

- Tilt or slope, derivative of the vertical displacement with respect to the horizontal; uniform tilt results in little surface damage while differential tilt results in a much higher potential for surface damage.
- Curvature, the derivative of slope or the second derivative of the vertical displacement with respect to the horizontal.
- Strain, derivative of the horizontal displacement with respect to the horizontal; tensile and compressive strains correspond to the concave and convex portions of the subsidence trough, respectively.

Idealized distributions of the above parameters and their relationships are shown in Figure 2.4.

2.2.2 Theories of Subsidence Prediction

Subsidence control generally involves subsidence prediction, damage assessement and prevention, often with regard to surface structures. Various theories have been established concerning subsidence movements, but the most commonly used generally fall into one of the following three categories: the profile function method (Brauner, 1973; NCB, 1975), the influence function method (Knothe, 1957; Kratszch, 1983), or the zone area method (Marr, 1975). Any one of these methods can be used to predict subsidence, the choice depending upon the application

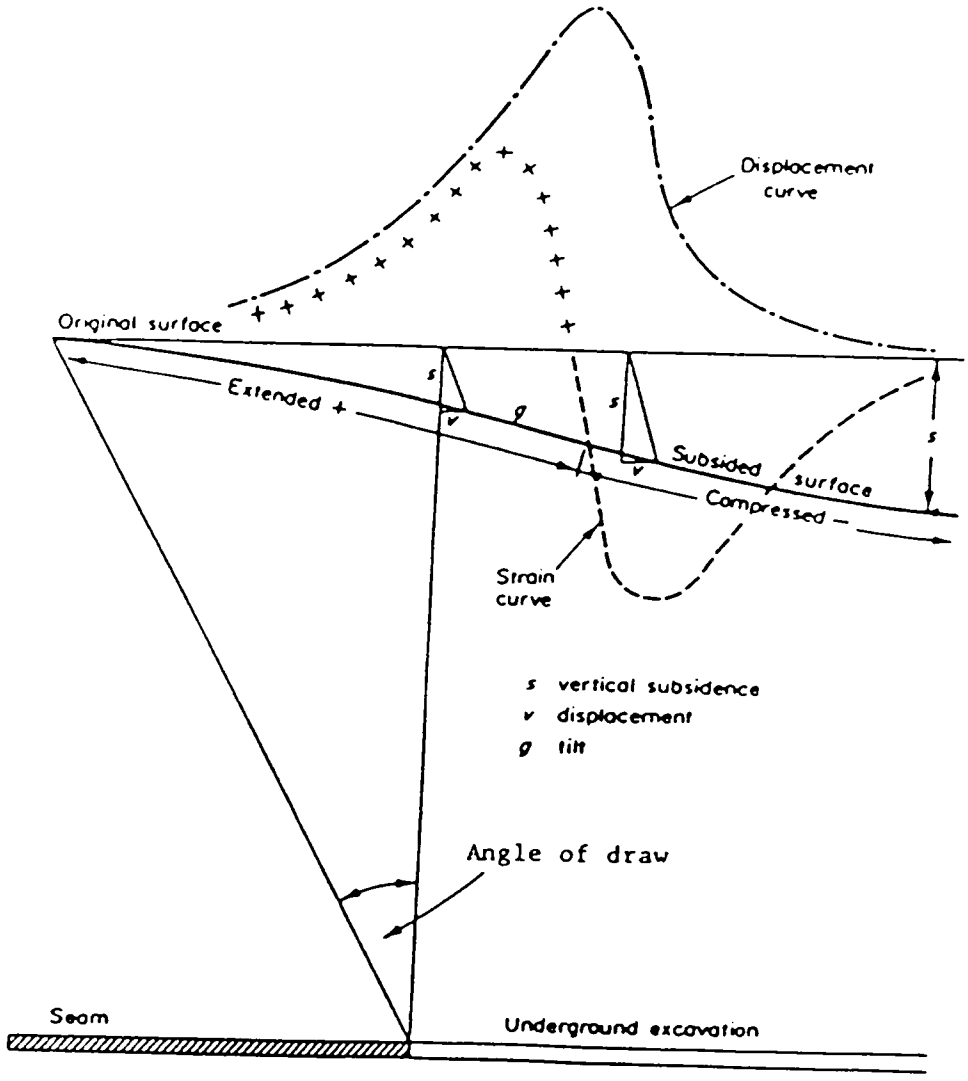

Figure 2.4 Elements of Ground Movement and Their Distribution (Karmis et al., 1985)

requirements and the site and mining factors.

Profile Function Method This method depends heavily on field measurements as its basis for fitting a profile function to the data collected from the measurements, based on a few parameters such as seam thickness and depth-to-width ratio (Kratzsch, 1983). In general, a function which is tangent or asymptotic to two horizontal lines is required (Karmis et al., 1983). The most complete and representative case of the application of this method is the study done by the National Coal Board of Britain and a result of their study, the widely-used NCB Subsidence Engineer's Handbook (NCB, 1975), which provides guidelines for predicting subsidence including strain distributions and damage assessment. Similar calculation charts and relationships have been developed for application in the United States by Karmis et al. (1986).

The advantage of such a method is that profile functions can be directly derived from observations and can be modified for simple subcritical profiles according to field data (Brauner, 1975). The main disadvantage is that three-dimensional problems and excavations of an irregular shape are usually very difficult to deal with using this technique.

Influence Function Method In this group of methods, it is common to seek a so-called influence function which is used

to describe the amount of influence exerted at the surface by infinitesimal elements of the extraction area. The total subsidence is then the sum of the elementary troughs of all extraction elements according to their position. A typical example of this technique is the Budryk-Knothe influence method, which was developed in Poland (Knothe, 1957). The influence function is given as:

$$f(x) = \frac{1}{r} \exp(-\frac{\pi x^2}{r^2}). \qquad (2\text{-}1)$$

where r = radius of influence = $h/\tan(\beta)$; h = mining depth; β = angle of influence; x = horizontal distance from the inflection point.

The subsidence at any point x, $s(x)$, is then given by

$$s(x) = \frac{Smax}{r} \int_{x_1}^{x_2} \exp(-\pi\frac{x^2}{r^2})dx \qquad (2\text{-}2)$$

Methods employing influence functions first appeared in 1932 and are now predominant in Germany and Poland (Kratszch, 1983), and are also becoming more and more widely used throughout the world. Their popularity lies in their advantage not being confined to rectangular extractions like the profile function method, and their ability to negotiate superposition problems.

Zone Area Method The zone area method is a slight variation of the influence method. The basic idea is to construct a series of circular zones or concentric rings around the surface point, the outer radius of the outer zone being equal to the radius of the area of influence (Marr, 1975). Mathematically, using seven zones, the subsidence can be expressed as (Goodman, 1980):

$$s/m = ax_1^n + bx_2^n + cx_3^n + dx_4^n + ex_5^n + fx_6^n + gx_7^n \qquad (2\text{-}3)$$

where x_1, x_2, x_3,... = proportional area of each zone extracted; a,b,c ... = corresponding zone factor for each zone; and n = influence constant.

The zone factors and influence constant are determined from field measurements. The subsidence at the surface is then obtained from the summation of the proportions of each zone or ring extracted.

The zone area method has the same advantage as the influence function method of being able to negotiate any mining geometry and superposition problems. Application of computer modeling can easily implemented to enable a large number of zones to be used for better accuracy. Calculations of strain, especially directions of strain, however, are usually difficult.

Specific models and parameters for application of any of the above three methods have been developed and tested

for different regions of the United States (Karmis et al., 1986).

2.2.3 Arching and Caving

Arching and caving are two closely-related phenomena in ground control. Even though the formation of a pressure arch does not necessarily entail caving, it is the sagging, sliding and separation of the beds immediately above an opening, or the failure of a portion of the strata above the opening, that induces the transfer of load to the unmined coal, or onto the packs or goaf behind the face in the case of longwall mining. The implications of the arching and caving effects in multiple seam mining depend on the shape, size and height of the arch, abutment pressure and stability of the pressure arch, existence of yielding pillars, and the height of caving as well as on the induced fracturing zone above the mined area (Figure 2.5).

There have been numerous theories developed concerning the strata movement in underground mining since Fayol (1885) first introduced the concept of arching. These theories are based mainly on the pressure arch and beam concepts. This concept of rock supporting itself through the transfer of a portion of the load originally supported by the later-mined-out material to the solid material, which is known as the abutment, is now widely used in rock

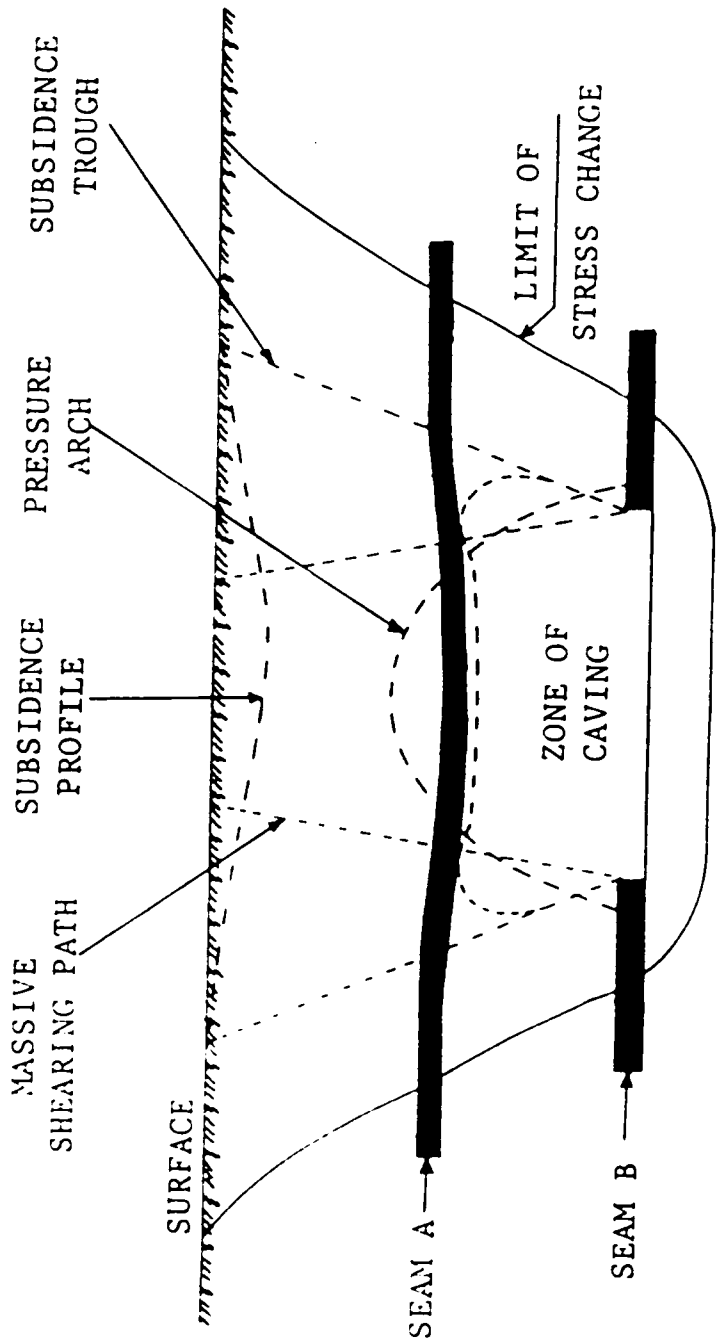

Figure 2.5 Schematic of Influence Profile After Total Extraction of Lower Seam

mechanics design and ground control. Table 2.2 summarizes the theories related to the pressure arch and the beam action concept of strata movements.

Regarding the application of the pressure arch theory, F. D. Wright (1973) pointed out that many of the formulas that have been developed to determine the maximum span and height of arches and the pressures on the abutments relate all these values solely to depth below surface. This indicates that geologic conditions and properties of the rocks are incorporated regionally. Formulas of this type may be very useful for a given mine site; however, they may be of little value when applied to another mine site where, for example, the in-situ stresses have an entirely different relationship to depth.

The main reason for the wide application of the pressure arch theory is the destressed zone inside the "dome" in combination with the yield pillar technique. Barrier pillars are designed so that much of the overburden pressure can be transfered to the barrier pillars if the distance between the barrier pillars is less than the maximum span of the pressure arch (Wright, 1973). The general principle is that pillars within the panel must be small enough to yield (Barrientos and Parker, 1974) or that other artificial methods are used to cause these pillars to yield (Wang et al., 1974).

The effect of the pressure arch on the overlying seam

Table 2.2 Summary of Some Pressure Arch and Dome Theories

Arching Theory		Reference
1. Pressure arch		
a. British:	s=opening width $s_{max}=3(d/20+20)$ $h=2s$	Holland, 1961
b. United States:	s=opening width $s_{max}=2\ell$ $h=(s^2-s_1^2)\frac{d}{s^2}$	Abel, 1982
2. Dome Theory		Denkhaus, 1964
a. Rigid dome: Insufficient cohesion	$s=\sqrt{\frac{8\sigma_c d}{w}(1-h/d)\log(1-h/d)}$ $s_{max}=\sqrt{2.96\sigma d/w}$ $h_{max}=0.63d$	
Sufficient cohesion	$s=\sqrt{\frac{8\sigma_c d}{w}(1-h/d)}$ $s_{max}=\sqrt{4\sigma_c d/w}$ $h_{max}=0.5d$	
b. Elastic fracture dome:	$h=[\frac{1+\sigma_t/wd}{2K}-0.5]\frac{s}{2}$	

s = span of dome or arch; s_1 = distance from pillar rib
h = height of dome or pressure arch
d = depth of opening below surface
σ_c = uniaxial compressive strength of rock
σ_t = uniaxial tensile strength;
w = specific weight of rock
K = ratio of lateral to vertical rock pressure
ℓ = load trasfer distance

is two-fold. On the one hand, the destressed zone can be taken advantage of by placing entries in this zone. On the other hand, high stresses will be transferred to the upper seam through the trajectory of load transfer. The determining factors are the shape and size of the pressure arch and the parting distance between the two seams.

2.3 Prediction of Interaction Effects

The study conducted by Dunham and Stace (1978) established the relationship between the amount of damage caused by a rib edge or remnant pillar and the major parameters governing the interaction mechanism. This was based on a number of case studies of interaction situations carried out mainly in the northeast coalfields of Britain, with emphasis on roadway stability and stability in the longwall faces. Results of the monitoring program are shown in Figure 2.6, which plots the mean working height against the distance from the face.

The results from all of the interaction sites indicate that the major governing variables affecting the degree of damage in roadways were as follows:

- The initial stability of the roadway;
- The vertical or perpendicular distance between the affecting rib edge and the roadway;
- The geometry of the affecting rib edge;

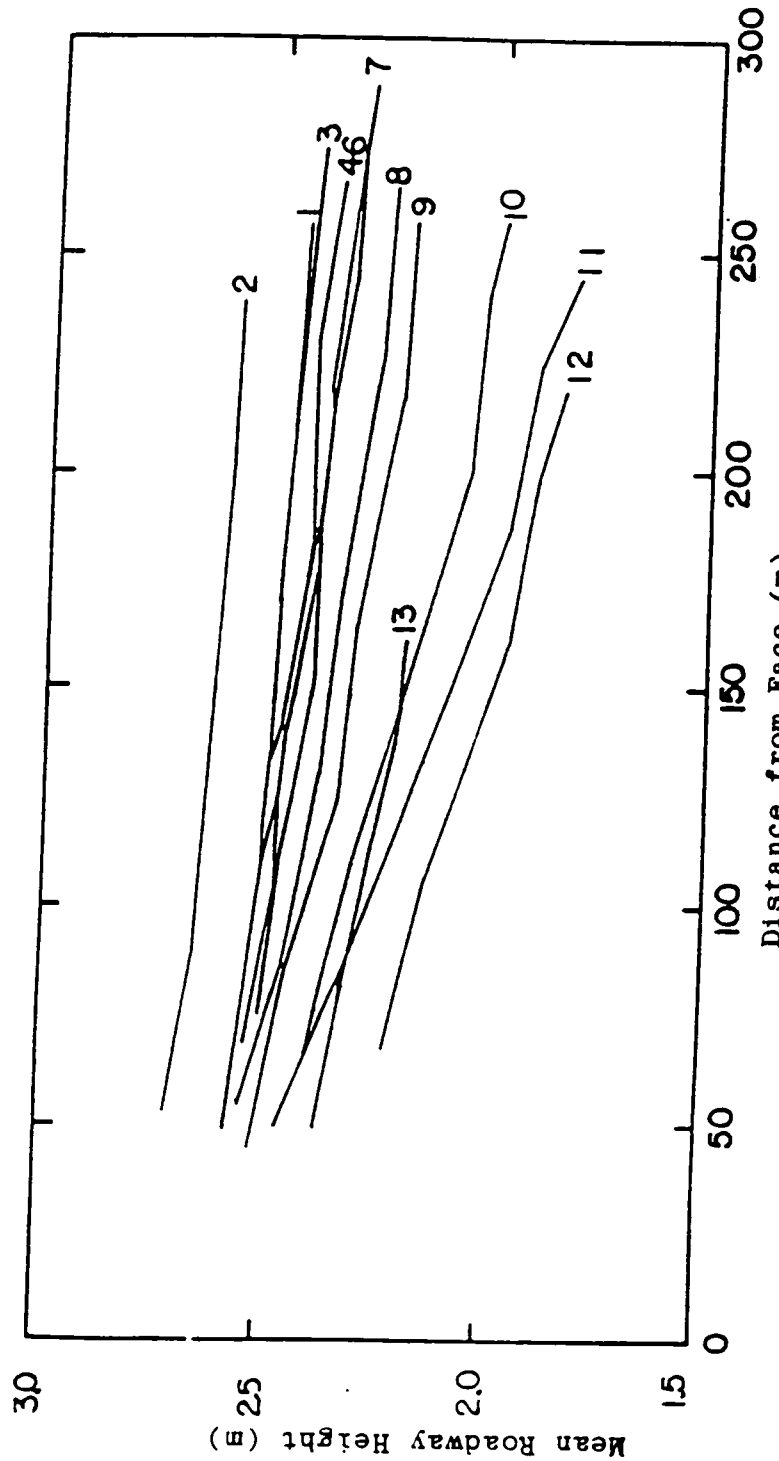

Figure 2.6 Mean Roadway Height Versus Distance from the Face (Dunham and Stace, 1978)

- The sequence of working of all seams in an area;
- The age factor; and
- The superimposition of two or more rib edges.

Final roadway assessment, based on the numerical scale obtained using the NCB/MRDE Roadway Nomogram, was divided into three categories:

- 1-5 Good conditions
- 6-10 Moderate conditions, maintenance required
- 11-18 Poor conditions, heavy maintenance.

A multiple linear regression model was then developed using four of the governing variables to predict roadway damage:

$$Y = 0.546 + 0.084x_1 - 0.003x_2 - 0.015x_3 + 1.427x_4 \qquad (2\text{-}4)$$

where Y represents a scale of roadway damage ranging from 1 to 5, defined as follows:

1. No effect.
2. Slight measurable effect, but roadway stability is unaffected.
3. Moderate effect, requiring a small amount of roadway maintenance.

4-5. Roadway damage is serious, heavy repair work will be required.

The four independent variables, represented by x_1, x_2, x_3, and x_4, respectively, were specified as:

- Initial stability
- Vertical seam interval
- Age of the rib edge
- Geometry of the rib edge

Numerical values for initial stability were calculated using the NCB/MRDE Roadway Nomogram. Geometry of the rib edge was given one of the following values:

1) Single rib edge.
2) Narrow pillar, superimposed abutments.
3) Isolated or semi-isolated remnant pillar.

Comparisons of the predicted damage and the original designated damage rating for the measured data show that reasonable prediction of interaction damage was realized in only 13 of the 21 cases.

Another similar study was reported by HRB-Singer, Inc. on the impact of overmining and undermining on the eastern underground coal reserve base (U.S.). A list of twelve input variables were identified. These were:

1) Percent of extraction in the previously-mined seam;
2) Distance between seams;
3) Seam thickness or pillar height in the previously-mined seam;
4) Span in the previously-mined seam;
5) Depth of overburden of the previously-mined seam;
6) Strength of roof in the previously-mined seam;
7) Strength of roof in the currently-mined seam;

8) Strength of floor in the previously-mined seam;

9) Strength of floor in the currently-mined seam;

10) Minimum pillar width in the previously mined seam;

11) Elapsed time since previous mining; and

12) Multiplier describing shape and distribution of remaining pillars.

Data were collected from four mines located in West Virginia and Pennsylvania, which were further divided into test blocks. Statistical analysis of the test data resulted in the following equations:

$$X_{1s} = 146.824 + 0.2718X_{3,} + 0.2563X_{52} + 0.0307X_{60} - 105.5506\log X_{61}$$

and

$$X_{1s} = 191.823 + 0.2266X_{3,} - 0.1583X_{52} + 0.0158X_{60} - 105.8583\log X_{61} \quad (2\text{-}5)$$

where X_{1s} = upper mine percent extraction; $X_{3,}$ = previous percent extraction; X_{52} = vertical distance between seams (ft.); X_{60} = overburden above previous mine (ft.); X_{61} = time elapsed between mining of seams (years).

The first model used only 31 of the 50 blocks while the second model used all of the 50 blocks.

Several authors (Engineers International, 1981; Webster, 1983) have questioned the coefficients determined in the above equations. The coefficient found for the first

variable in the first equation was b1=+0.2266 while that in the second equation was b1=+0.2718. These positive coefficients, argues Webster, indicate that the higher the percent extraction in the lower previously-mined seam, the higher the percent extraction can be expected in the upper seam. He further argues that this is reasonable for near-total extraction, where a more uniform extraction results in a more uniform subsidence profile; for partial extraction, however, this is doubtful. The seemingly contradictory results may have come from the statistical procedure and the related assumptions. For example, all the regression variables used are more likely than not to be interdependent, which may cause the linear regression technique to be unviable for the analysis.

A second approach, called the engineering model, was proposed by HRB-Singer, Inc. and consists of a series of engineering judgements based on theories of rock mechanics, subsidence, seam interaction and on working rules. Using the 12 input variables defined previously, the setps of the process can be described as follows:

1) Determine whether subsidence will occur. If it will, calculate the maximum subsidence and percent subsidence. A percent coal loss is then assigned.

2) Determine whether high stress-zone effects will occur. If they will, assign a coal loss percentage based on the geometry and on the strength of the roof and floor

in the current seam. The coal loss percentage is the adjusted according to the pillar pattern, the pillar alignment and the depth of the previously mined seam.

3) The actual coal-loss percentage is then reported as the larger of the percentages found in steps one and two.

This approach may have the best potential for the application of knowledge-based expert systems, which--as a branch of artificial inteligence--is quickly finding its way into mining applications.

Based on statistical analysis of 44 case studies, Webster et al. (1984) developed an empirical model for predicting upper seam damage using a damage factor. The formula is given as:

$$DF = 1239 + Y - 18.83X \qquad (2\text{-}6)$$

where DF is the damage factor, with positive values indicating no interaction problems; X is the percent of extraction in the underlying seam; and Y is the ratio of innerburden thickness to lower seam height multiplied by the time elapsed after previous mining in years. To adjust for the effects of geologic structure, Eq. (2-6) is written as:

$$ADF = DF + (Z-50) \qquad (2\text{-}7)$$

where ADF is the adjusted damage factor and Z is the percent of hardrock in the innerburden. A nomogram was pro-

duced as shown in Figure 2.7, which can be used directly for design purposes.

The damage rating originally used for the case studies was later related to the subsidence factor (Figure 2.8), where damage was rated on a scale of 0 to 5 with 0 indicating no damage and 5 indicating very severe damage. Two important points should be noted in Figure 2.8. First, this figure shows a strong association between upper seam damage and maximum subsidence. Second, there is considerable variability in the relationship, attributable to the different structural conditions in the roof and the spatial locations. It should also be noted that this statistical model was the first to take into consideration the effects of geology. This is the direction which should be taken in future research when building any new models.

Hladysz (1985) took a different approach from the above damage rating methods in presenting a risk analysis of multiple-seam mining. He stated that the most important effect created by longwall mining is the caving because this influences the rock mass stability. Based on Polish experience and on his theory, the distance between the extracted coal seam and the surface can be divided into three zones (Figure 2.9): the zone of full caving, the zone of fracturing, and the zone of subsidence.

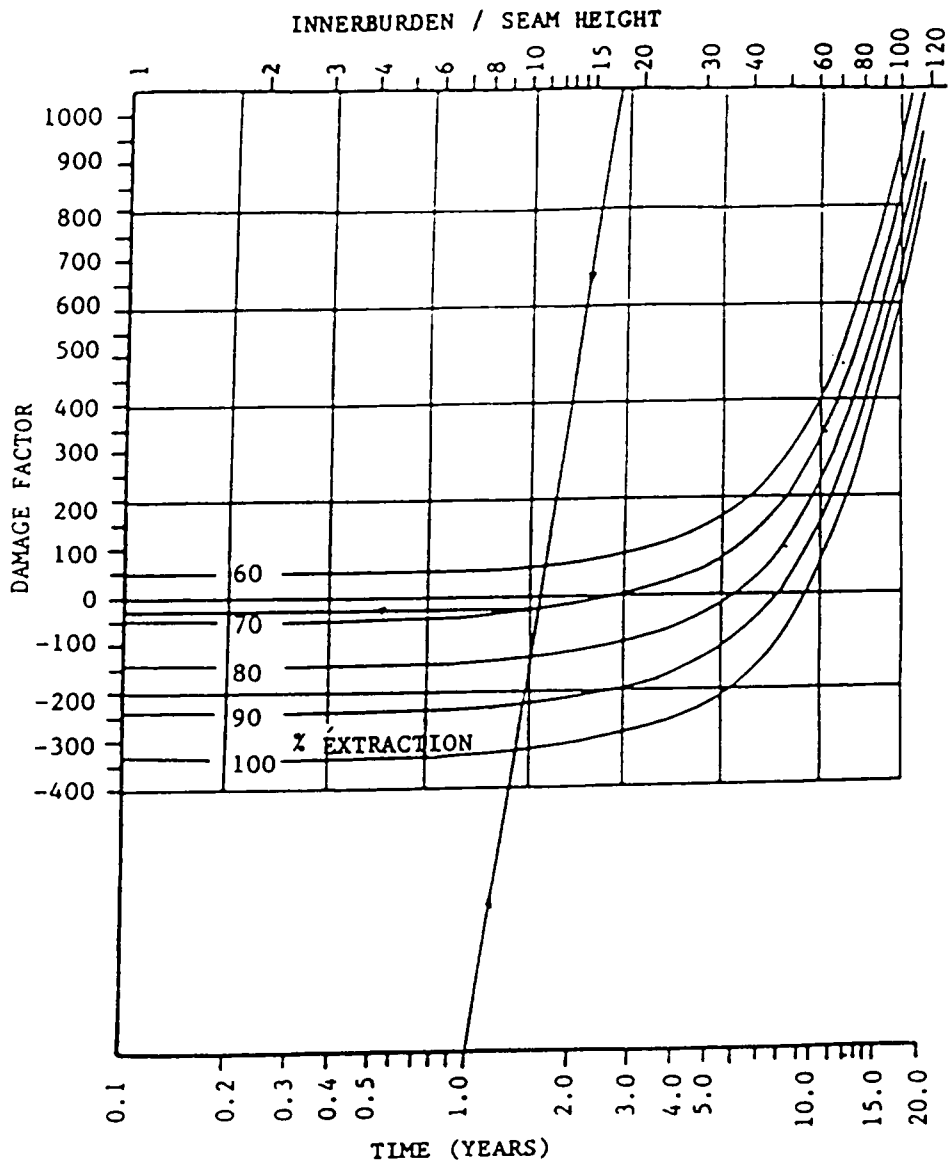

Figure 2.7 Nomogram for Upper Seam Damage Prediction (Webster, 1983)

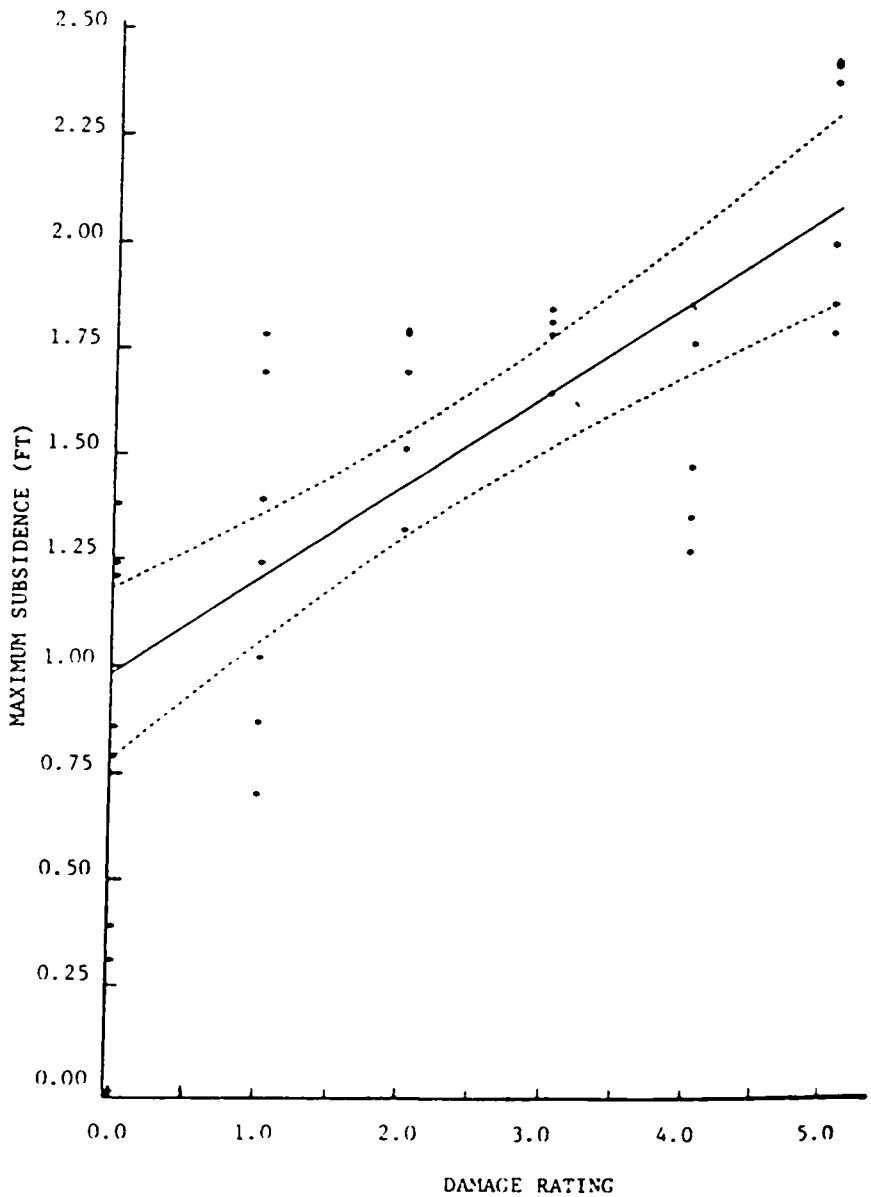

Figure 2.8 Relationship between Upper Seam Damage Factor and Maximum Upper Seam Subsidence (Webster, 1983)

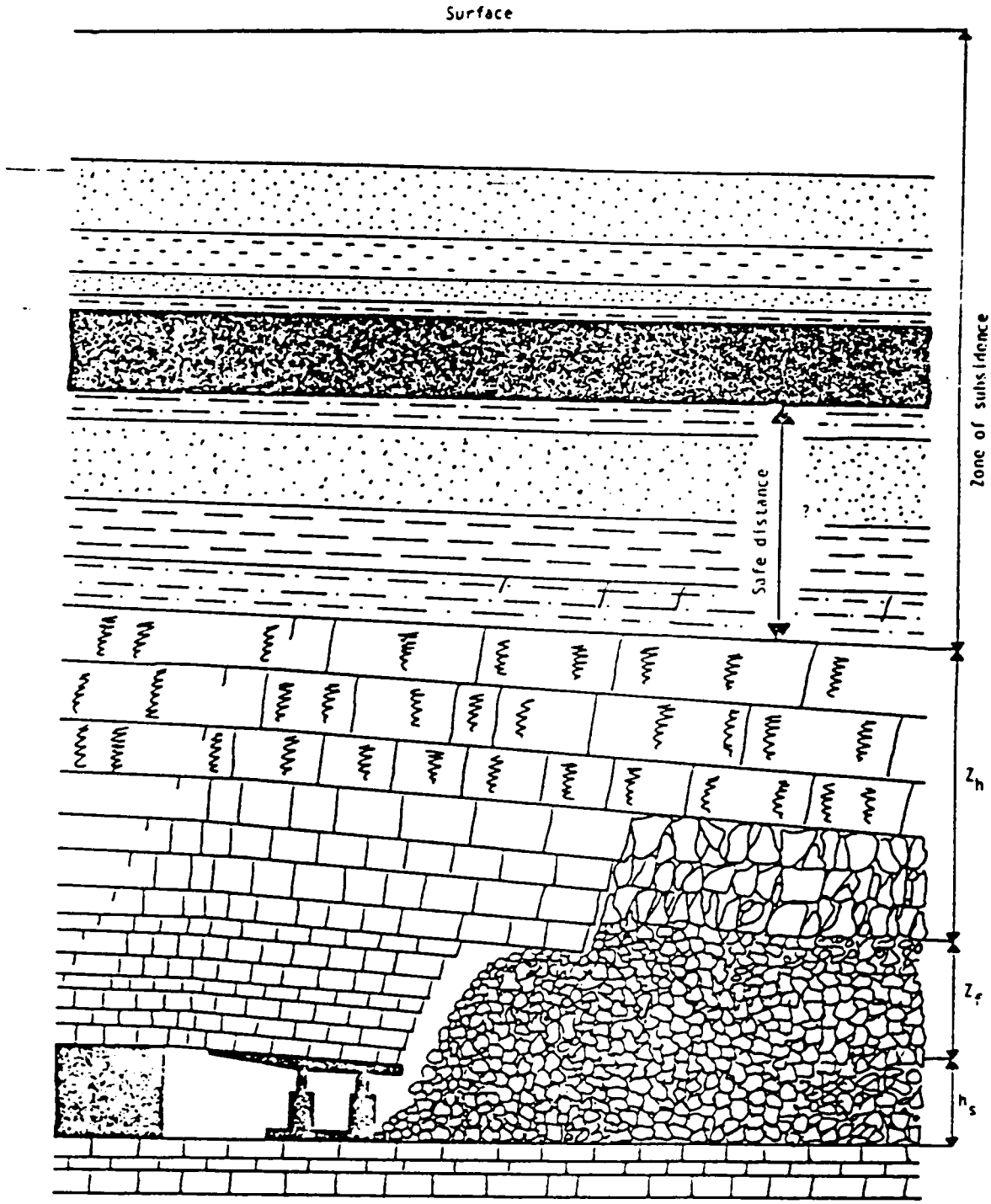

Figure 2.9 Various Zones Created after Mining of a Lower Seam (Hladysz, 1985)

Zone of Full Caving In this zone, roof rocks exist as a caving debris which consists of rock blocks or loose rock material. The height of this zone is given by the following formula:

$$Z_f=1.11h_s+0.33 \qquad (2\text{-}8)$$

where Z_f is the height of the full caving zone in meters, and h_s is the thickness of a coal seam or the height of a longwall face.

Zone of Fracturing Within this zone rock strata also lose their continuity due to jointing and separation of high intensity. This is also a completely destressed rock mass in a close vicinity to the full caving zone. The height of that zone can be calculated as:

$$Z_h=(1.5 \text{ to } 2.5)\ h_s \qquad (2\text{-}9)$$

The sum of these two zones is called the maximum height of the caving.

Zone of Subsidence This zone reaches the surface of the earth with a decreasing rate of separation and joint intensity.

Hladysz further states that it is obvious that the minimum distance between two coal seams should be greater than the high caving zone of the lower coal seam. However, it was pointed out that determination of the high caving zone

will not yield predictions of possible effects of undermining. According to the method used in Poland, he gave the following empirical equation for calculating the critical distance between two seams as follows:

$$M = \frac{D}{h_s} \qquad (2\text{-}10)$$

where M is the index of undermining, D is the parting thickness, and h_s is as defined before.

If D > 6.3, the upper seam can be mined safely after undermining. Eq. (2-10) gives a critical innerburden thickness as:

$$D_c = 6.3h_s. \qquad (2\text{-}11)$$

It should be pointed out here that these equations are based on European experiences and should be applied with caution due to the significant difference in entry development between Europe and the U.S.

There have been considerable attempts to predict interactions in multiple-seam mining, as reviewed in this section. These models are based on statistical analysis of case study data and are usually site specific. As a result, the conclusions are often descriptive; more detailed information on design cannot be obtained from these models.

2.4 Stability in Overmining

2.4.1 Impact on Future Mining

Interaction due to trough subsidence, caving and arching can affect the roof, pillar and floor of the upper seam. Of all the disturbances to a superjacent seam engendered by the mining of an underlying bed and the subsequent subsidence, certainly that which hascaused the most difficulty is the disturbance to the roof of the superjacent seam (Stemple, 1956). Although pillar load increases when mining crosses the gob line to the solid side of the lower seam, as recorded by Chekan et al. (1985), the increase is usually not large enough to cause any major problems except when it is over remnant pillars.

Depending upon the strata characteristics and degree of extraction in the mined lower seam, upper seam damage can occur due to any one or any combination of the following factors: high stress anomalies that lead to fracture; bed separation; innerburden slumping that affects ventilation; or high tensile stresses that may cause roof falls (Webster, 1984). If the lower seam is developed but pillars are left to support the upper seam, then the lower seam workings, which remain idle and open for long periods, will be subject to roof falls and may become heavily caved (Lazer, 1965). When pillars of any substantial size are left in the lower seam, high stresses are transmitted

through the innerburden to the overlying seam. The upper seam reacts to these stresses, resulting in cracking of the roof and floor. Squeezing and crushing of the coal, sometimes accompanied by falls of the top and heaving bottom, may occur due to an aggravation by the subsidence process of conditions already inherent in the seam (such as soft floor and other natural occurrences) in combination with mining methods not best suited for extraction under such conditions (Stemple, 1956). Negative interactions have resulted in delayed production, reduced coal recovery, and increased cost for extra support, injuries and the cleaning up of roof flls. Figure 2.10 shows how the extraction ratio is affected in overmining operations as a function of rock type and parting thickness.

2.4.2 Design Considerations

Design techniques which have been successfully adapted for multi-seam mining are often of the descriptive type. In room-and-pillars mining, these often concern where and how pillars should be located.

Pillar layering, or pillar columnization, is considered the traditional approach to multi-seam mining, especially when parting thickness is less than 50 ft. (Stemple, 1956; NCB, 1972). This technique involves careful mapping of the workings and pillars in the previously-mined seams, and subsequently locating each pillar in the seam being mined

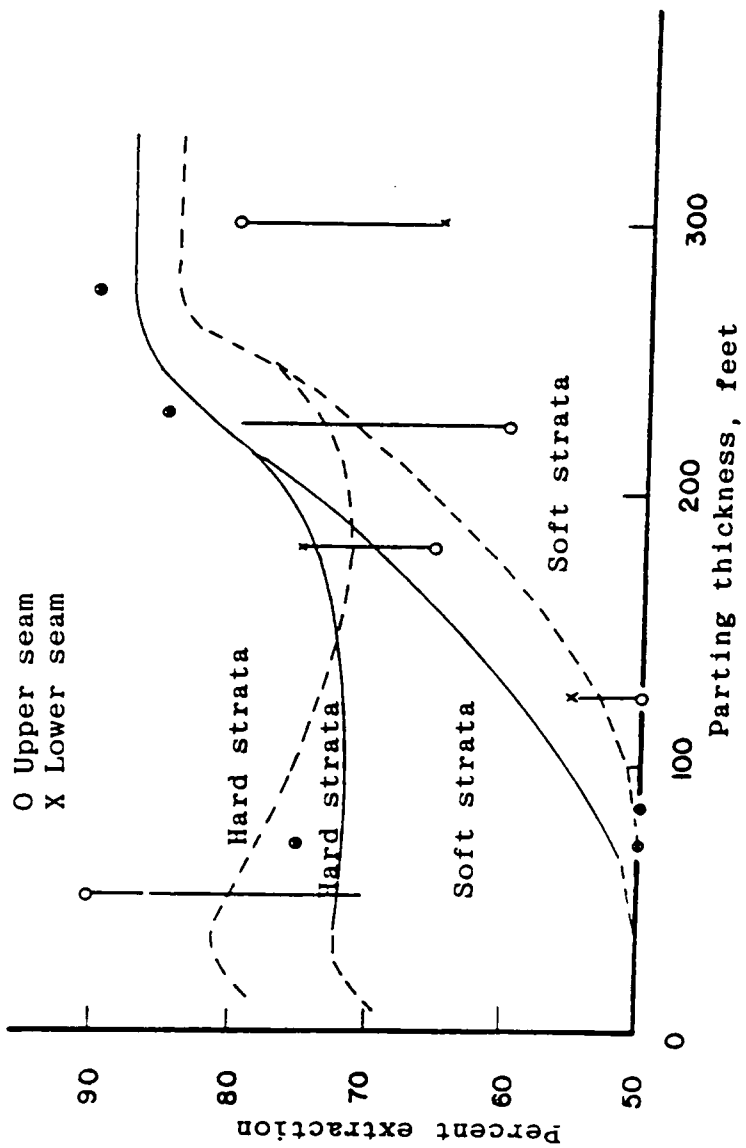

Figure 2.10 Effect of Innerburden Thickness on Extraction When Mining above a Previously-Mined Seam (Engineers International, 1981)

directly above or below a pillar in the previously-mined seam (Figure 2.11). Pillar lines should be kept long and straight to reduce shearing of the adjacent strata at the edges of barrier pillars (Holland, 1951).

In this type of design, since pillar sizes are designed for the maximum load, the pillars are often oversized and thus reduce the reserve recovery (Peng and Chandra, 1980). This design also tends to produce a piston of ground stresses through the pillars, which can cause unwanted overbreak in the lower workings. Pillar columnization also contributes to floor heaving problems due to the failure of floor strata (Britton, 1980).

When all seams are being designed for mining, Holand (1951) recommends that extraction in the lower seam be complete with no pillars or large remnants left in place. Advantage can also be taken of destressed zones over the gob, if the gob is free of remnant pillars. Roadways can be located in the destressed areas, thereby eliminating any chance of producing a piston of ground stresses through superimposed pillars.

Salamon (1964), in his considerations for multi-seam mining in the design of bord and pillar mining, states that when the vertical distance between the two seams is more than 0.75C where C is pillar center distance, the alternating influence of bords and pillars is negligibly small (Figure 2.12). This statement also suggests that interac-

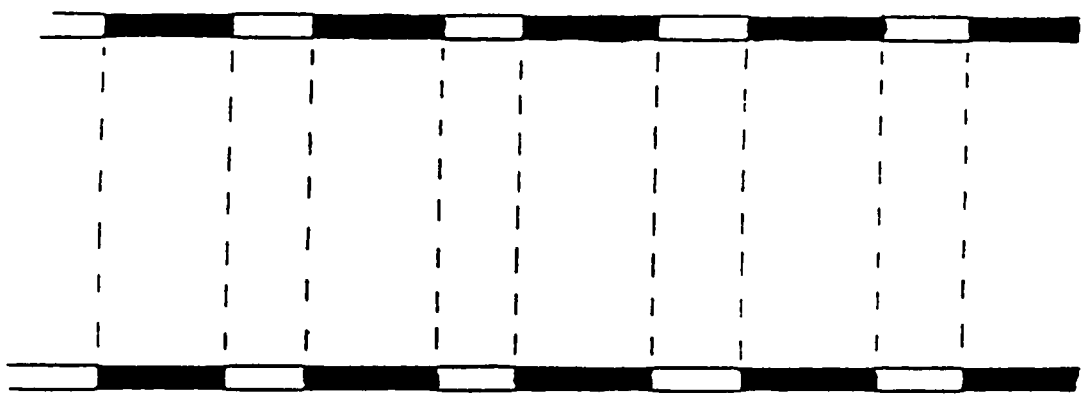

Figure 2.11 Pillar Columnization (NCB, 1972)

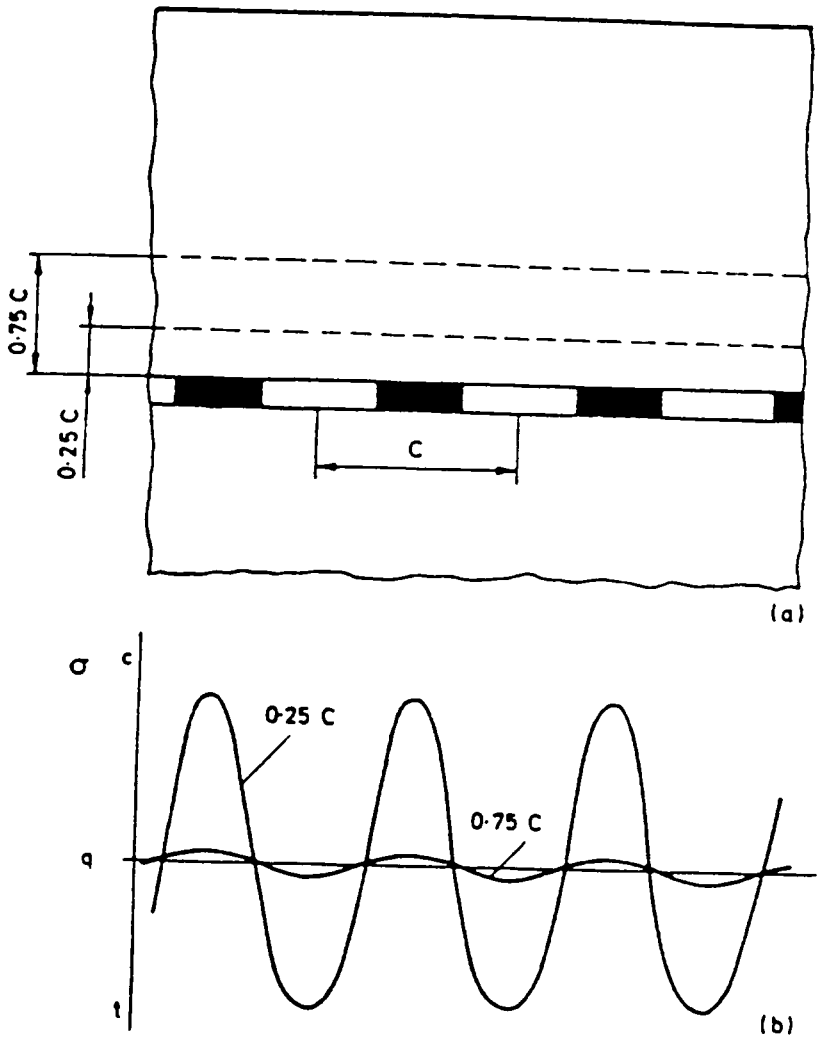

Figure 2.12 Upper Seam Stresses as a Function of Room Center Distance and Vertical Distance From Lower Seam (Salamon, 1964)

tion is larger with larger pillar center distance even when extraction ration remains the same. The stress picture is almost the same for both the roof and floor strata horizons.

He further pointed out that the situation is more complicated in the vicinity of a solid rib-side or a barrier pillar. The roof is exposed to much greater strains than is the floor.

Salamon concludes that panel pillars need not be superimposed if the distance between seams is greater than 0.75 to 1.00 times the pillar center distance. If the parting between two seams is less than this value, the superposition of the panel pillars is recommended. If it is known that a given parting is unlikely to collapse, then minimum safety factors can be used for the individual workings, and pillar sizes can be determined for all seams in turn. Finally, the largest pillar dimension determined by this calculation is used in all seams.

As for the sequence of mining, Salamon (1964) states that there does not appear to be any significant advantage to adopting a definite sequence for the mining of the various seams.

For protection of longwall workings against the effects of interaction, a similar approach to the columnization design, known as the pyramid support design, is taken (Figure 2.13). In this design, each of the succeeding seams

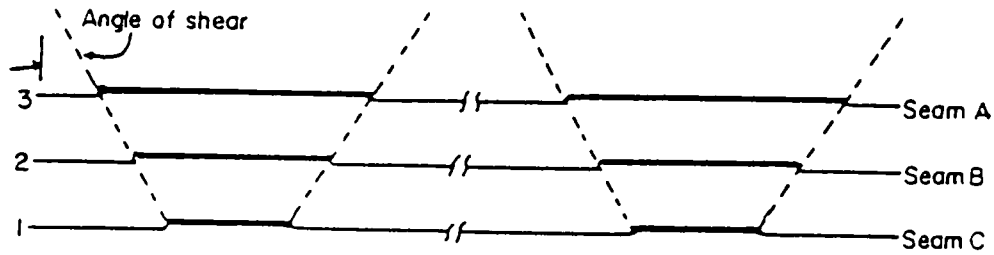

Ascending order of extraction

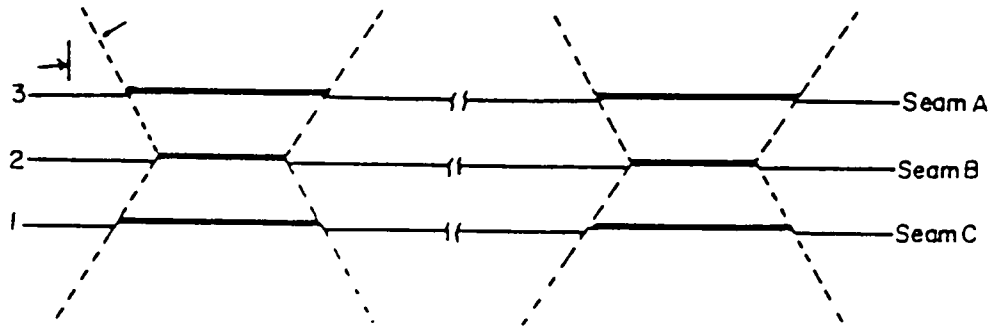

Extraction of intermediate seam first

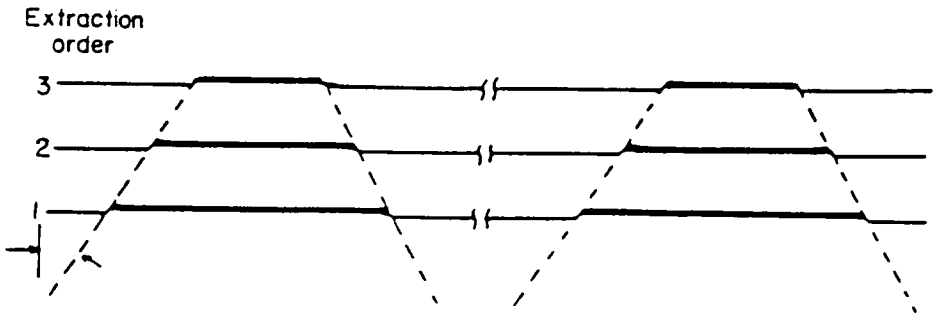

Descending order of extraction

Figure 2.13 Pyramid Pillar Support Design (King and Whittaker, 1970)

support the extraction units of the previously-mined seam. The face line should be orientated along, as opposed to perpendicular to, old rib-edges in other seams (Scurfield, 1970; Whittaker, 1974). Location of the face in such a destressed situation, as stated by Whittaker and Pye (1975), will promote excellent strata control conditions both on the face and in the gates. Such a scheme of composite layout, however, involves increasing successively the size of the rib pillar, which is wasteful of reserves.

An alternative layout which incorporates gate protection and conservation of reserves is the location of remnant rib pillars down the central axis of the present face, as shown in Figure 2.14 (Whittaker, 1972). This staggered pillar layout has the following advantages (Whittker, 1972; Whittaker, 1974, Whittaker and Pye, 1975; Whittaker and Singh, 1979):

- The fractures are kept intact much better than with other layouts since the face is moving on end relative to the orientation of the main vertical interaction fractures.
- Only a small length of the face is affected at any one time.
- Convergence on the face is not affected providing that the interaction fractures are kept constrained.
- A more even subsidence profile and more balanced strain profile are produced at the surface than with

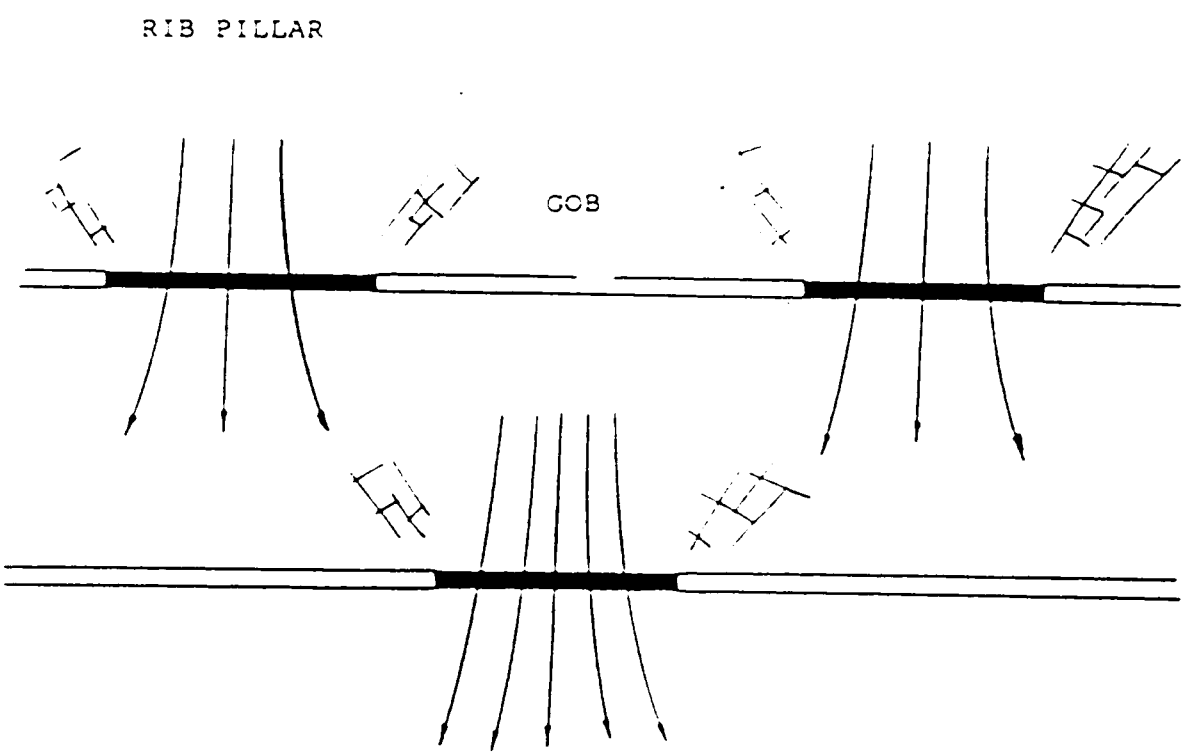

Figure 2.14 Remnant Pillars Located Down the Central Axis of the Present Face (Whittaker and Pye, 1975)

other layouts. This layout is, however, more likely to increase slightly the overall subsidence (Whittaker and Singh, 1979).

- The successive build-up of localized high-pressure regions, as occurs in the columnized layout, is avoided.

III. CASE STUDIES AND STATISTICAL ANALYSES

Recorded cases of interaction in multi-seam mining abound and date back to the late 1800's and early 1900's (Eavenson, 1923). These case study data have provided valuable information on many aspects of ground control in multi-seam mining and on the ground control mechanisms involved (Wu, 1987). This chapter deals with the construction of a computer data base of case studies and analyses of these cases.

3.1 Data Collection for Case Studies

Case studies of overmining operations have been collected in order to:

1) identify damage types and failure modes;
2) isolate factors affecting overmining interactions;
3) establish empirical models for prediction of possible interaction; and, finally,
4) lay preliminary groundwork for further studies.

Data collection was implemented through extensive literature research, contacts with operating mines and with research institutions engaged in studies of multi-seam mining (Eavenson, 1923; Holland, 1949; Holland, 1951; Hasler, 1951; Stemple, 1956; Lazer, 1965; Peng and Chandra, 1980; Engineers International, 1981; Haycocks and Karmis, 1983;

Su et al., 1984; Chekan, et al., 1985; Chekan, et al., 1986). The collected data were assembled on a computer data base. Where available, specific details of damage and subsequent analytical studies were also collected. Table 3.1 shows a typical example of a case study.

A total of 93 cases has been compiled, with each case containing the following information:

- Geological Factors
  - Overburden thickness and structural features;
  - Innerburden thickness and lithological compositions;
  - Percent of hard rock in innerburden;
  - Nature of immediate roof and floor in both seams;
  - Height of both seams;
  - Geological discontinuities;
  - Ground water conditions.
- Mining Variables
  - Method of extraction in both seams;
  - Geometries of mine layout;
  - Excavation height in lower seam;
  - Percentage of recovery in lower seam;
  - Time elapsed since mining of the lower seam.
- Assessment of Ground Control Conditions
  - spatial locations of observation in relation to lower seam workings;
  - description of any problems encountered during over-mining;

Table 3.1 An Example of a Case Study

SOURCE OF INFORMATION:	Stemple, 1956
NAME/LOCATION OF MINE:	Cambria County, PA
LOWER SEAM:	
Bed Name:	Lower Kittanning
Thickness:	38"
Method of Extraction:	Room-and-Pillar, complete recovery; only coal left was in barrier pillars
Extraction Ratio:	90%
Immediate Roof:	Shale, fairly firm
Immediate Floor:	Fireclay
INNERBURDEN:	
Thickness:	130-150 ft.
Nature of Strata:	Shales with 20- to 40-ft. thick bed of sandstone lying 5- to 30 ft. above lower seam
Percent of Hardrock:	20%
M-Index:	43.8
UPPER SEAM:	
Bed Name:	Lower Freeport
Thickness:	52"
Method of Extraction:	Room-and-Pillar
Immediate Roof:	Sandy shale, generally very firm
Immediate Floor:	Fairly soft shaley fireclay
OVERBURDEN:	
Cover thickness:	620 ft.
Nature of Strata:	Predominantly shales with several sandstone beds 15- to 40-ft. thick, lying mostly at about 150 to 250 ft. above the upper seam
TIME AFTER MINING OF LOWER SEAM:	7.5
GROUND WATER:	Not present
ASSESSMENT OF GROUND CONTROL CONDITIONS:	
Location:	Mining over gob/solid coal interface
Description:	Some bending and disruption of strata when entries crossed over line between lower gob and solid barrier pillars
Possible Mechanism:	Cantilever beam action by innerburden
Damage Rating:	2 - Moderate Damage
Control Method:	Unknown

- possible causes or mechanisms of success or failure;
- subsequent studies and methods adopted for the control of negative interaction.

Damage was also quantified using an indexing system on a scale of 0 to 5, which is indicative of the severity of damage, as defined in Table 3.2.

3.2 Statistical Analysis

Statistical techniques used range include from simple statistics such as mean, standard deviation, and frequency, to multivariate analysis such as factor analysis and multiple linear regression.

3.2.1 Location of Mining

Location of mining is divided into the following four types:

Type 1 - RP, Mining over remnant pillars;

Type 2 - GB, Mining over gob/solid coal interface areas;

Type 2 - RB, Mining over robbed areas;

Type 4 - X, General, other locations or unspecified.

The first three types are self-explanatory. Type 4 includes almost all favorable locations or locations which were not clearly specified. These locations include areas outside of the subsidence trough, those near the center of a supercritical and uniform subsidence trough, areas sup-

Table 3.2 Extended Upper Seam Damage Rating for Overmining Operations (After Webster, 1983)

Damage Rating	Conditions
0 - No damage	Normal conditions; conditions no worse than mining in undisturbed areas.
1 - Negligible Damage	Fractures present in upper seam, but no associated roof problems; no displacements; no difficulty of mining due to lower seam extraction.
2 - Moderate Damage	Fractures with visible movement; occasional broken roof and/or coal; water entering; mined with minimum or no extra support.
3 - Considerable Damage	Roof problems encountered; seam broken; some bottom heaves and pillar spalling; mined with increased timber support and slate work; occasional loss of coal.
4 - Severe Damage	Major roof problems encountered; entire entries caved; bottom heaved; top broken; coal crushed or cut out; mined with heavy support or certain amount of coal lost
5 - Very Severe Damage	Coal abandoned; mining too dangerous or too costly to continue; large amount of coal lost.

ported by regularly disturbed pillars left in the lower seam, or areas where extraction in the lower seam was low.

The location of mining relative to lower seam workings is of paramount importance, as most of the interaction damage was located in isolated areas. The effects of the location of mining are best illustrated in Figures 3.1 and 3.2 and in Tables 3.3 and 3.4, in which the frequency of upper seam damage and damage rating are shown as functions of mining location in upper seam. The first three locations show similar statistics of appreciable damage, being the three most troublesome locations in overmining operations. Over 84% of the cases examined in these locations showed appreciable damage as compared to 24% in Type X locations (Table 3.5). The most severe damage was usually reported in areas over remnant pillars or over gob and coal interface areas.

In many of the cases, lower seam workings such as remnant pillars were not known to exist until after damage had occurred. The statistics given here should serve as a guide as to where interaction can be expected. The logical and most important first step is naturally identification of the location of these structures, through careful mapping of lower seam workings, in order to avoid unnecessary damage.

Block diagram showing the effects of location of mining by location type. ROBBED represents mining over robbed areas in the lower seam, etc. GENERAL includes all other locations, including those not specified in the original reports. Number in each box is total number of cases.

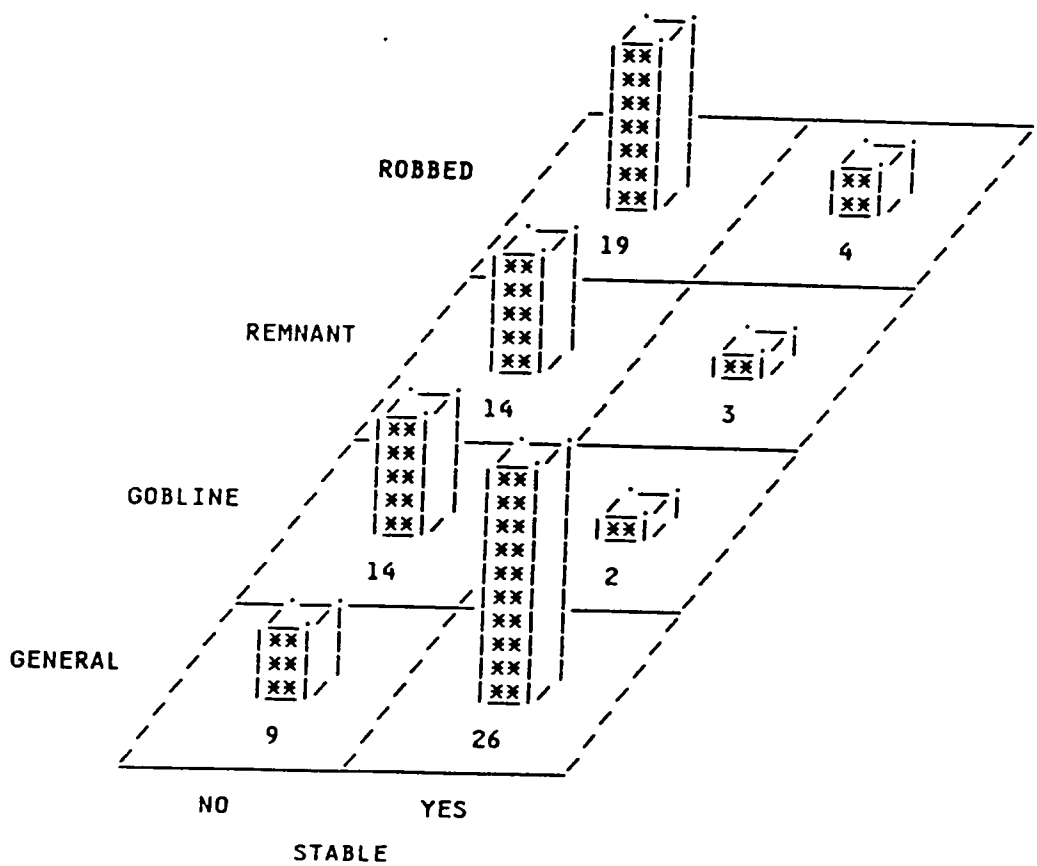

Figure 3.1 Block Diagram Showing the Effects of Mining Location - Four Locations

Block diagram showing the effects of location of mining with respect to lower seam workings. Type R & G includes mining over remnant pillars, mining over gobline areas, and mining over robbed areas. Type X represents mining in all other areas, including those not specified in the original reports. Number is each box is total number of cases.

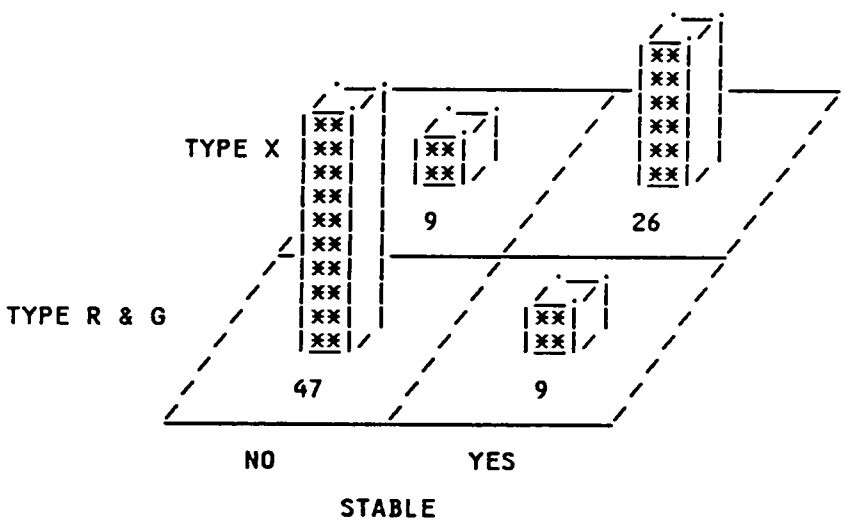

Figure 3.2 Block Diagram Showing the Effects of Mining Location - Two Locations

Table 3.3 Statistics Showing the Effects of Mining Location

LOCATION	DAMAGE RATING (DR, See Table 2.1)					
FREQUENCY PERCENT ROW PCT COL PCT	0	1	2	3	4	5
GENERAL	17 18.58 48.57 94.44	9 9.89 25.71 52.94	6 6.59 17.14 54.55	3 3.30 8.57 15.79	0 0.00 0.00 0.00	0 0.00 0.00 0.00
GOBLINE	0 0.00 0.00 0.00	2 2.20 12.50 11.76	0 0.00 0.00 0.00	7 7.69 43.75 36.84	4 4.40 25.00 25.00	3 3.30 18.75 30.00
REMNANT	0 0.00 0.00 0.00	3 3.30 17.65 17.65	1 1.10 5.88 9.09	0 0.00 0.00 0.00	7 7.67 41.18 43.75	6 6.59 35.29 60.00
ROBBED	1 1.10 4.35 5.56	3 3.30 13.04 17.65	4 4.40 17.39 36.36	9 9.89 39.13 47.37	5 5.49 21.74 31.25	1 1.10 4.35 10.00

Table 3.4 Statistics Showing the Effects of Mining Location

LOCATION	DAMAGE RATING (DR, See Table 2.1)					
FREQUENCY PERCENT ROW PCT COL PCT	0	1	2	3	4	5
TYPE R&G: REMNANT GOBLINE ROBBED	1 1.10 1.79 5.56	8 8.79 14.29 47.06	5 5.49 8.93 45.45	16 17.58 28.57 84.21	16 17.58 28.57 100.00	10 10.59 17.86 100.00
TYPE X: GENERAL	17 18.68 48.57 94.44	9 9.89 25.71 52.94	6 6.59 17.14 54.55	3 3.30 8.57 15.79	0 0.00 0.00 0.00	0 0.00 0.00 0.00

Table 3.5 Summary of Upper Seam Damage Statistics

Location of Mining	Number of Cases	Appreciable Damage	Percentage (%)
Type R & G	57	48	84
Type X	36	9	25
Total	93	57	61

3.2.2 Upper Seam Subsidence

The earliest, and probably the most complete, measurement of upper seam subsidence was reported in 1931 by Auchmuty. In this study, an underground limestone mine was being mined over a coal seam mined several years before. Surveys were made of both the surface and mine level. It appears that the action in the limestone mine was similar to that observed on the surface. A base line, survey stations, and vertical movements are reproduced in Figure 3.3.

Other reports on subsidence, taken from multiple-seam mining operations, have shown somewhat erratic numbers, possibly due to inconsistent observations or to the irregularity and lack of uniformity of recovery in the lower seam. Often, measurements have been started long after the lower seam has been mined out, giving only a partial picture of the situation. As shown in Table 3.6, upper seam subsidence ranges from 0.1 to 0.8 of seam height. The numbers are usually lower than most surveying results on surface subsidence over more completely extracted mines. It should also be noted that the gradual type of subsidence often observed on the surface is not always found underground. A sudden dropping of the pavement (floor) was also frequently encountered in many of the 93 cases studied. On several occasions, coal-cutting machines or conveyor belt sections of several hundred feet in length were dropped

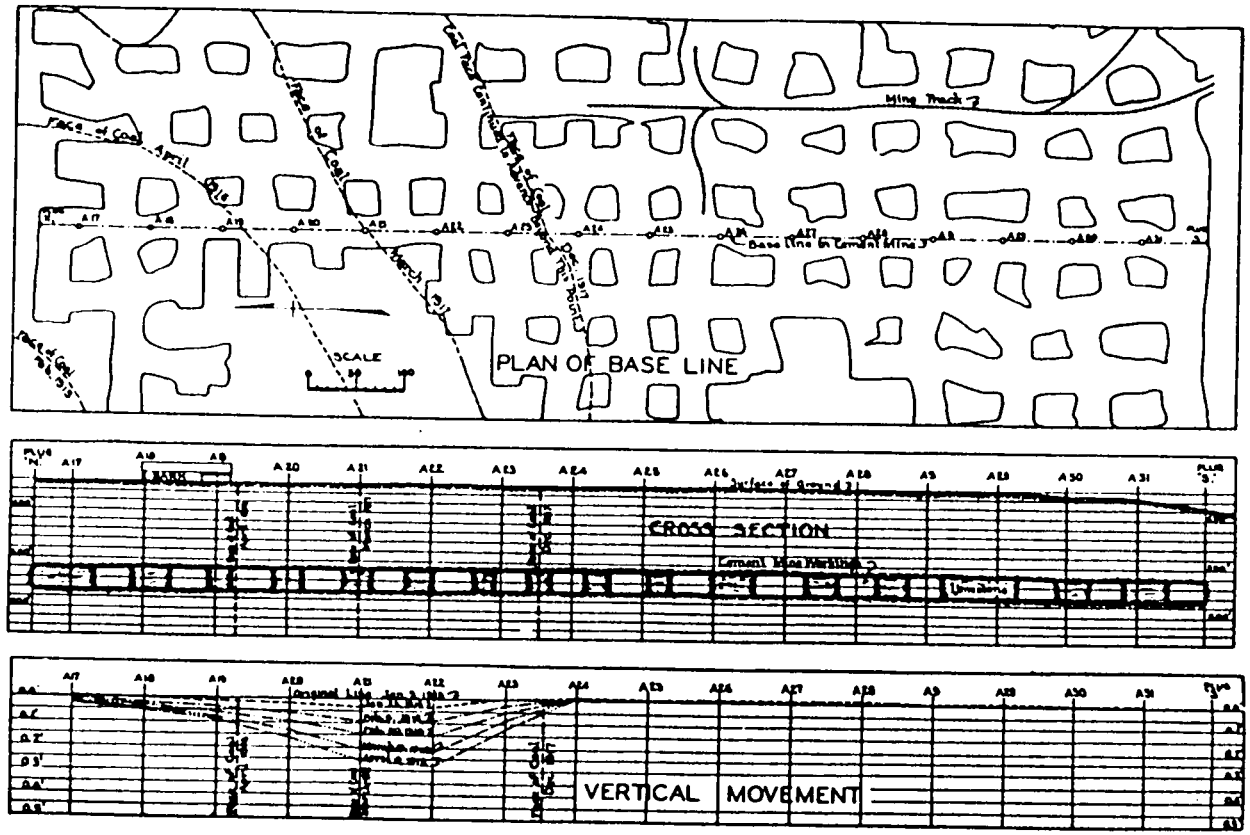

BASE LINE, STATIONS A17 TO A31, IN CEMENT WORKINGS.

Figure 3.3 Subsidence Survey of a Limestone Mine Being Mined Over a Previously Mined Coal Seam (Auchumty, 1931)

Table 3.6 Examples of Upper Seam Subsidence

Innerburden Thickness (h, ft.)	Lower Seam Thickness (s_1, in.)	Maximum Subsidence (Smax, in.)	Subsidence Factor (Smax/s_1)	Ref.
96	96	18	0.188	(1)
80	132	18	0.136	(2)
26-35	96	36-48	0.500	
101	102	12	0.118	
92	102	8.4	0.082	
38	110	43	0.391*	
26	96	36	0.375	(3)
50	60	8	0.133	(4)
11	45	36	0.800**	
150	48	6	0.125	
40	51	6	0.118	
95	72	2-18	0.250***	(5)

(1) - Paul et al., 1932
(2) - Holland, 1949
(3) - Eavenson, 1942
(4) - Stemple, 1956
(5) - Chekan, 1985

* Sinkhole-type subsidence, massive interseam failure
** Upper seam dropping down to lower seam
*** Subsidence started 200 ft. outside of gobline

down in their entirety by from a few inches up to a foot.

Another phenomenon, not mentioned in the reported case studies but probably occurring quite frequently, is sinkhole subsidence. This type of subsidence occurs as a result of the collapse of the overburden into a mine opening, due to deterioration of ground conditions in the mined lower seam over time. This is probably the reason, in some cases, that abrupt vertical displacement of the upper seam has occurred even when the lower seam was mined many years before and extraction ratio was not high. The main factors contributing to this type of subsidence are the water and air percolating downward to the lower seam through the cracks induced by lower seam mining, causing weathering in the lower seam roof, coal and floor. Sinkholes, however, are usually in the range of 1.5 to 45 ft. in diameter (Bruhn et al., 1980) and the effects of sinkhole-type subsidence are therefore local compared to those of trough subsidence.

3.2.3 Empirical Relationships

Statistical analysis of the case study data has yielded some useful empirical relationships, which can be used to predict the possibility of interaction damage given certain variables.

Scatter plots of the data, as shown in Figures 3.4 and 3.5, have shown a clear separation between two groups of

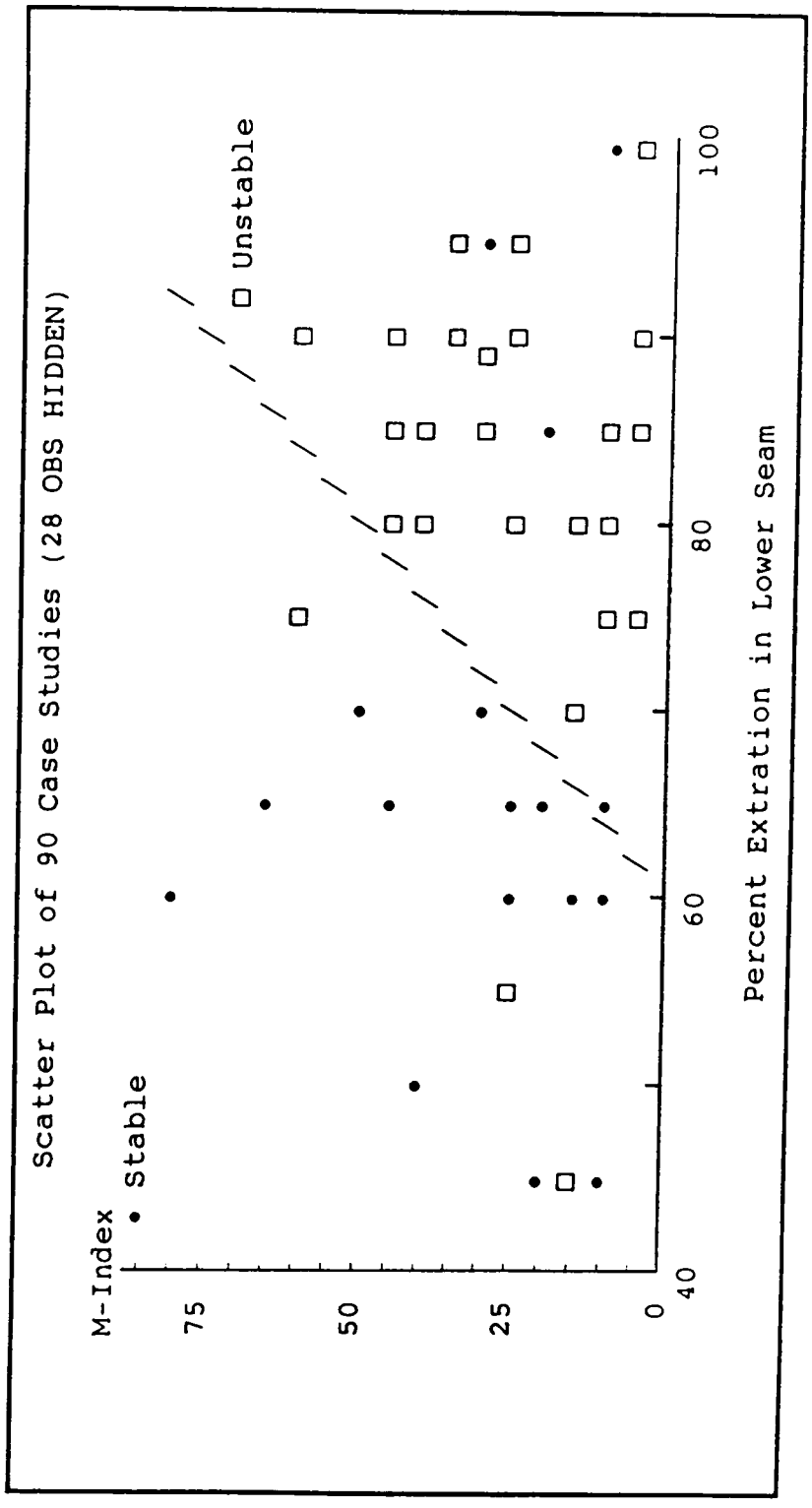

Figure 3.4 Scatter Plot of Case Studies Without Time Effect

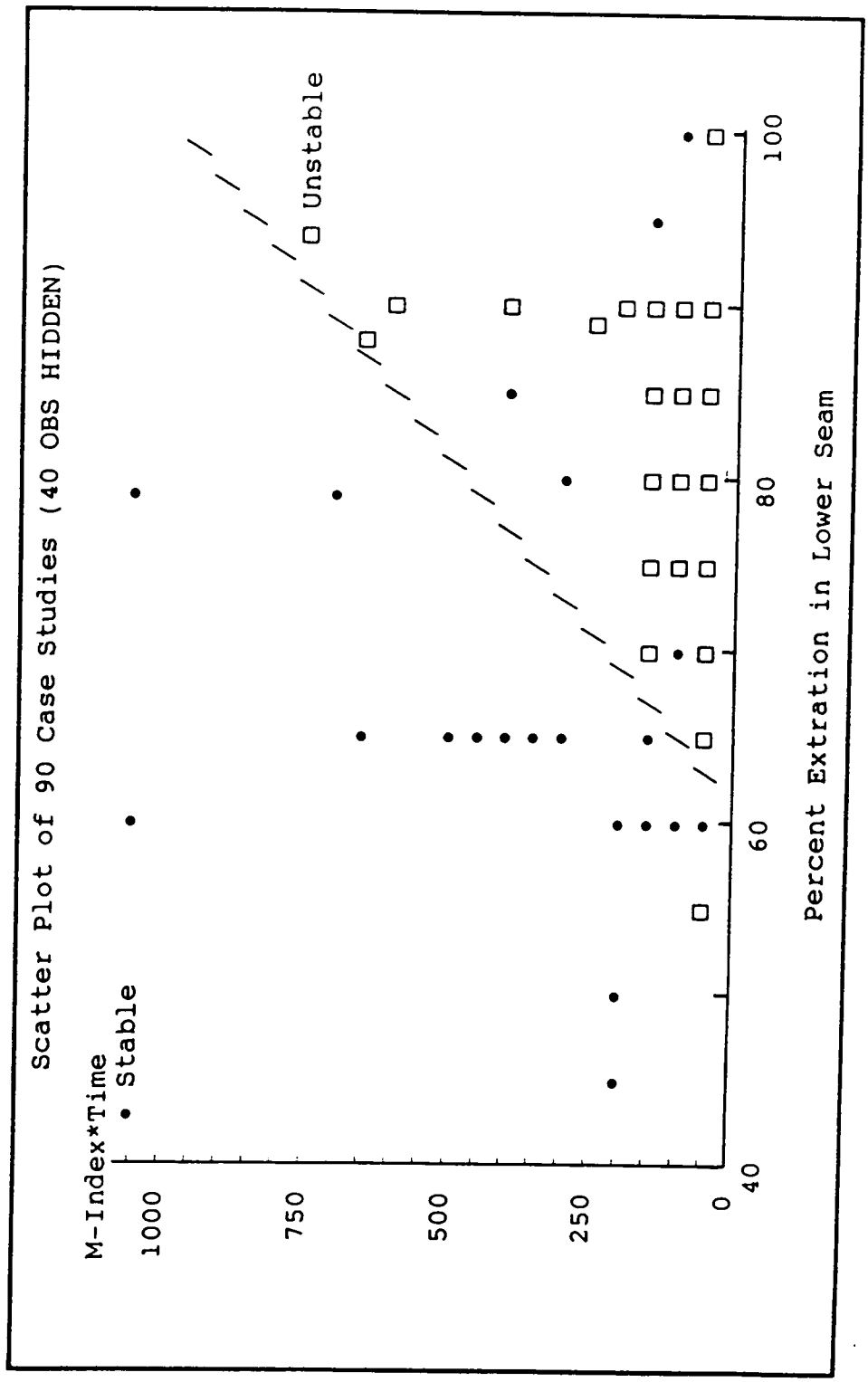

Figure 3.5 Scatter Plot of Case Studies With Time Effect

data: stable - those with damage ratings 0 and 1, and unstable - those with damage ratings 2 and above. Based on Figures 3.4 and 3.5, the M-Index method has been developed. The method predicts a critical M-index, which is the minimum index value required if no appreciable damage is anticipated for the upper seam, given by

$$\text{M-Index} = -224 + 3.5x \qquad (3\text{-}1)$$

where x is the percentage of lower seam extraction ($x \geq 62$); and M-index the ratio of the innerburden thickness and lower seam excavation height.

Figure 3.5 is a scatter plot of critical M-Index with time effects:

$$\text{M-Index} = (-972.8 + 15.1x)/t \qquad (3\text{-}2)$$

where t is time elapsed since mining of the lower seam.

From Equations (3-1) and (3-2), a critical innerburden thickness can be calculated:

$$\text{IBTc} = \text{M-Index}*\text{LST} \qquad (3\text{-}3)$$

where LST is lower seam thickness in feet.

The design applications, the critical M-index method is represented by the nomogram shown in Figure 3.6. If a calculated critical innerburden is greater than the actual value of innerburden thickness, then interaction is likely to cause damage.

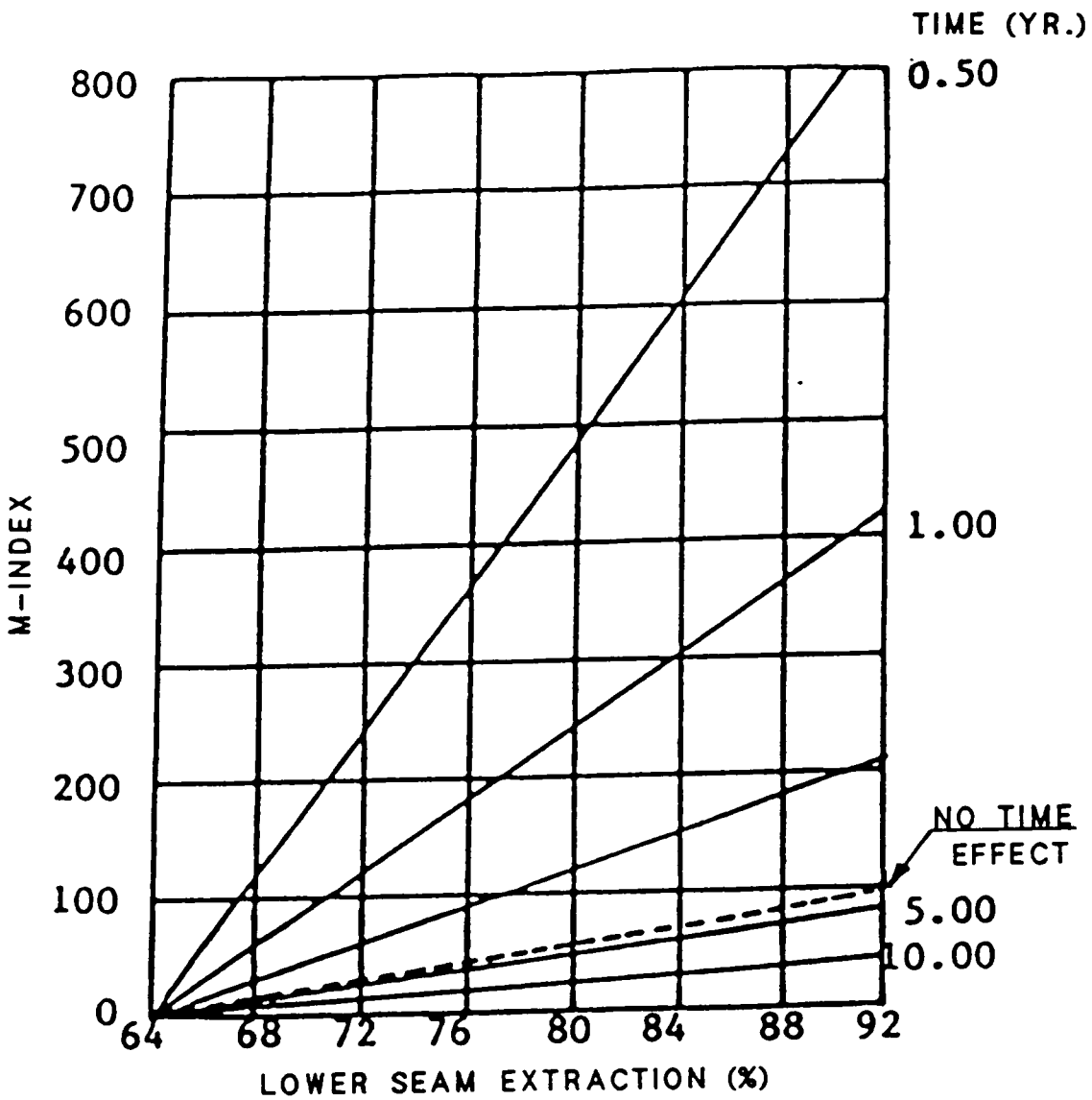

Figure 3.6 Nomogram for Prediction of Critical M-index

The relative difference between the actual M-index and the calculated M-index, expressed in terms of the actual M-index, is introduced as the stability factor:

$$S.F. = \frac{y - (-972.8 + 15.1x)/t}{y}$$

$$= 1 - \frac{(972.8 + 15.1x)/t}{y} \qquad (3.4)$$

where y is the M-index = innerburden thickness/lower seam height.

From the above definition, an S.F. of zero indicates the critical condition with a positive meaning stable and negative meaning an unstable situation. The larger the absolute value of S.F. is, the stronger the indication.

The possibility of interaction can also be assessed using a probability model which was developed based on the frequency distribution of damage cases as a function of the M-Index (Figure 3.7). Linear regression gives the following function:

$$Pm = 0.196 + 0.803e^{-0.0169y} \qquad (3\text{-}5)$$

where Pm is the probability of interaction damage.

Finally, a multiple regression model was also developed using stepwise regression techniques. This model predicts a Damage Rating as:

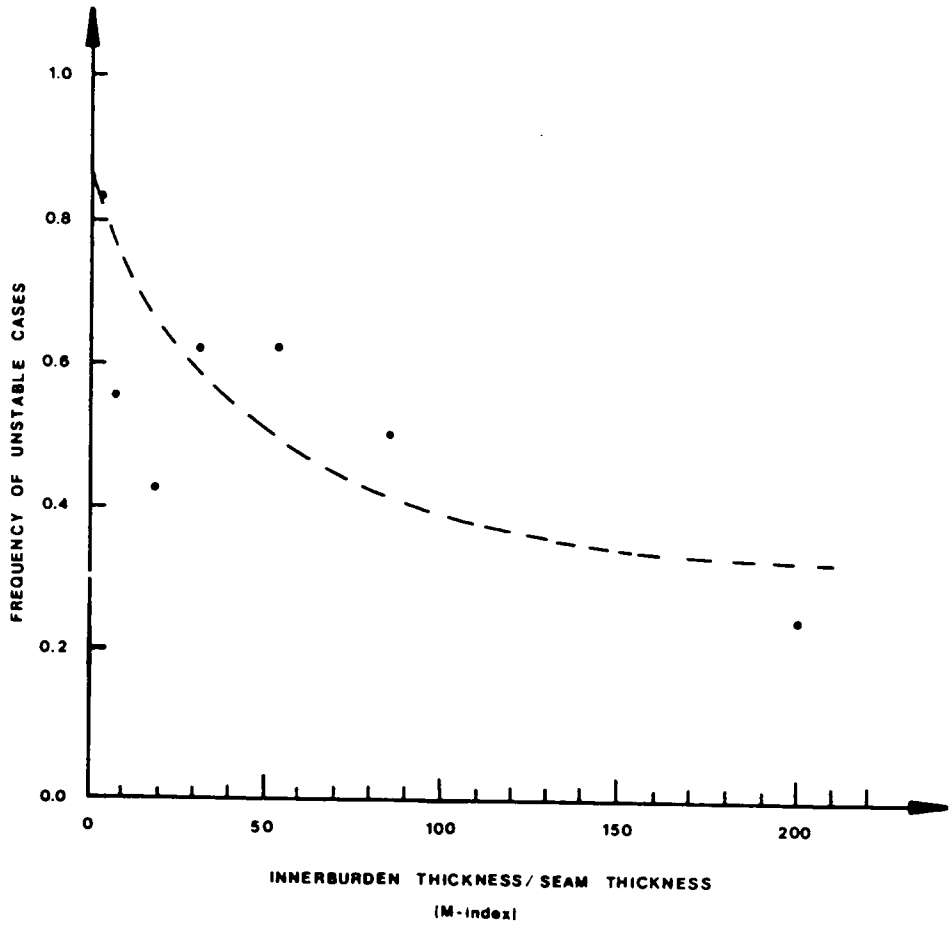

Figure 3.7 Frequency Distribution of Unstable Cases as a Function of M-index

$$DR = -1.28+1.804xLOC-0.00053 \frac{IBT}{LST}t +0.0347*LEXT \quad (3-6)$$

where LEXT is the lower seam extraction percentage. Other variables are as defined previously.

LOC was entered as the most important factor, as already shown in Section 3.2.1. The model can explain about 52% of the variance, with the remainder being due to geological factors which could not be quantified in this model. To incorporate these geological factors, a classification scheme has been developed and will be discussed in Chapter 5.

It is important to note that these models, because they are based on field data, can be used as a preliminary check for the possibility of interaction damage. For the same reason, their applications should be restricted to the Appalachian coalfields, where these data were collected.

3.3 Summary of Failure Modes in Overmining

The following is a summary of failure modes, contributing factors, and their effects, which have been reported in the case studies based in turn on general observations and subsequent analysis. This is information can be used in future studies to quickly identify the interaction mechanisms.

1. Massive shearing (Figure 2.3)

Factors:

- Strong massive innerburden such as sandstone
- Extremely large excavation height and extensive excavation in lower seam
- Very low ratio of innerburden thickness to excavation height
- Relatively shallow overburden so that thrust arch is not easily formed
- Inherent weak planes (e.g. fault planes)

Effects:

- Extensive area of large vertical displacement
- Coal and roof entirely cut out or crushed at shearing boundaries

2. Local Shearing (Figure 3.8)

Factors:

- Remnant pillars left in lower seam
- Lack of uniformity in extraction and pillar robbing in lower seam
- Brittle innerburden
- Relatively large excavation height
- Inherent weak planes

Effects:

- Grades due to uneven relative vertical displacement
- Abrupt displacement cutting out coal
- Coal may be crushed alone shearing plane

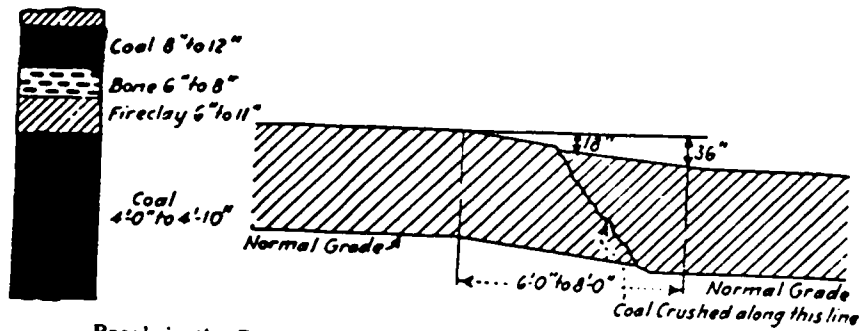

Break in the Redstone Seam when Passing from Solid Coal to Robbed Area in the Pittsburgh Seam

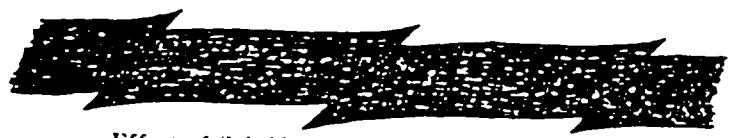

Effect of Subsidence Movement in the Low Main Seam, Bewicke Main Colliery; Note Bending, Shearing, and Readjustment of Level

Figure 3.8 Local Shearing Failure (after Holland, 1949)

- Effects are local and isolated

3. Bending of Upper Seam (Figure 3.9)

Factors:

- Over gob/solid coal interface
- Soft or ductile strata (e.g. soft clay or soft shale)
- Tension zone in subsidence trough

Effects:

- Fractured coal due to low tensile strength
- Heavy grades causing difficulty in mining
- Gradual bending accompanied by fracturing may cause dangerous roof conditions for an extent of several hundred feet

4. Fracturing (Figure 3.10)

Factors:

- Caving of lower seam or roof falls
- High pressure due to arching
- Low ratio of innerburden thickness to excavation height
- Weak strata with low bulking factor

Effects:

- Fractured upper seam coal and roof
- Roof falls
- Water percolating through overburden to upper seam
- Water and air entering upper seam causes roof rock to weather
- Ventilation problems (e.g. disruption)

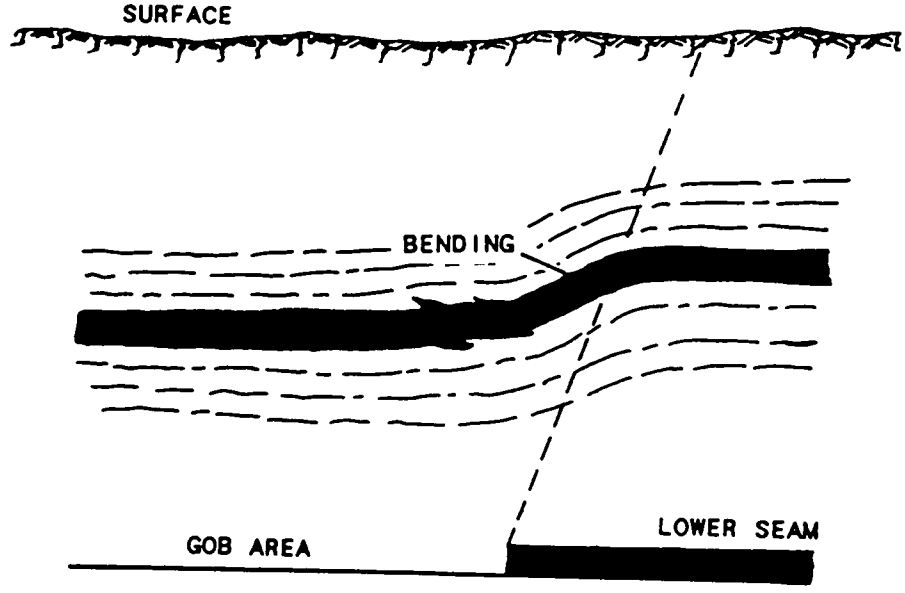

Figure 3.9 Bending of Upper Seam due to Subsidence

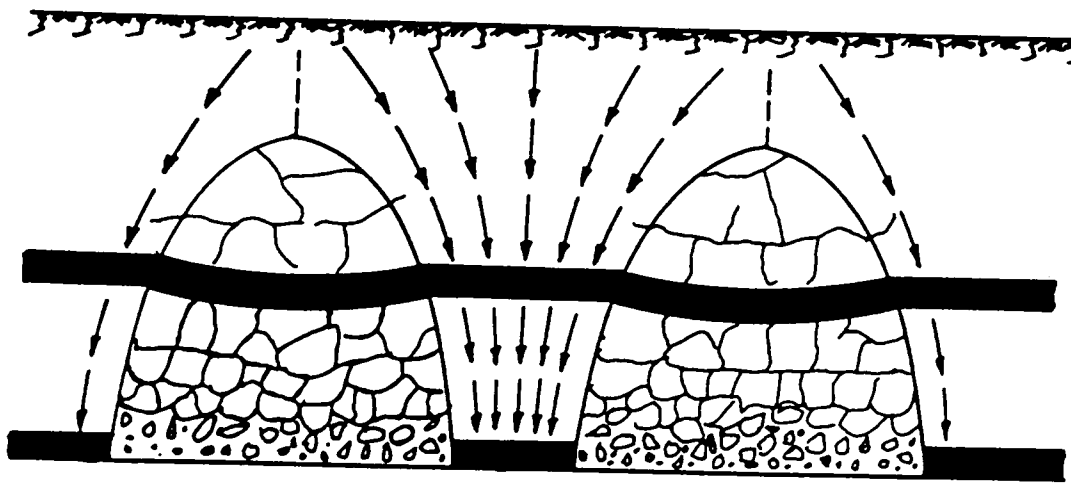

Figure 3.10 Load Transfer and Formation of Pressure Arch Creating Fracturing and Squeezing

- Water in upper seam drained to lower seam to leave dry conditions in upper seam

5. Squeezing (Figure 3.10)

Factors:

- High pressure transferred by remnant pillar
- Arching effects shifting loads
- Soft floor
- Large overburden thickness

Effects:

- Pillar crushing
- Floor heaves
- Roof falls

6. Bed Separation (Figure 3.11)

Factors:

- Stress relief
- Low bonding strength between coal and roof or between coal and floor
- Sagging of strong innerburden strata
- Beam action by strong innerburden

Effects:

- Coal dropping away from the roof
- Floor dropping away from the coal
- Interruption of ventilation

It is important to realize that, more often than not, a combination of the above failure modes will occur, due to the complex nature of geological and mining conditions.

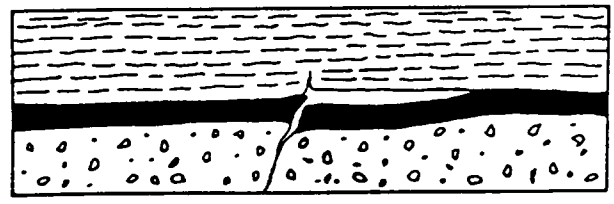

COAL SEPARATED FROM ROOF THROUGH SHEARING

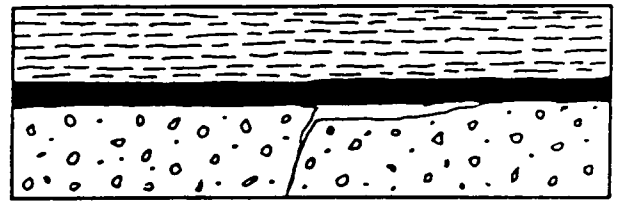

COAL SEPARATED FROM FLOOR THROUGH SHEARING

a. MOST LIKELY OVER REMNANT PILLAR OR GOB EDGES

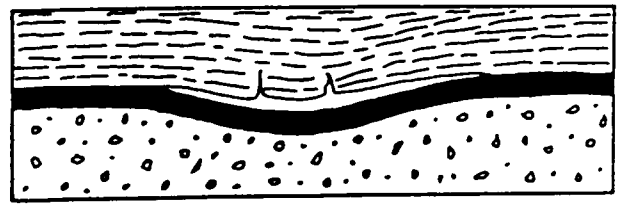

COAL SEPARATED FROM ROOF THROUGH BENDING

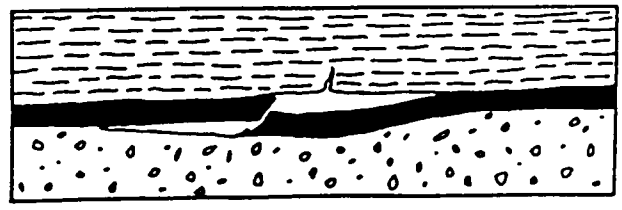

COAL SEPARATED FROM FLOOR THROUGH BENDING AND SHEARING

b. MOST LIKELY TOWARDS CENTER OF SUBSIDENCE TROUGH

Figure 3.11 Bed Separation

Nevertheless, given sufficient information regarding the controlling factors, the potential failure modes can be predicted so that advance planning can be made in order to minimize interaction effects accordingly.

VI. ANALYSIS OF INTERACTION MECHANISMS

Having identified the various mechanisms of upper seam interaction, this chapter provides quantitative analyses of each mechanism. Determination of the extent and magnitude of interaction by each mechanism, including zones of caving and fracturing, tensile strain and width of tension zone, as well as the influence of stress increase by remnant pillars, can help to locate areas of potential hazard and to predict the magnitude of expected damage.

4.1 Subsidence Model

4.1.1 Selection of Subsidence Model

The Budryke-Knothe method, with modifications made for upper seam subsidence prediction, has been chosen for the following reasons:

1. the method has been successfully used for surface prediction in the Appalachian coalfields; and

2. the method has the flexibility necessary to allow for irregular mine geometries and superposition.

Using this method, the subsidence at any point A is given by (Figure 4.1):

$$S(x) = \frac{Smax}{r} \int_{-a}^{x} e^{-\pi \frac{x^2}{r^2}} dx \qquad (4\text{-}1)$$

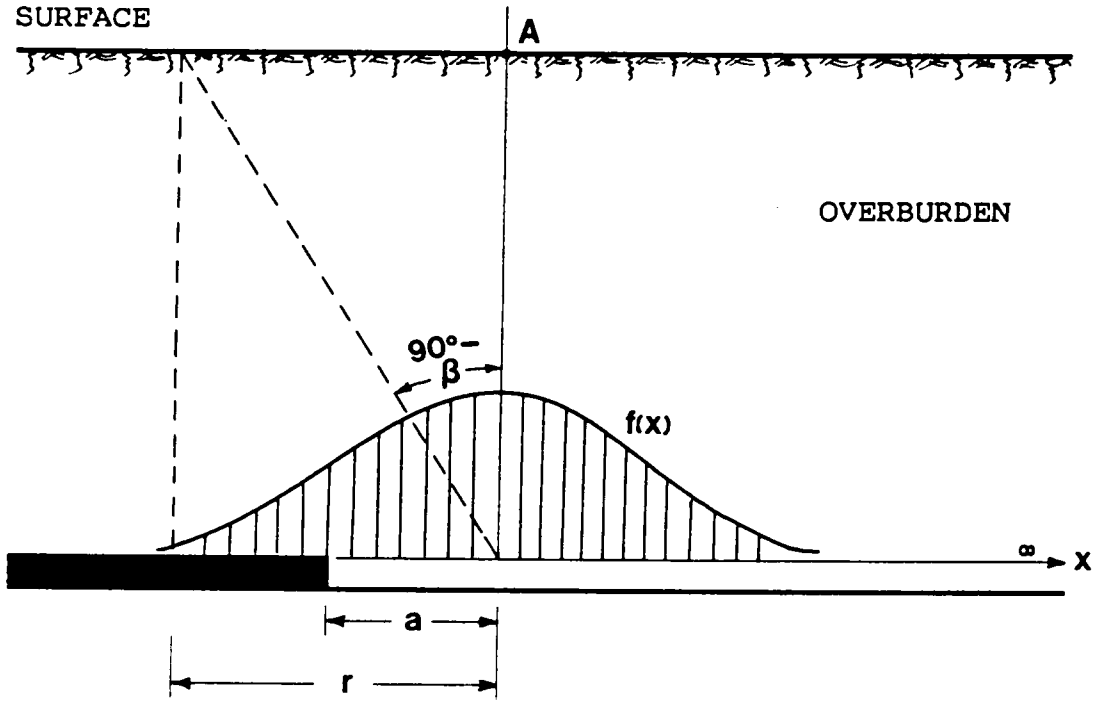

Figure 4.1 Subsidence Prediction Using the Influence Function Method

where r = average radius of influence = h/tan(β); h = distance from lower seam level; β = angle of influence; x = horizontal distance from the inflection point; Smax = maximum subsidence.

Tensile strain at the upper seam level, which is a measure of the intensity of disturbance, can be calculated by the following equation:

$$\varepsilon(x) = brK(x) = 2\pi b \frac{Smax}{r} \left(-\frac{x}{r}\right) \exp(-\pi x^2/r^2) \qquad (4\text{-}2)$$

where b = constant, and is found to be equal to 0.3 for horizontal seams by the finite element method. A value of 0.35 for b can be derived from results reported by Karmis et al. (1987), based on case studies relating strain to curvature.

The subsidence factor Smax/m is a function of the excavation geometry of the lower seam and lithology of the strata. Based on case studies, an empirical formula has been derived for the Appalachian coalfields:

$$Smax/m = (-0.0071*n+0.825)(1-e^{-60\ell/n}) \qquad (4\text{-}3)$$

where Smax = maximum subsidence; m = extraction height of the lower seam; n = percent of hardrock in strata; ℓ = width/depth ratio = w/D; w = excavation height of the lower seam; and D = distance from the lower seam.

4.1.2 Correction For Upper Seam Level

The subsidence factor defined above, as in most subsidence control literature, is the maximum subsidence for the surface. Although subsurface subsidence can be treated as surface subsidence with reasonable accuracy, it is generally believed that subsidence at the upper seam level is greater than that at the surface. This is because as the strata subsides, caving at the lower seam level and subsequent strata movement create voids in the strata; otherwise the surface subsidence factor would always be 1.0 under supercritical conditions.

In a super-critical subsidence situation, if the surface subsidence factor, a_s, is 1.0, it is reasonable to assume that maximum subsidence at all levels below the surface and above the mined seam is 1.0. Then, if the subsidence factor for the surface is less than 1.0, the subsidence factor at a distance z from the surface, a(z), can be written as:

$$a(z) = a_s + \frac{da}{dz} f(z) \qquad (4\text{-}4)$$

where a(z) = maximum subsidence factor at level z; $a_s \leq a(z) \leq 1.0$; a_s = subsidence factor at surface; z = distance from surface; f(z) = function of z; and da/dz = rate of change of maximum subsidence factor.

Assuming that the maximum subsidence at the excavation level is a_ℓ for super-critical conditions, and that the difference between a_s and a_ℓ is lineraly ditributed in the strata, da/dz can be computed as:

$$da/dz = \frac{a_\ell - a_s}{D} \qquad (4\text{-}5)$$

where D = distance from the surface to lower seam level.

The subsidence factor at distance z from the surface, satisfying boundary conditions, is then:

$$a(z) = a_s + \frac{a_\ell - a_s}{D} z. \qquad (4\text{-}6)$$

4.1.3 Determination of Other Parameters

Angle of Influence: The angle of principal influence is the angle between the horizontal and the line connecting the inflection point to the "zero" subsidence limit, as represented by β in Figure 4.1. This parameter is required when using the Knothe's method to predict subsidence and its value has a great significance on vertical movements and strain distribution. Its value is dependent on the geological characteristics of the overburden (or innerburden) and on the depth of mining. If the angle of influence for each rock type comprising the innerburden is known, then the parameter for the whole strata can be estimated using the

principles of superposition, given the percentage of each rock type. Figure 4.2 shows how the average tanβ is calculated for a two-layer (or two-type) strata, expressed by the following equation:

$$\tan\beta = \frac{h}{d + r} = \frac{h}{d + h_1/\tan\beta_1 + h_2/\tan\beta_2} \qquad (4\text{-}7)$$

where β = average angle of influence

$h = h_1 + h_2$ = innerburden thickness;

h_1, h_2 = thickness of layer 1 and 2, respectively;

d = distance of inflection point from the rib edge.

Expanding Equation (4-7) to include n rock types, we have

$$\tan\beta = \frac{h}{d + \Sigma h_i/\tan\alpha_i} \qquad i=1,2,\ldots,n \qquad (4\text{-}8)$$

where $h = \Sigma h_i$; and h_i = thcikness of layer i.

As is the practice in both subsidence control and multi-seam mining, a percentage of hardrock is usually used to represent the geology of the overburden (innerburden). Equation (4-8) is then sufficient for most purposes if an estimate of the angle of influence for each rock type can be obtained. In a study for the Appalachian coalfield, Karmis et al. (1987) gave an estimate of 2.31±0.40 for tanβ.

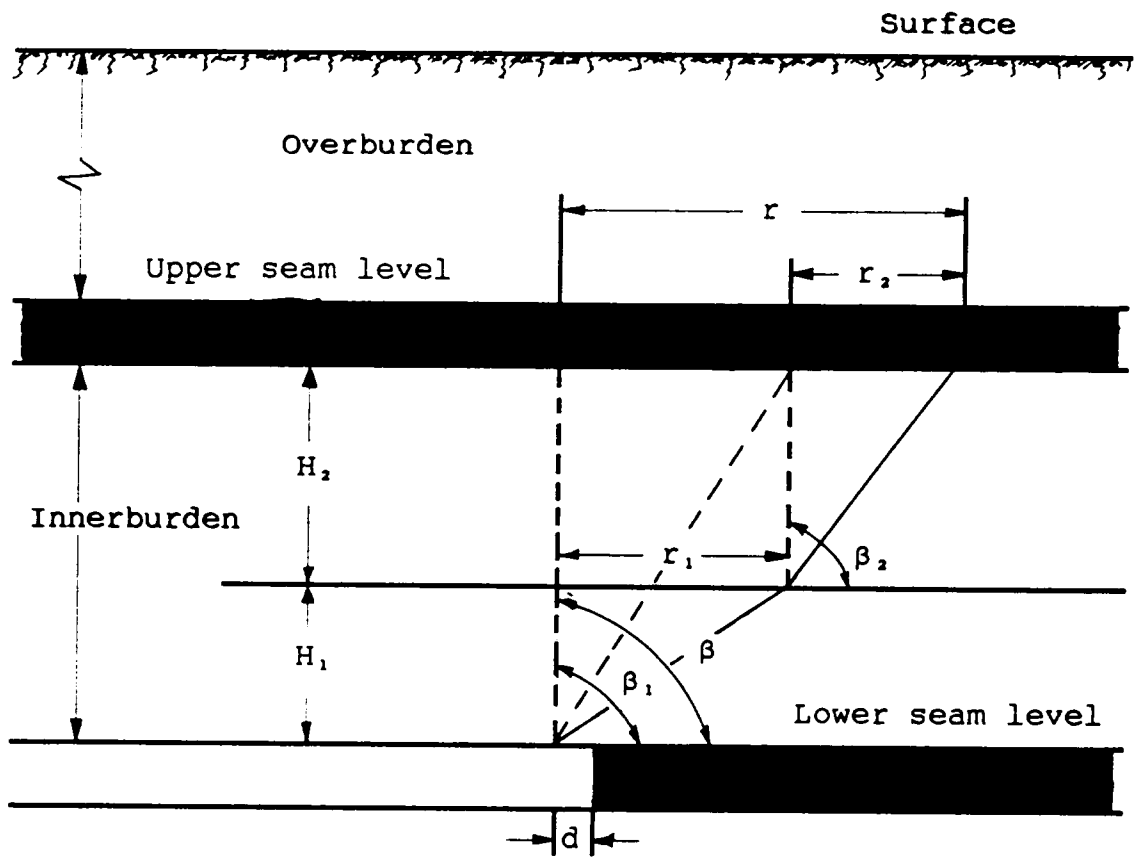

Figure 4.2 Determination of Average Angle of Influence

Location of Inflection Point: The location of the inflection point, whose offset is represented by d in Figure 4.2, is a function of the innerburden thickness (h), excavation geometry (W/H), and rock properties, and is usually expressed in terms of the innerburden thickness h. It determines the transition point from tension to compression and ultimately the width of the tension zone.

In the Appalachian region, the following empirical equation has been developed for the prediction of the inflection point location on the surface over an area extracted by either longwall or room-and-pillar methods (Schilizzi, 1987):

$$d/H = 0.29 - \frac{0.6}{W/H - 0.5}. \qquad (4\text{-}9)$$

Substituting the innerburden thickness, h, for the overburden depth, H, the offset of the inflection point for the upper seam can be estimated.

When super-critical conditions exist, which are usually the case for the upper seam in multi-seam mining situations, the inflection point becomes independent of the geometries (W/H). In a similar study (Karmis et al., 1981), the inflection point was found to be 0.20H over the gob. This corresponds to a W/H value of 1.2 in Equation (4-9). However, a larger d/H value is obtained for a greater W/H value using the same equation. The apparent

discrepancy can be attributed to the fact that geologic conditions are not included in the prediction equations. The equations described above represent the average geologic conditions, or about 30% of hardrock in the strata, based on the data presented. Taking these conditions into account, a modified equation has been developed for the prediction of the inflection point based on the above studies and on CMRI (1981):

$$d/h = 0.20 + (\eta/100 - 0.30)0.29$$
$$= 0.113 + 0.29\eta/100 \qquad (4\text{-}10)$$

where h is the innerburden thickness; and η is the percent of hardrock in the innerburden.

4.2 Mining Over Remnant Pillars

4.2.1 Pressure on Remnant Pillars

Remnant pillars left in the lower seam may create high pressure to an overlying seam, due to the continued subsidence of the strata on both sides of the pillar and to support provided by the pillar. The special feature of a remnant pillar is that abutment pressure zones on both sides of it superimpose and can form a much greater maximum pressure in the center of the pillar, if the pillar is not too wide. Therefore, remnant pillar pressure exceeds abutment pressure both in magnitude and extent of influence. The

influence of a remnant pillar on upper seam stress distributions is illustrated by the photoelastic models in Figure 4.3.

The magnitude of the strata load bearing on the pillar is governed by the size of the pillar, mining geometry, and loading angle of the strata. Any load from the undermined strata that is not taken up by the goaf (caved area) is passed as an additional load to the pillar, which may or may not be transferred to the overlying seam, depending on the strata characteristics and innerburden thickness. The pressure peak, or the pillar's absorption of pressure, is limited by the strength of the coal.

Estimation of loading conditions at the lower seam involves determination of the following parameters defining load distribution:

1. Peak stress;

2. Width of yield zone or distance into abutment at which peak stress will occur;

3. Distance into waste gob at which stress recovers to cover load or reaches a portion of cover load for subcritical conditions;

4. Distance into abutment at which stress decays to cover load.

The most commonly-accepted empirical methods for pillar-loading analysis are those developed by King (King and Whittaker, 1971) and Wilson (1972, 1983). Both theories

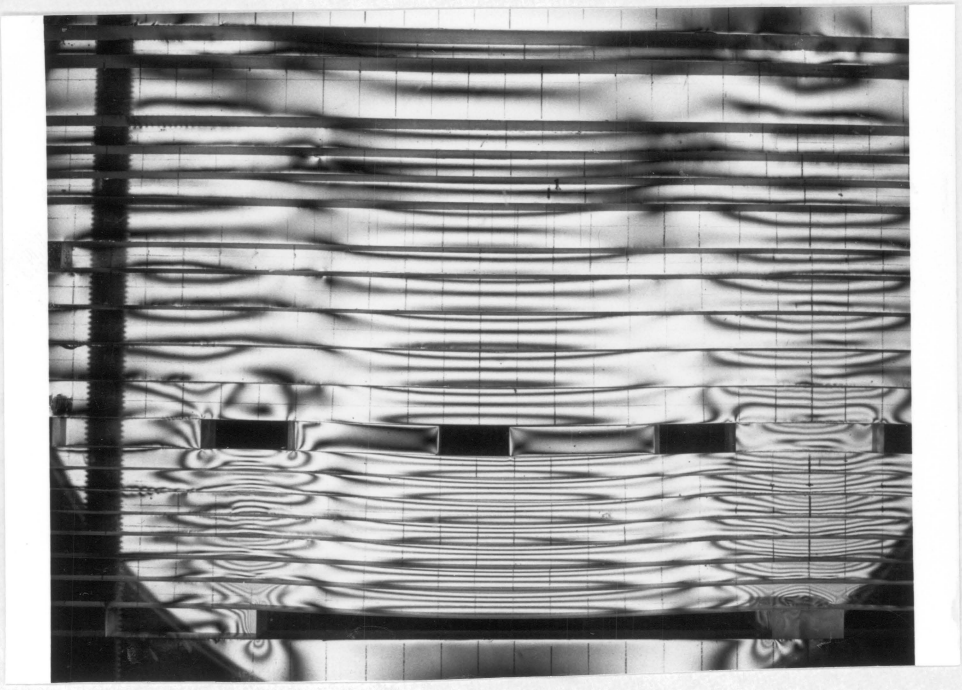

a. With Remnant Pillar

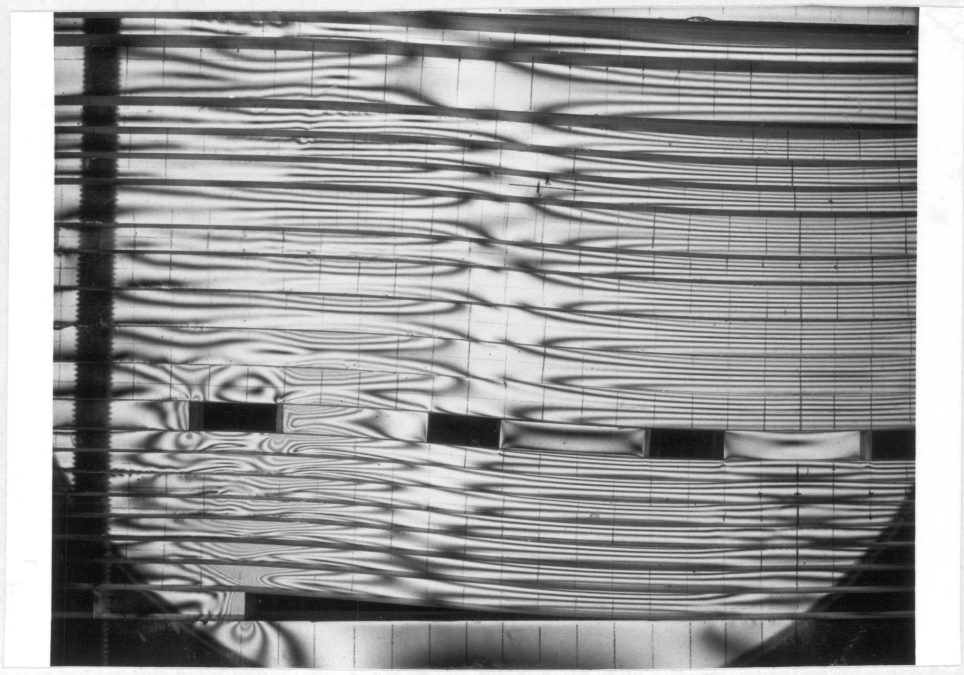

b. Without Remnant Pillar

Figure 4.3 Body-Loaded Photoelastic Models Showing the Effect of a Remnant Pillar on Upper Seam Stress Concentration

assume a constant pillar loading angle and a reloading distance dependent upon it. The angle of pillar loading, according to King and Whittaker, is equal to the angle of draw. Wilson's 17° or 0.3H distance into the gob is based on observations in U.K. coalfields, and indicates that the caving is well-behaved with the shaley overburden. The overburden in the U.S. coal regions usually contains stronger strata such as sandstone and limestone, indicating a larger angle of pillar loading. For Eastern U.S. coal seams, a value of 21° has been found to be more appropriate (Mark and Bieniawski, 1987).

4.2.2 Upper Seam Stress Concentrations

For relatively shallow mines, a simple method for estimating average stress concentrations on the upper seam over a remnant pillar has been derived by extending the theories discussed above. According to King and Wilson, the strata within the triangle or the trapezoid over the gob is assumed to be completely relieved from the remaining strata, and represents the load supported by waste while the remaining sections of the strata above are transferred to the pillars (Figure 4.4). By the principle of stress continuity over the pillars, it can be assumed that, above the lower seam level, average load can be estimated in the same manner done for pillar loading at the lower seam.

As shown in Figure 4.4, load transfer to the upper seam

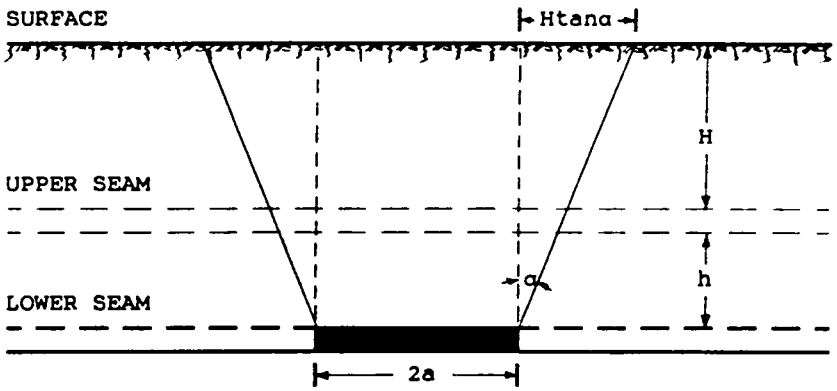

$$\ell c = 1 + \frac{H\tan\alpha}{2(a + h\tan\alpha)}$$

a. SUPERCRITICAL LOADING CONDITION ($w>(H+h)\tan\alpha$)

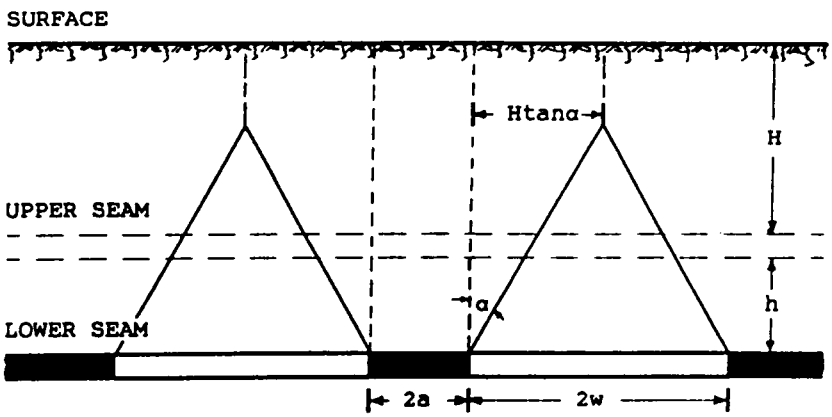

$$\ell c = \frac{1}{2H}\left[\left(\frac{w}{\tan\alpha} - h\right) + \frac{(w + a)(2H + h - w/\tan\alpha)}{a + h\tan\alpha}\right]$$

b. SUBCRITICAL LOADING CONDITION ($w<(H+h)\tan\alpha$)

Figure 4.4 Pillar Loading Conditions for Estimating Upper Seam Load Concentration

can be identified as one of two situations:

1. Super-critical, when $w > (H+h)\tan\alpha$

2. Sub-critical, when $w < (H+h)\tan\alpha$

Application of the tributary load theory, combined with the pillar loading analysis, leads to the following relationships for average load concentration in the upper seam.

- For super-critical conditions:

$$\text{l.c.} = 1 + \frac{H\tan\alpha}{2a + 2h\tan\alpha} = 1 + \frac{H\tan\alpha}{2(a + h\tan\alpha)} \quad . \qquad (4\text{-}11)$$

- For sub-critical conditions:

$$\text{l.c.} = \frac{1}{2H}\left[\left(\frac{w}{\tan\alpha} - h\right) + \frac{(w + a)(2H + h - w/\tan\alpha)}{a + h\tan\alpha}\right] \qquad (4\text{-}12)$$

where l.c. = average load concentration factor;

$2a$ = width of the remnant pillar;

h = innerburden thickness;

H = overburden thickness to upper seam;

α = angle of pillar loading;

$2w$ = panel width.

The maximum load concentration is about 1.5 times the average. The magnitude and location of load concentration on the upper seam depends on the width of the remnant pillar (2a), thickness (h) and characteristics (α) of the innerburden and overburden (H). As can be seen from Equa-

tions (4-11) and (4-12), narrow pillars tend to create higher stress concentrations than do wide pillars.

Experience has shown that the tributary load theory is no longer applicable in deep mining conditions. For this situation, modified analytical solutions for elastic foundations can be used to calculate the stress distributions when the overburden depth is large in relation to the width of remnant pillars. According to Budavari (1983), when the ratio of mining depth to the half opening width is greater than 4~5, deep-level conditions can be expected. That is, the depth of mining can be assumed to be infinite, and errors resulting from solutions based on this assumption will be negligibly small. Details of the mathematical derivations are listed in the Appendix I. Numerical integration on the computer is used in carrying out the computation. Table 4.1 lists all formulas for calculations of abutment load and related parameters which would be required for load distribution estimates at the lower seam level.

4.2.3 Strain Analysis

The effects of a remnant pillar on upper seam stability can also be evaluated by using the subsidence concept. The strain distribution at the upper seam level over a remnant pillar is usually larger than that over a gobline because of the superposition of strain from both sides of the

Table 4.1 Formulas for Calculations of Load Distribution (Adapted from Brady and Brown, 1985)

Relevant Parameters	Weak seam, strong roof and floor	Weak roof, seam and floor
Peak Stress	$\sigma_p = kp + C_o$	
Width of Yield Zone	$x_b = \frac{s}{F}\ell n(\frac{p}{p^*})$	$x_b = \frac{s}{2}[(\frac{p}{p^*})^{1/(k-1)} - 1]$
Load Carried by Yield Zone	$A_b = \frac{s}{F}k(p-p^*)$	$A_b = \frac{s}{2}p^*[(\frac{p}{p^*})^{k/(k-1)} - 1]$
Load Decay Distance	$\ell = 2C + x_b$	
Load Recover Distance		
for $W > 2D\tan\alpha$	$x_a = D\tan\alpha$	
for $W < 2D\tan\alpha$	$x_a = W/2$	
Load Deficiency		
for $W > 2D\tan\alpha$	$A_w = \frac{\gamma D^2}{2}\tan\alpha$	
for $W < 2D\tan\alpha$	$A_w = \gamma D(\frac{W}{2} - \frac{W^2}{8D\tan\alpha})$	

Definition of Variables:

k = triaxial loading factor, $= (1+\sin\phi)/(1-\sin\phi)$
ϕ = angle of internal friction
α = angle of pillar loading, equal to angle of draw
D = depth of mining
s = height of excavation
W = panel width

$F = \frac{k-1}{\sqrt{k}} + (\frac{k-1}{\sqrt{k}})^2 \tan^{-1}\sqrt{k}$, where $\tan^{-1}$ is in radians

p^* = support resistance + strength of broken material, $= ps + 14.5$ psi
p = original vertical stress, $= \gamma H$

$C = \frac{A_w + px_b - A_b}{\sigma_p - p}$

C_o = in situ uniaxial compressive strength of the strata

pillar. From Equation (4-4), the strain can be calculated for each side of the pillar, with the total strain being the sum of the two:

$$\varepsilon(x) = \varepsilon(x_1) + \varepsilon(x_2). \tag{4-13}$$

If the distance from the center of the pillar is defined as x, then

$$\varepsilon(x) = 2\pi b \frac{S_{max}}{r}\left[-\frac{x-B-d}{r}\right)e^{-\pi\left(\frac{x-B-d}{r}\right)^2} + \frac{x+B+d}{r}\, e^{-\pi\left(\frac{x+B+d}{r}\right)^2}\Bigg] \tag{4-14}$$

where B = half pillar width = 1/2PW; b = strain factor, usually 0.3 for flat seams; r = influence radius, H/tanβ; d = distance of inflection point from pillar edge; x = distance from the center of the pillar.

Maximum strain occurs when the masimum strains from both sides of the pillar superimpose, i.e., when B satisfies the following equation,

$$B = 0.41r - d.$$

As for the location of maximum strain given B, maximum strain occurs when

$$\frac{\partial \varepsilon(x)}{\partial x} = 0.$$

That is, when x satisfies the following equation:

$$\ell n\left[\left(2\pi\left(\frac{x-B-d}{r}\right)^2-1\right)/\left(2\pi\left(\frac{x+B+d}{r}\right)^2-1\right)\right]=-\frac{4\pi(B+d)}{r^2}x \quad . \qquad (4\text{-}15)$$

In this equation x can be numerically solved on a computer.

The distinction made between wide and narrow remnant pillars can also be seen from the strain distributions. Figure 4.5 shows the horizontal strain at the upper seam level as a function of the remnant pillar width. When pillar width is greater than 4r-2d, supermposition of strains from the two sides of the pillar ceases to exist. Maximum tensile strain occurs when pillar width is equal to 2r-2d. Strain superimposition still exists for a pillar width of less than 2r-2d, but maximum strain is no larger than the maximum induced by one abutment (side) of the remnant pillar. Naturally, when pillar size is so small that the overburden pressure will crush the pillar, the effect produced by the remnant pillar may be negligible. It can be seen that this analysis agrees well with the results based on lower seam pillar-loading conditions.

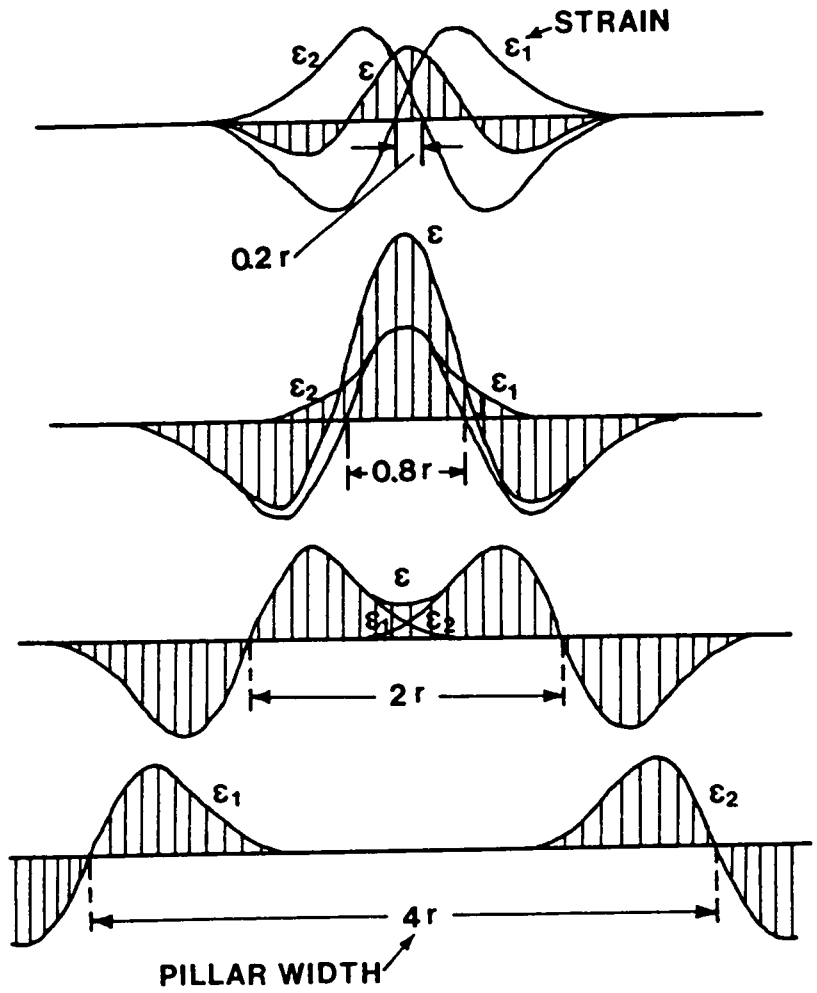

Figure 4.5 Relationship Between Width of Remnant Pillar and Upper Seam Strain Distributions

4.3 Mining Over Gob Line Interfaces

4.3.1 Subsidence Wave and Strata Movement

The effects of trough subsidence on the upper seam can be viewed from the various zones that are created during the subsidence process (Figure 4.6). As the panel advances in the lower seam, the upper seam will experience a subsidence wave. This wave constitutes a tension zone near the front line of the lower seam, followed by a zone of lateral compression, sometimes accompanied by shearing. In some strata structures, if the innerburden is comprised of massive and strong rock such as sandstone, the cantilever action assumed by the innerburden against the strata's tendency to subside will create some stress concentrations in areas beyond the gob line and towards the boundaries of the trough. The result is not only a highly fractured and destressed zone in the identified tension zone, but also a stress concentration zone outside of the identified tension zone due to load transfer. This explains why, in many case studies, high ground pressure is often recorded at a distance from the gob line. The thickness and geological features of the innerburden are important parameters controlling the magnitude of strain and the width of the tension zone.

As shown in Figure 4.6, the subsidence at the top edge of the layer immediately above the coal seam (level 1) is

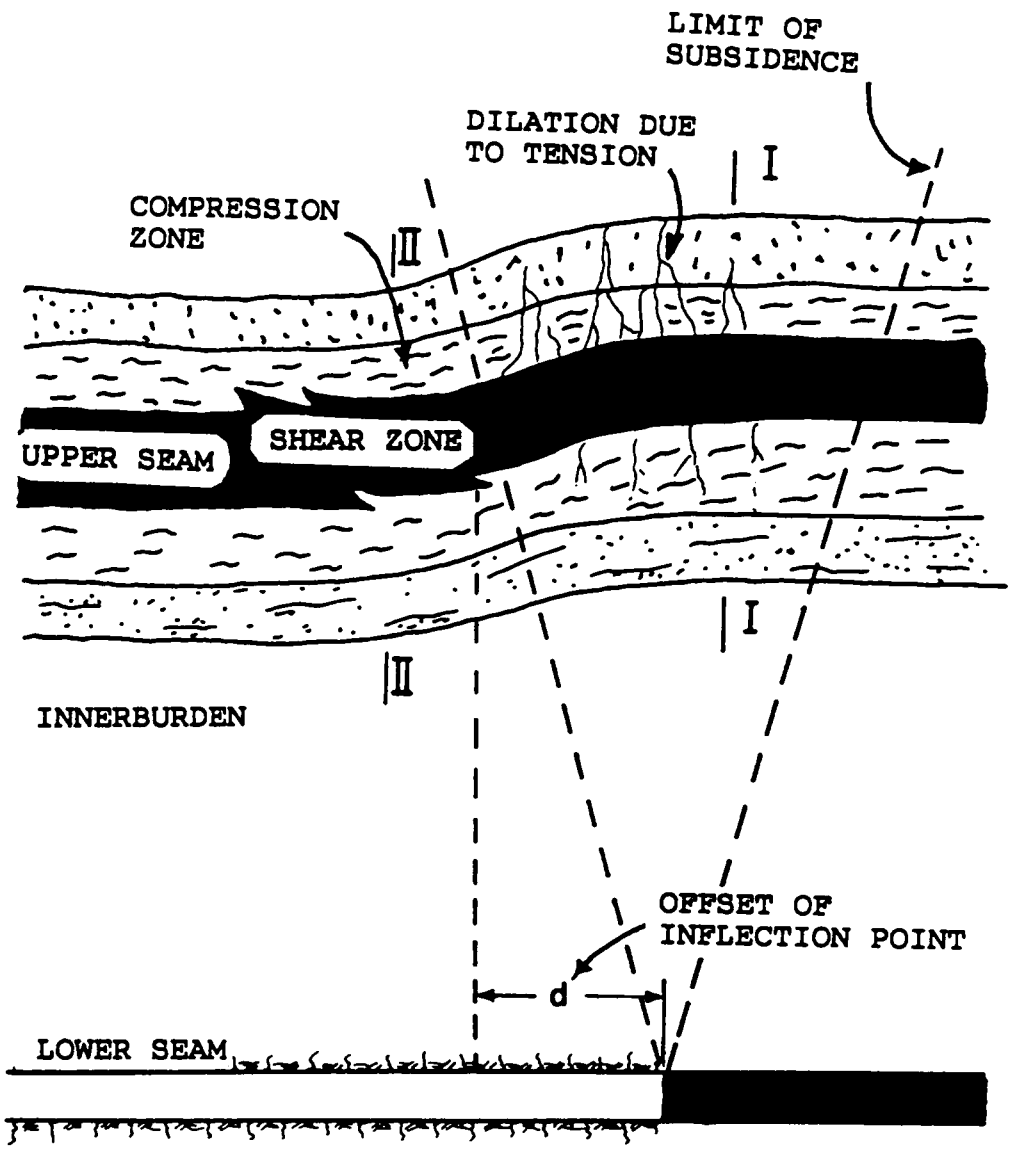

Figure 4.6 Subsidence Wave and Strata Movement after Mining of Lower Seam

greater than that at the bottom edge of the layer immediately below the coal seam (level 2) for Section I-I. The reverse is true for Section II-II. The dividing line is the line which connects the inflection point of each level. It is then not difficult to conclude that Section I-I of the strata, or the coal seam, is undergoing vertical compression, and that Section II-II of the strata is undergoing vertical tension. It is also known from section 4.1 that the strata between the inflection point and the trough boundary are undergoing horizontal tension and the strata on the other side of the inflection point is undergoing compression, horizontally. Therefore, the complete state of strata conditions above the gob line area is known.

4.3.2 Tensile Strain and Tension Zone

The most detrimental effect of the subsidence wave is the tension it creates, because most coal measure rocks have very low inherent tensile strengths (practically zero). If substantial tension is identified, the rock is expected to be completely dilated, and a stress-relief zone is created if load can be shed onto unbroken rocks (Figure 4.6). Therefore, the application of the subsidence concept to overmining analysis involves determination of two critical parameters: the width of the various zones, expecially that of the tension zone, and the magnitude of the tensile strain (Figure 4.7).

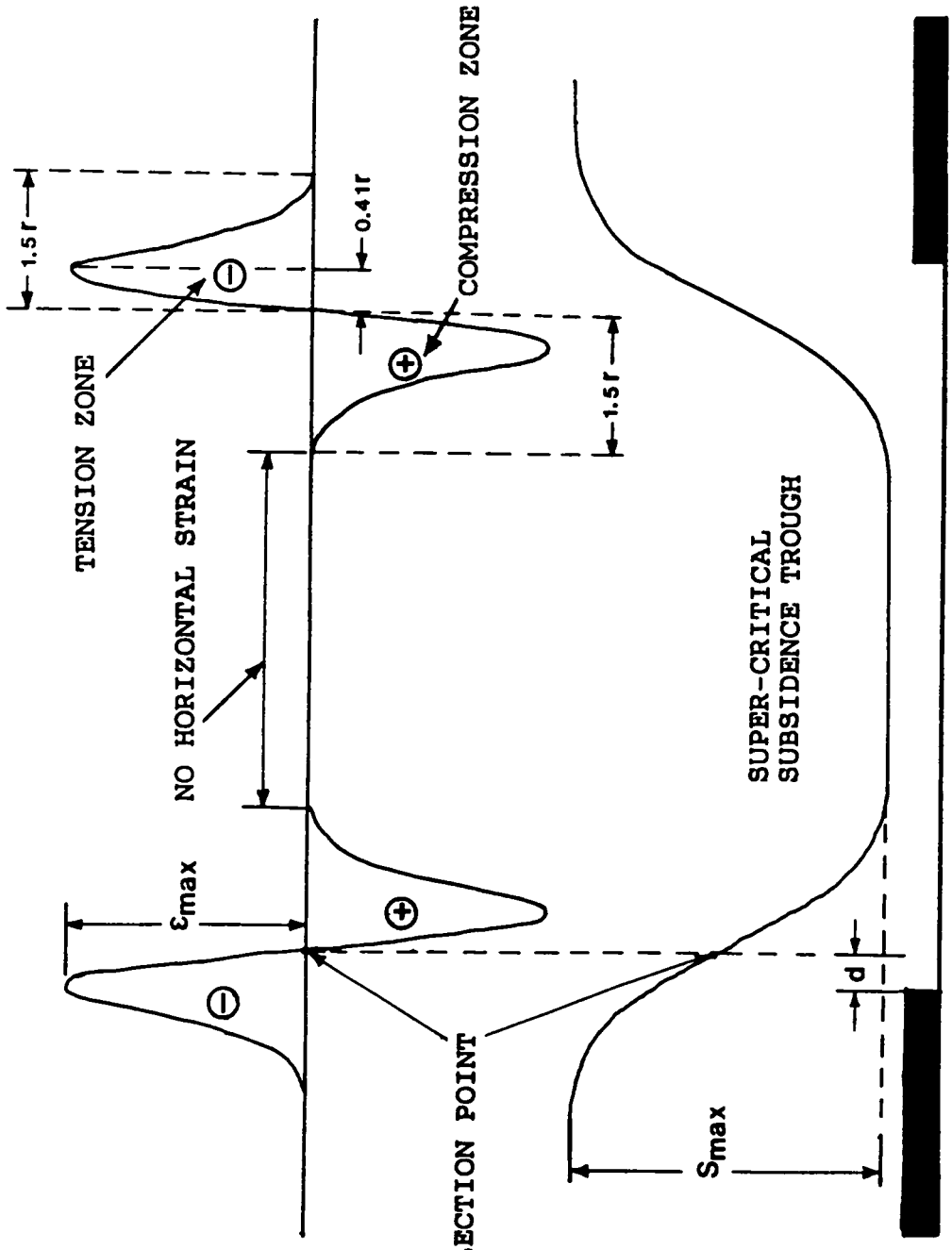

Figure 4.7 Use of Subsidence Theory to Determine Critical Areas in Upper Seam

It has been shown that the inflection point determines the transition from tension to compression. Extending from the inflection point in both directions, the boundaries of both the tension zone and the compression zone is at approximately 1.5r based on numerous computations and field observations, where r = h/tanβ is the influence radius.

Tensile strain (or compressive strain) is given by Equation (4-2). The maximum tensile strain at the upper seam level is given by:

$$\varepsilon_{max} = 1.52b\frac{Smax}{r} \text{ , } (1/1000) \qquad (4\text{-}16)$$

occurring at 0.41r from the point of inflection in the direction of the trough boundary.

Equation (4-16) can be rewritten as:

$$\varepsilon_{max} = 1.52\frac{as}{h/tan\beta} = 1.52b\frac{a}{h/s}tan\beta$$

$$= 1.52b\frac{a}{M\text{-}index}tan\beta \qquad (4\text{-}17)$$

where M-index = h/s; a = subsidence factor.

Using Equation (4-17), a strain chart is generated for tanβ=1.0 (Figure 4.8). For values of tanβ other than 1.0, the maximum strain is obtained be multiplying the value of tanβ by the strain value from the chart.

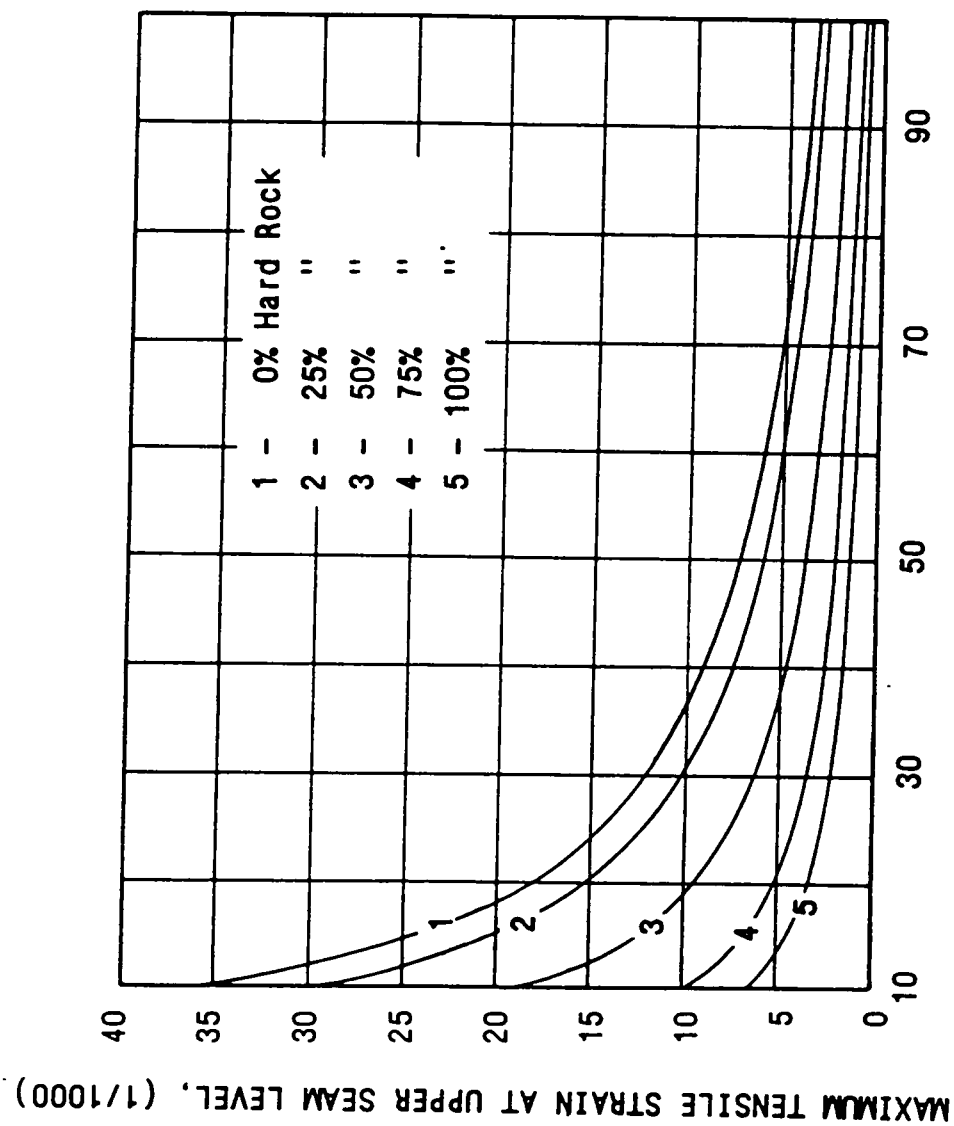

Figure 4.8 Estimated Maximum Upper Seam Tensile Strain as a Function of M-Index and Rock Properties

4.4 Interseam Shear Failure

4.4.1 Interseam Failure under Normal Condiditons

Interseam failure results from the mining of an underlying seam, usually when the parting distance is less than 33 feet (Barko, 1982) and the innerburden is comprised of brittle-type rocks. The conditions for interseam shear failure are also critically affected by opening widths and by uniformity of extraction in the lower seam. In some extreme cases, such failure can extend through to the surface, as shown in Figure 2.3, cutting off large sections of coal. If the height of caving is given by the following equation:

$$h_c = \frac{h_s}{K - 1} \qquad (4\text{-}18)$$

where h_c is the height of caving, h_s is the mining height, and K the bulking factor under pressure, then h_c will extend to the surface when K approaches unity.

If the innerburden is well separated from the upper seam and caving does not occur, complete extraction of the lower seam will leave the innerburden in a clamped beam condition. In this case, the stability of the innerburden against shearing can be analyzed by comparing the maximum shearing stress and shear resistance mobilized by the innerburden. From the theory of elasticity, the maximum

shear stress in a clamped beam is given by:

$$\tau_{max} = \frac{3qL}{4t} \qquad (4\text{-}19)$$

wherq is the distribution load; L is the beam span; and t is the beam thickness.

For an innerburden composed of multiple layers, the innerburden can be treated as a composite beam (Figure 4.9). Assuming that the deformation curves of all individual layers are compatible, the weight density of the beam is adjusted to take into account the fact that a strong layer overlain by a weaker one will be loaded by a part of the weight of the weaker layer as well as that of itself (Merril, 1958). The adjusted weight density is given by:

$$q_n = \frac{E_1 h_1^3 (\gamma_1 h_1 + \gamma_2 h_2 + \ldots + \gamma_n h_n)}{E_1 h_1^3 + E_2 h_2^3 + \ldots + E_n h_n^3} \qquad (4\text{-}20)$$

where q_n is the adjusted weight density; E_i is the Young's Modulus for layer i; h_i is the thickness of layer i; and γ_i is the unit weight of layer i.

In actual computation, the contributing load is calculated upwards, including first one layer (n=1), then two layers (n=2), and so on until the calculated load q_{n+1} is smaller than q_n. The layers above the nth layer do not influence the load distribution. Using this procedure, the maximum shear stress can be calculated for each layer. The

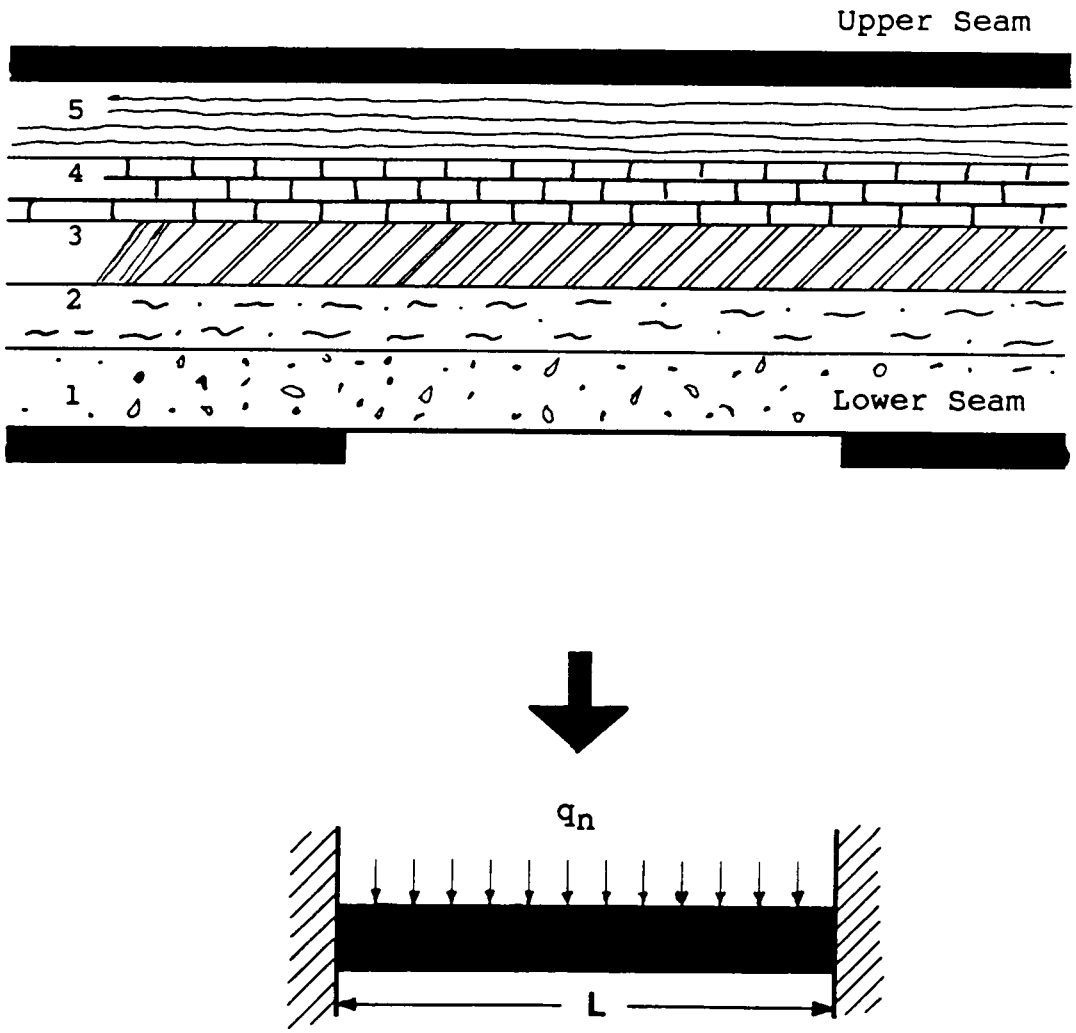

Figure 4.9 Multi-Layered Innerburden as a Composite Beam

resulting maximum shear stress is then compared with the shear strength, given by the Mohr-Coulomb criterion:

$$\tau_s = C + \sigma_n \tan\phi \qquad (4\text{-}21)$$

where τ_s = shear strength of rock material; C = cohesion of rock material; σ_n = normal stress on the failure plane; and ϕ = angle of internal friction.

4.4.2 Interseam Failure Resulting from Weak Planes

In addition, an innerburden with geologically weak planes such as faults may also be subject to this type of failure. In the case of a fault plane being disturbed by the removal of the lower seam, there may be a sudden dislocation of the workings due to reactivated fault movements (Figure 4.10). The determining factors are the stress field and characteristics of the fault plane, including those of any filling material.

The stability, or shear resistance of such a fault plane, is adequately described by the Mohr-Coulomb criterion, modified to take into account the effect of pore pressure (Sibson, 1977):

$$\tau_f = C + \mu(\sigma_n - P_f) \qquad (4\text{-}22)$$

where τ_f = shear resistance; C = cohesion of fault plane; μ = coefficient of friction; σ_n = normal stress on the fault plane; and P_f = pore pressure.

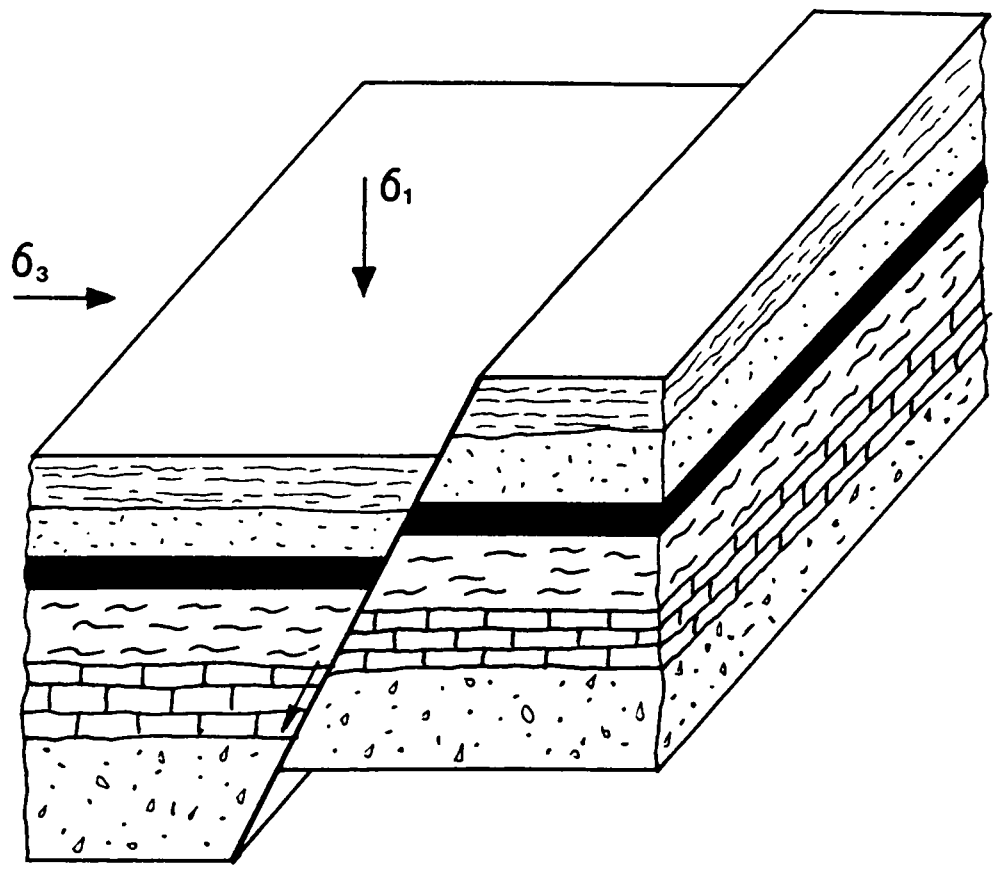

Figure 4.10 Intensified Dislocation of Upper Seam due to Reactivated Fault Movement

A second failure related to weak planes, with a smaller scale of influence, is a well-separated fault plane cutting off the entire innerburden. When the lower seam is removed to a certain extent, the innerburden fails as a hanging beam clamped at one end and free at the other (Figure 4.11a). Protection against such a failure can be achieved by leaving a large pillar (or a group of pillars) at the intersection between the fault plane and the lower seam, as shown in Figure 4.11b.

4.5 Caving and Pressure Arch

4.5.1 Arching Mechanism

As has been reviewd in Chapter 2, many theories have been developed concerning pressure archs. The most fundamental concept for the formation of a pressure arch is the fact that rock structures can support themselves by redistributing the ground pressure - a process known as load transfer. As an opening is created, the origianl stress state is disturbed and a stress redistribution results. If the roof (or pillar) can still sustain the concentrated stress, no arch will be formed. When the roof fails, either in tension or shearing, the strata will cave onto the gob, separating the failed roof material from the remaining strata. An arch is formed when load is shed onto solid abutment or onto caved but compacted waste material,

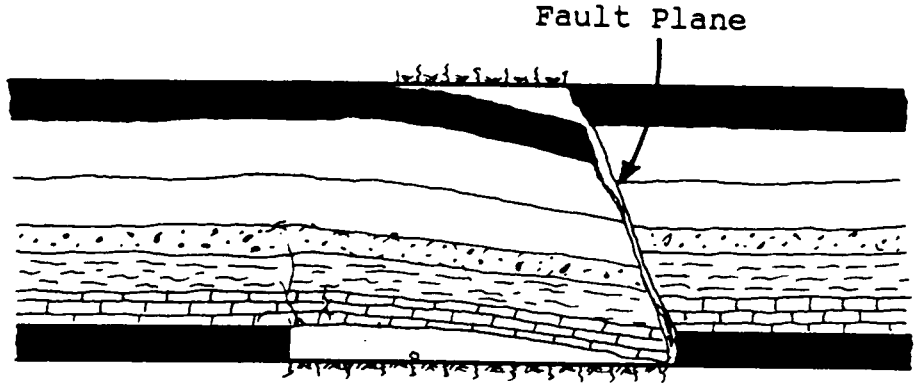

a. Interseam Failure Along a Fault Plane

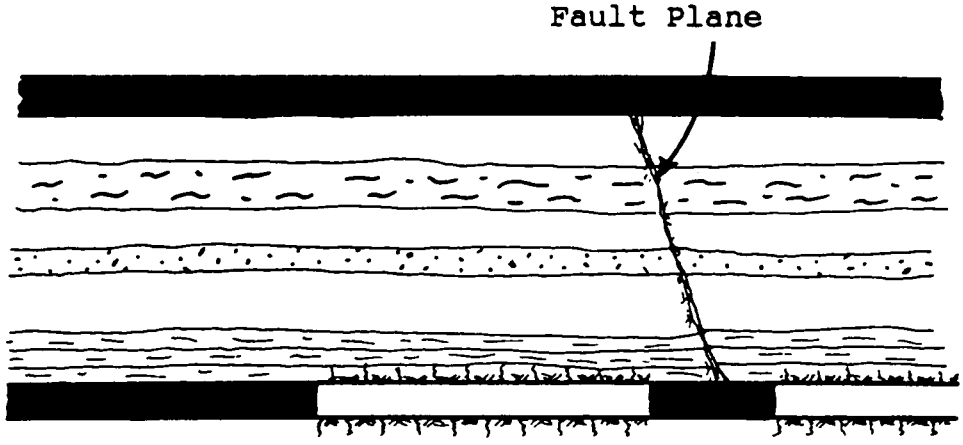

b. Protection Against Interseam Failure
Near a Fault Plane

Figure 4.11 Interseam Failure Resulting from Geologically Weak Planes and Protection Against Same

creating zones of stress relief and stress concentration.

Caving and arching are two closely related strata movements. In fact, it is the caving and sagging of the strata above the gob that creates the pressure arch. The effects on an overlying seam are dependent on the relative location of mining in the upper seam with respect to the arch geometry and the height of caving/fracturing.

4.5.2 Extent of Effects on Upper Seam

While the height of the pressure arch or caving limits the vertical extent of interaction, the width of the pressure arch determines the horizontal extent.

The height of caving and fracturing zones follows a geometric function of the height of mining based on extensive field measurements, given by the following equation modified from Peng (1983):

$$h_{c,f} = \frac{100h}{ah + b} \pm c \qquad (4\text{-}23)$$

where hc,f = height of caving or fracturing (ft.); h = height of mining, (ft.); and a, b, c = constants characteristic of strata properties.

Table 4.2 lists the values of the corresponding constants, a, b, and c.

The two critical parameters defining an arch are the arch width and arch height. If either the opening width is

Table 4.2 Constants for Calculating Caving and Fracturing Height (After Peng, 1983)

Rock Type	Caving Zone			Fracturing Zone		
	a	b	c	a	b	c
Hard	0.640	16.0	8.2	0.366	2.0	29.2
Medium Hard	1.433	19.0	7.2	0.488	3.6	18.4
Soft	1.890	32.0	4.9	0.945	5.0	13.1
Weathered	2.134	63.0	3.9	1.524	8.0	9.8

$$h_{c,f} = \frac{100h}{ah + b} \pm c, \text{ feet}$$

h - Height of mining, feet

greater than the maximum width or the depth of mining less than the arch height, no arch will be formed although there will still be load transfer along an arch-shaped path. Arch shapes, as described in hapter 2, can be in the form of an ellipse, a circle, or a parabola, with the most commonly-used form being parabolic.

Using the load transfer concept, the maximum width of the pressure arch is two times the load transfer distance (LTD), which is given by:

$$LTD = -848 + 159\ell n(D) \qquad (4\text{-}24)$$

where D is depth of mining of the lower seam in feet.

The height of the pressure arch can be derived as follows (Figure 4.12).

Assume a parabolic function:

$$y'^2 = 2px'.$$

The tangential line MT to the parabola at (d, w/2) has the function:

$$y' = \frac{p}{y'_o}(x' + x'_o) = \frac{p}{y'_o}x' + \frac{p}{y'_o}x'_o.$$

The slope of line MT is then p/y'_o, and

$$\frac{p}{y'_o} = \tan\alpha$$

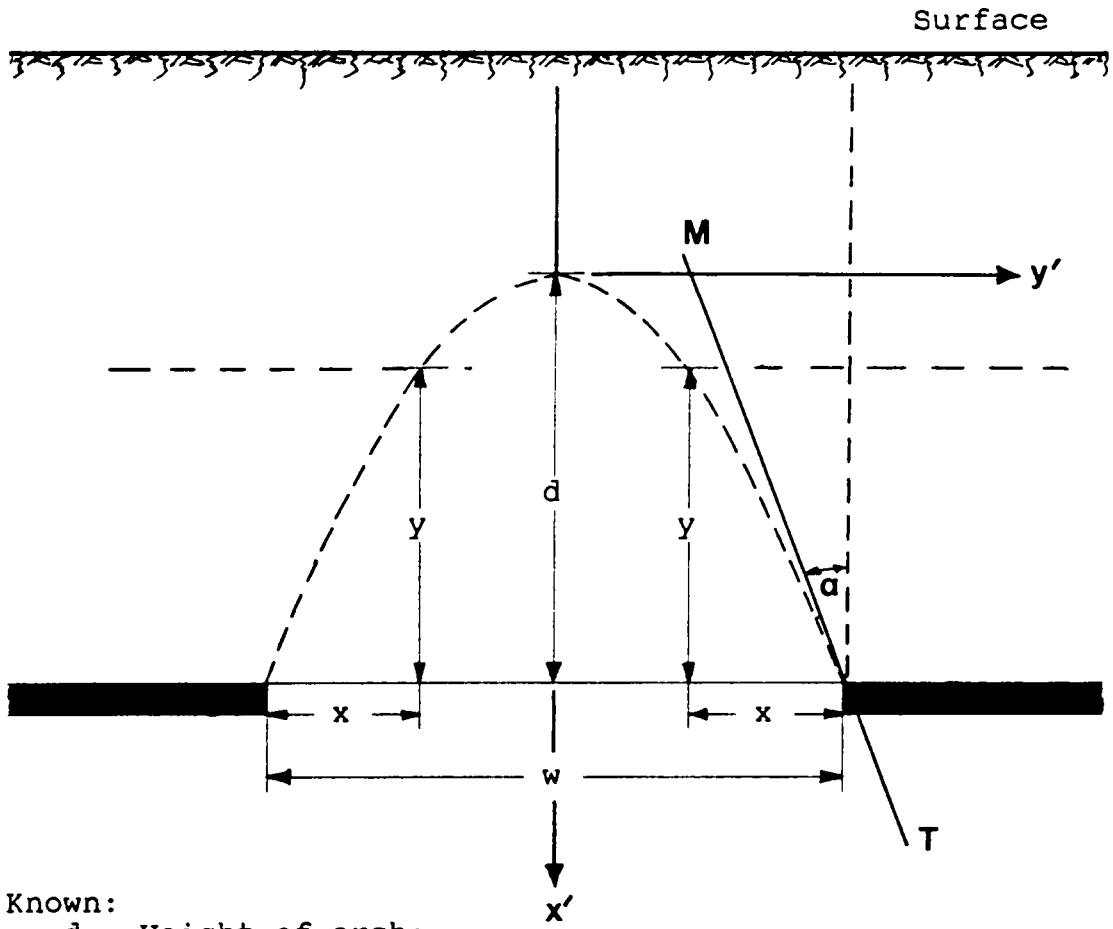

Known:
d = Height of arch;
w = Width of arch;

Find:
x = Horizontal distance from abutment edge;
y = Vertical distance from seam level.

Assume:
Parabolic form of arch.

Equation of a parabola:

$$y = \frac{d}{w^2}\left[w^2 - (w-2x)^2\right]$$

$$x = \frac{w}{2}\left(1 - \sqrt{1-y/d}\right)$$

Figure 4.12 Interaction Effects due to Pressure Arching and Determination of Arch Geometry and Critical Areas

or

$$p = y'_o \tan\alpha.$$

At the abutment edge ($x'_o=d$, $y'_o=w/2$), the slope of the tangential line should coincide with the tangent of the pillar loading angle $\tan\alpha$.

Therefore, the arch is completely defined by the equation:

$$y'^2 = 2px' = 2(\frac{w}{2}\tan\alpha)x' = (w\tan\alpha)x'$$

Now, let $y' = w/2$. Substituting and solving, we have

$$x'\Big|_{y'=w/2} = d = \frac{w^2/4}{w\tan\alpha} = \frac{w}{4\tan\alpha}$$

Therefore,

$$d = \frac{w}{4\tan\alpha} \qquad (4\text{-}25)$$

Thus, the height of the pressure arch is determined by the opening width (w) and the rock properties ($\tan\alpha$). It must be noted that if the arch height from Equation (4-25) is greater than the depth of mining, it must be concluded that no arch will be formed.

Once the height of the pressure arch is determined, the

path of the pressure arch at the upper seam level can be obtained by the equation (Figure 4.12):

$$x = \frac{w}{2}(1 - \sqrt{1-y/d}) \qquad (4\text{-}27)$$

where x = distance from the ribside; y = distance from the lower seam; and other variables as defined previously.

Influenced areas in the upper seam can thus be determined by the parameters associated with caving, fracturing and the pressure arch.

V. GEOMECHANICS CLASSIFICATIONS

Because of the diversity and variations of geology and of the structural settings in coal deposits, it is often difficult to quantify many critical geologic factors in ground control. Consequently, most are ignored in quantitative evaluations, although many play a very important role in upper seam stability and are actually in many cases the dominating factors. This chapter develops a roof-rating system for multi-seam mining to incorporate these geologic factors.

5.1 Basic Considerations for Classification

When mining over a previously-mined seam, trough subsidence, arching and block-shear mechanisms can be used to evaluate the effects of interaction between seams. Applications of these mechanisms have met with varying degrees of success for prediction of interaction damage. Studies relating upper seam damage to strata subsidence, for exmaple, have demonstrated considerable variation. These variations are attributable in large part to a complex interaction between geologic and mining factors. To develop a realistic model for multi-seam mine design, it is essential to incorporate the many geologic and mining factors involved in multi-seam mining. A roof-rating system

is especially needed for multi-seam mining operations during overmining. The rating system must be based on two basic considerations, geologic and spatial, and must include factors commonly found in geomechanics classification systems as well as factors which are peculiar to multi-seam mining. Geologic factors describe the strata characteristics and the structures under consideration, while spatial factors define the geometric locations and orientations of upper seam structures with respect to the subsidence trough, lower seam remnant structures and geologic discontinuities.

It is conceivable that some factors will have a more prominent effect on interaction and roof stability than others. For example, the location of the roof structure under consideration is usually more important than ground water in terms of interactive effects on the upper seam. This fact is taken into account by assigning different weights to the various factors. The precise weighting can be determined based on sources such as:

1. Existing classification systems;
2. Statistical analysis of case studies;
3. Engineering Experience.

Supposing there are n factors under consideration, then the weight each factor receives must satisfy the following condition:

$$\sum_{j=1}^{n} w_j = 1 \qquad (5\text{-}1)$$

where w_j = weight of each factor on roof stability.

For example, the spatial location Type R & G can be seen from Table 3.5, i.e. when mining in areas over remnant pillars or gob line areas, to be the most troublesome. Of the 57 cases of Type R & G, 48 cases, or 84.2%, showed appreciable damage while of the 36 cases of Type X, only nine cases, or 25%, showed appreciable damage. Since 25% of the cases in areas of Type X recorded damage, it can be assumed that on the average, damage rate is 25% without location effect. Then of the 57 cases in Type R & G, 57(.25)=14.3 damage cases can be assumed to be without the effects of spatial location. Therefore, only (48-14.3)=33.7 damage cases were associated with the effects of location, which gives as percentage:

$$\frac{48-57(0.25)}{57} = .574 = 57.4\%$$

This number will serve as a guide when assigning a weight to the location factor. On the other hand, a very favorable rating of the M-Index will almost offset the effects of spatial location, which should provide an indication as to the weight of the M-Index.

It should also be noted that any disturbance caused by

mining of the lower seam will intensify the effects of unfavorable geologic discontinuities.

5.2 Effects of Major Factors in Multi-Seam Mining

Four distinct types of factors in multi-seam mining are the elapsed time since mining of the lower seam, spatial location of the roof structure, the M-index, and the condition and orientation of geological discontinuities. These factors are extremely important in determining the magnitude of interaction effects. The following is a discussion of how these factors and others affect the basis of the rating system.

5.2.1 Time Factor

The effects of time are reflected in whether the interaction is purely active, active/passive, or purely passive. These interaction states are defined as bwing when:

1) Undermining is currently active or concurrent with upper seam mining, a purely active condition;
2) Undermining is complete but the ground is still in the process of settling, an active/passive condition;
3) Undermining is complete and the ground has settled, reaching a new state of equilibrium, a purely passive condition.

Conceptually, if I_i is defined as an interaction func-

tion, then for the three states of interaction, I_i will be:

$$I_1 = f_1(x_1,x_2,\ldots,x_k,t,s)$$
$$I_2 = f_2(x_1,x_2,\ldots,x_k,t)$$
$$I_3 = f_3(x_1,x_2,\ldots,x_k) \qquad (5\text{-}2)$$

where $x_1,x_2,\ldots,x_k$ = the geologic and mining variables; t = time after beginning of mining of the lower seam; s = sequencing factor in simultaneous mining.

Case studies and statistical analysis presented in Chapter 3 have shown that, in most situations, a period of two years proves to be adequate, although in some instances it may take five, ten, or even fifteen years for the strata to settle. The effects of time factor on interaction and the use of time in interaction prediction have already been discussed in Chapters 2 and 3 (see also Figures 2.7 and 3.6).

5.2.2 Spatial Locations

Chapter 3 has identified the location of mining with respect to lower seam structures as being one of the most important factors affecting interaction in multi-seam mining. The effect of spatial location is most noticeable when the innerburden distance between the two seams is relatively small. As demonstrated in Chapter 4, superimposition of strain and pressure from both sides of a remnant pillar increase the intensity of disturbance. Upper seam

damage is normally concentrated in the tension zone created over gob/coal interface areas by trough subsidence.

To incorporate the effects of the spatial location factors into the classification system, the upper seam is divided into different zones according to their location relative to the subsidence trough and the remnant pillars. In trough subsidence, three zones are identified: the tension, the compression, and the no-strain zone, as shown in Figure 4.7. Narrow pillars tend to create more severe problems than do wide pillars because a) narrower pillars create higher stress concentrations at the lower seam level and thus transfer higher stresses to the upper seam level; and b) superposition of tensile strains from the two edges of a pillar gives rise to higher strains than do wider pillars. Structures over very wide pillars can be treated as if they were located over abutments because interaction between the two edges of the pillar no longer exists. Entries placed inside the destressed zone over gob areas will experience relatively few problems.

5.2.3 M-Index

To take into account the effect of the innerburden thickness and of the mining height, the M-index is used for classification. The M-index determines whether upper seam mining is located in the caving zone, the fracturing zone, or the subsidence zone. This relative index is a better

measure than is the absolute value of the innerburden thickness because, for a constant innerburden thickness, a larger lower seam extraction height (smaller M-index) is more likely to cause interactions than is a smaller one. Furthermore, a seam lying very close to the lower seam will most likely be in the caving zone, and thus will almost certainly undergo severe damage. Using an average minimum bulking factor of 1.1 (under pressure), the caving height in terms of lower seam thickness can be given as

$$\frac{h_c}{h_s} = \frac{1}{1.1-1} = 10$$

This indicates that when the M-Index is less than 10, severe damage is almost certain to occur in the upper seam. This analysis also agrees well with the nomogram shown in Figure 2.7. From Figure 2.7, it can be seen that when the M-index is less than 10, the damage factor is always less than -100, indicating severe damage.

5.2.4 Geological Discontinuities

Discontinuities here refer primarily to joint sets in the roof. A highly-jointed roof will almost invariably cave after coal is extracted. The determining factors for instability are the spacing, length and orientations of the joints in relation to the upper seam layouts.

The effect of these joint sets is further manifested in

multiple-seam mining. This manifestation results from the fact that roof structures, with the presence of geological discontinuities which are oriented in unfavorable directions, are very prone to the tension and high rock pressure created by the subsidence of the strata and load transfer. As an example, Figure 5.1 shows two extreme cases of orientation of the joint set with respect to the subsidence trough. Case (a) is the worst possible combination because the strike of the joint system is parallel to the direction of the trough, and the tension is exerting the greatest negative effect on the joints. For the same reason, case (b) is the best possible combination, as far as the direction of the joint set and that of the subsidence trough are concerned.

Rating of the geological discontinuities is based on Bieniawski's (1983) Rock Mass Rating system with modifications introduced by Grenoble (1985). Table 5.1 lists the weights assigned to different strike-dip combinations. According to Grenoble (1985), an influence coefficient is assigned to each joint set in the roof by the calculation:

$$JIC = (EFAC)(DFAC) + SFAC \qquad (5\text{-}3)$$

where JIC = joint influence coefficient; EFAC = $1/\cos(\theta)$; θ = angle between the joint and the normal to the strike of the entry (deg.); DFAC = weight factor due to the dip; SFAC = weight factor due to the spacing.

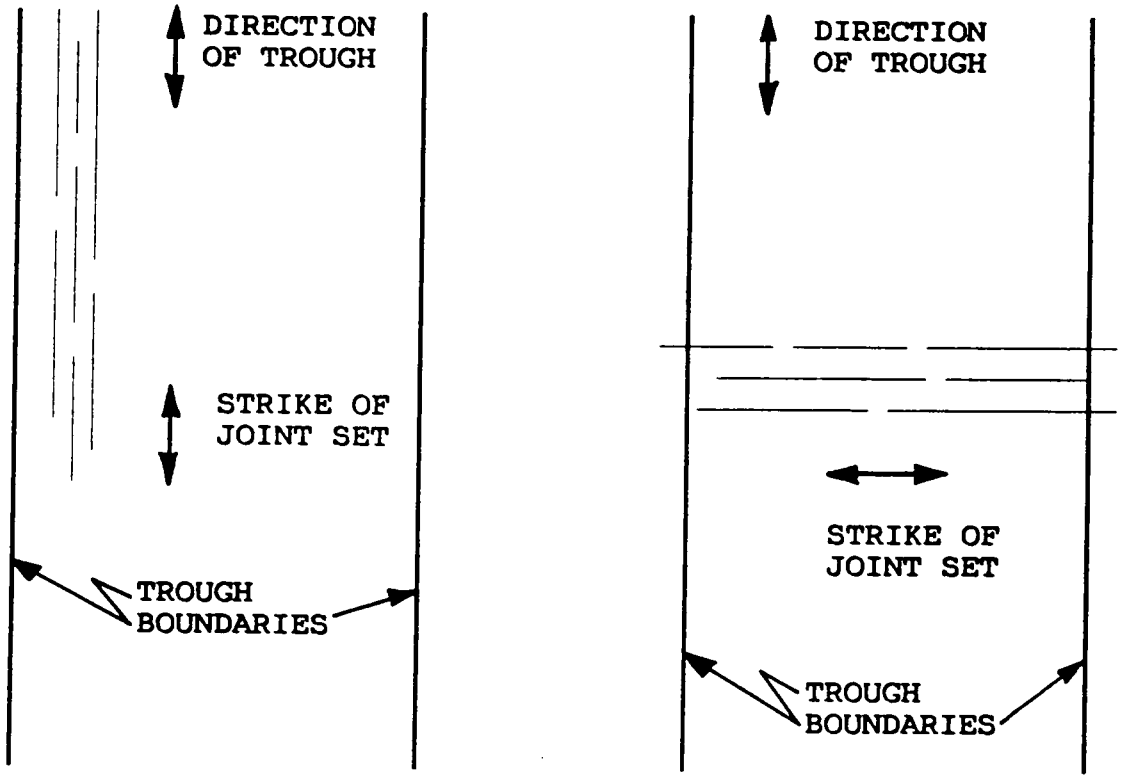

a) Worst possibel direction combination of joints and subsidence

b) Best possible direction combination of joints and subsidence

Figure 5.1 Possible Combinations of Joint Orientation with Respect to Subsidence Trough

Table 5.1 Weights Assigned to Different Strike/Dip Combinations (Bieniawski, 1983)

Strike perpendicular to tunnel axis				Strike parallel to tunnel axis		Dip 0-20° Perpendicular/ parallel
Drive with dip		Drive against dip				
Dip 45-90°	Dip 20-45°	Dip 45-90°	Dip 20-45°	Dip 45-90°	Dip 20-45°	
Weight						
1	2	3	4	5	3	4/2

SFAC is 0.5 when the ratio of opening width-to-joint spacing is between 1 and 2, and is 1 when this ratio is greater than 2. A large JIC indicates that the joint set is likely to cause problems while a low value means that the joint will have little influence on roof stability. Figure 5.2 shows a nomogram for estimating JIC.

5.2.5 Other Factors

There are other factors which mainly affect the behavior of roof structures. Classification of the distance to the first competent strata is based on the studies performed by Ealy et al. (1979) and on a roof-rating system proposed by Kester and Chugh (1980). Rock structures constituting the immediate roof are classified according to study results by Moebs, Ellenberger, and others (1982) on the relationship of geology to mine-roof conditions. Geologic structures such as paleochannels, scours, slickensides, and clay veins are not uncommon in the Appalachian region, and have been identified as to contributing to roof falls (Moebs and Ellenberger, 1982). These structural anomalies, especially under the influence of strata subsidence, constitute a discontinuity in the upper seam roof and pose a potential hazard.

The rating of ground water is usually based on the amount of water or joint water pressure and the sensitivity of the rock to moisture. It should be noted that, in over-

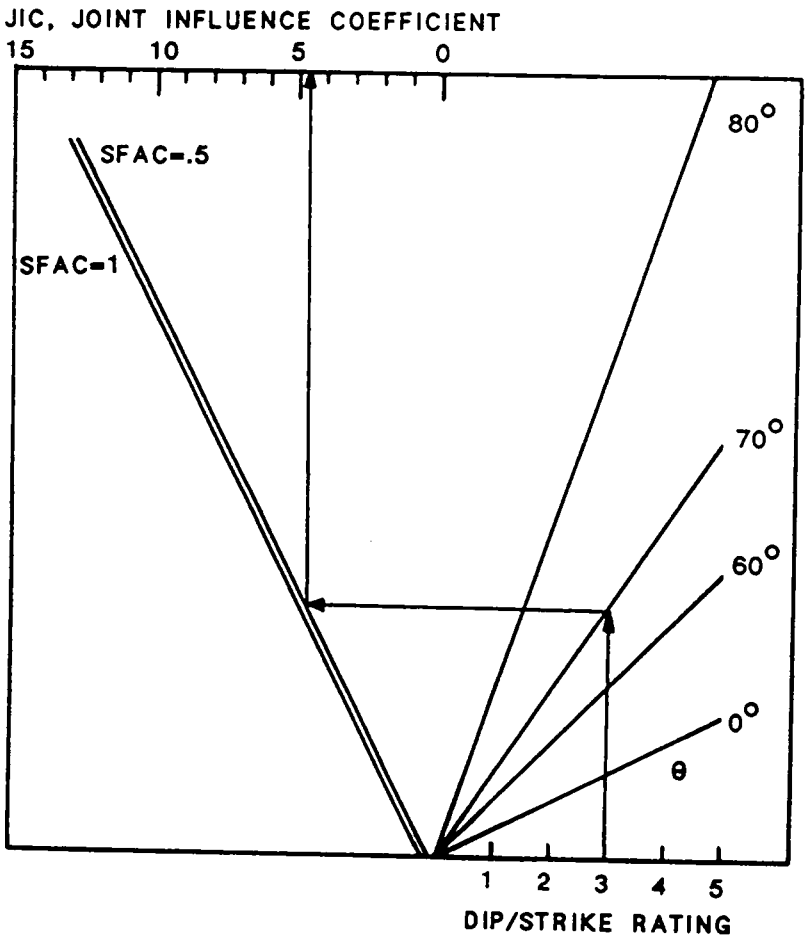

Figure 5.2 Nomogram for Estimating Joint Influence Coefficient

mining, ground water may be less of a problem after the lower seam has been mined if water is drained to the lower seam through cracks created in the innerburden. On the other hand, depending upon the degree and extent of fracturing of the innerburden and overburden strata, surface water may percolate to the upper seam, increasing the difficulty of upper-seam mining.

5.3 The Roof Rating System

After careful examinations of current geomechanics classification systems and factors peculiar to multi-seam mining, a multi-seam roof-rating (MSRR) system is developed. The system includes the following seven basic parameters:

1. Roof Rock - Type of rock constituting the immediate roof of the upper seam;
2. Roof Structure Location - Location of the roof structure in relation to lower seam remnant pillars and/or the subsidence trough;
3. Joint Sets - Jointing system in upper seam roof rock, including effects of joint spacing and orientation;
4. M-Index - Ratio of innerburden thickness to excavation height of the lower seam;
5. Distance to First Competent Stratum;

6. Time Factor - Time elapsed since mining of the lower seam (in years);
7. Ground Water - Ground water conditions and sensitivity of rock to moisture.

The complete rating scheme is summarized in Table 5.2. As can be seen, each parameter is classified into five categories, with a rating ranging from very poor to very good. A rating coefficient is assigned to each category. Since each factor will necessarily have a different weight according to its importance to upper-seam roof stability, a weighted average rating is introduced for the final overall rating in order to allow for maximum flexibility of the MSRR system.

Let n = total number of factors being evaluated,

w_j = weight of factor j, given based on the total number of factors under consideration;

RC_{ji} = rating coefficients as assigned in Table 5.2.

Then, the final overall rating is given as

$$r = \frac{\Sigma w_j RC_j}{\Sigma w_j} \qquad (5\text{-}4)$$

If, for example, two factors are being evaluated with weighting points of 10 and 20, and the rating for the two factors are poor and very good, respectively, the overall rating is then,

$$r = \frac{(10)(-1)+(20((2)}{10+20} = 1.0$$

Table 5.2 Multiple-Seam Mining Roof Rating (MSRR) Scheme

Factors (RC)*	Very Good (+2)	Good (+1)	Fair (0)	Poor (-1)	Very Poor (-2)
Immediate Roof Rock (IRR) (Weight=15)	Massive, clean, smooth gray sandstone or sandy sandstones; some massive hard shales		Interbedded shale and sandstone; crystallized sandstones and conglomerate	Thinly laminated shale beds	Slumps, deposits, channel scours, fire clays, kettlebottoms, slickensides, pinchouts
Roof Structure Location (RSL) (Weight=15)	Within undisturbed zones	Within zones of no-horizontal strain of subsidence trough	Within compression zone over remnant pillars or gob	Within tension zone over gob area or wide remnant pillars or over roobed areas	Over narrow remnant pillars
Joint Sets (JS) (Weight=30)***	JIC** < 2.5	2.5 - 3.5	3.5 - 6.0	6.0 - 10.0	JIC > 10
M-Index (Weight=15)	>60	35 - 60	20 - 35	10 - 20	< 10
Distance to First Competent Stratum (DFCS) (Weight=10)	< 1.5 m (< 5 ft.)	1.5 - 3.1 m (5 - 10 ft.)	3.1 - 7.6 m (10 - 25 ft.)	7.6 - 10.7 m (25 - 35 ft.)	> 10.7 m (> 35 ft.)
Time Factor (TF) (Weight=10)	> 5 years	2 - 5 years	1 - 2 years	0.5 - 1 years	<0.5 years
Ground Water (GW) (Weight=5)	Completely dry in upper and lower seam	Completely dry in upper seam, mostly dry in lower seam	Moist only in both seams	Moderate pressure upper seam wet	Severe problems, wet ground, roof rock very sensitive to water

* RC = Rating Coefficient
** JIC = Joint Influecne Coefficient
*** Weight for joint set is points per set.

indicating an overall good roof.

This weighted rating system allows the roof to be rated in the absence of certain factors, as is often necessary in mining engineering. As with any classification systems, the engineer must exercise his judgement as to whether the information on certain variables can be ignored and the reliability of the rating if such is the case. The system also provides flexibility for modification to widely differing applications, where some factors become more important than others, or where factors need to be added to the system.

5.4 Correlation With Upper Seam Subsidence

Methods have been presented for estimating upper seam subsidence and strain in Chapter 4. In incorporating the roof-rating system into damage prediction as a function of maximum subsidence at the upper seam elevation, the following empirical equation has been proposed:

$$DR = a_0+bSmax+ax_1+ax_2+ax_4+ax_5 \qquad (5\text{-}5)$$

where DR = damage rating, defined in Table 3.2; Smax is the maximum subsidence at the upper seam level, and

$$x_j = \begin{cases} 1 & \text{for roof rating } j,\ j=1,2,4,5 \\ 0 & \text{for all others.} \end{cases}$$

Figure 5.3 shows plots of damage rating against maximum

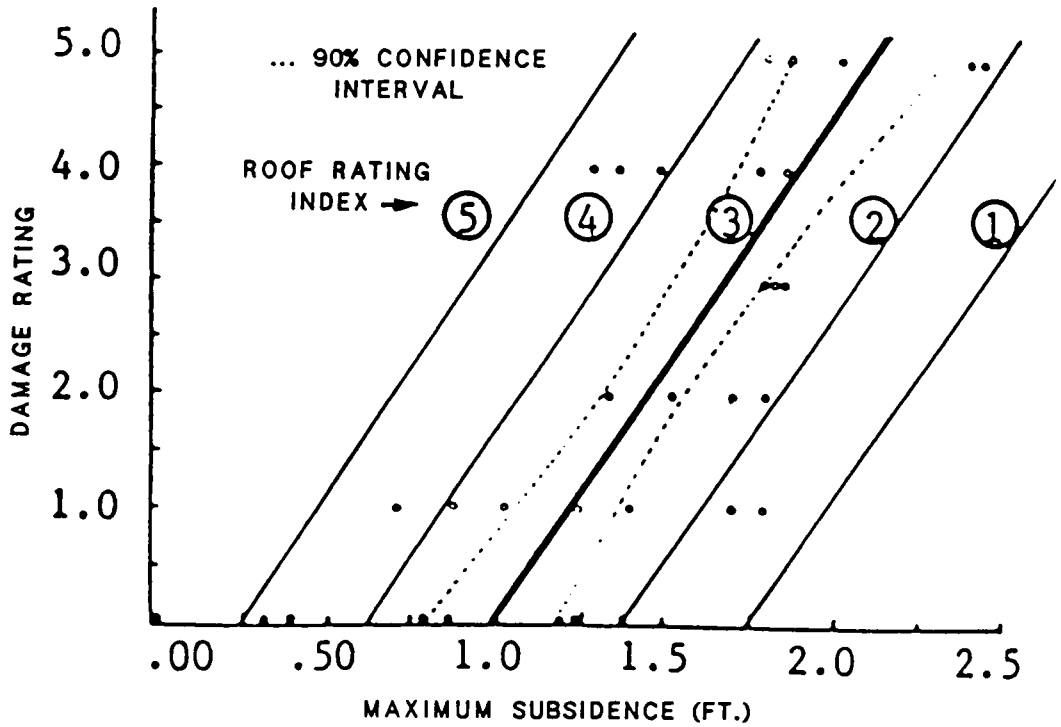

Figure 5.3 Damage Rating vs. Maximum Upper Seam Subsidence

subsidence. If the roof rating is three, an average condition is indicated which is expressed by the first two terms as:

$$DR = a_0 + bSmax.$$

Analysis using multiple linear regression with indicator variables yields:

$$DR = 4.59Smax - 4.54 + \Sigma a_j x_j \qquad (5\text{-}6)$$

where a_1=-3.35, a_2=-1.67, a_3=0.0, a_4=1.67, a_5=3.34.

Since the magnitude of ground control problems in upper workings can be elated to the magnitude of subsidence at that elevation, it is also related to the magnitude of strain at that elevation. Figure 5.4 plots damage rating against maximum tensile strain in the upper seam. Tensile strain can be calculated using Eq. (4-2).

In correlating the severity of damage to the magnitude of strain, the stability factor as defined in Chapter 3 is introduced. Plots of the stability factor against the estimated maximum tensile strain are shown in Figure 5.5. A positive stability factor indicates stable conditions while a negative value indicates potential ground control problems.

Correlation of the stability factor with the maximum tensile strain gives an empirical equation of the form:

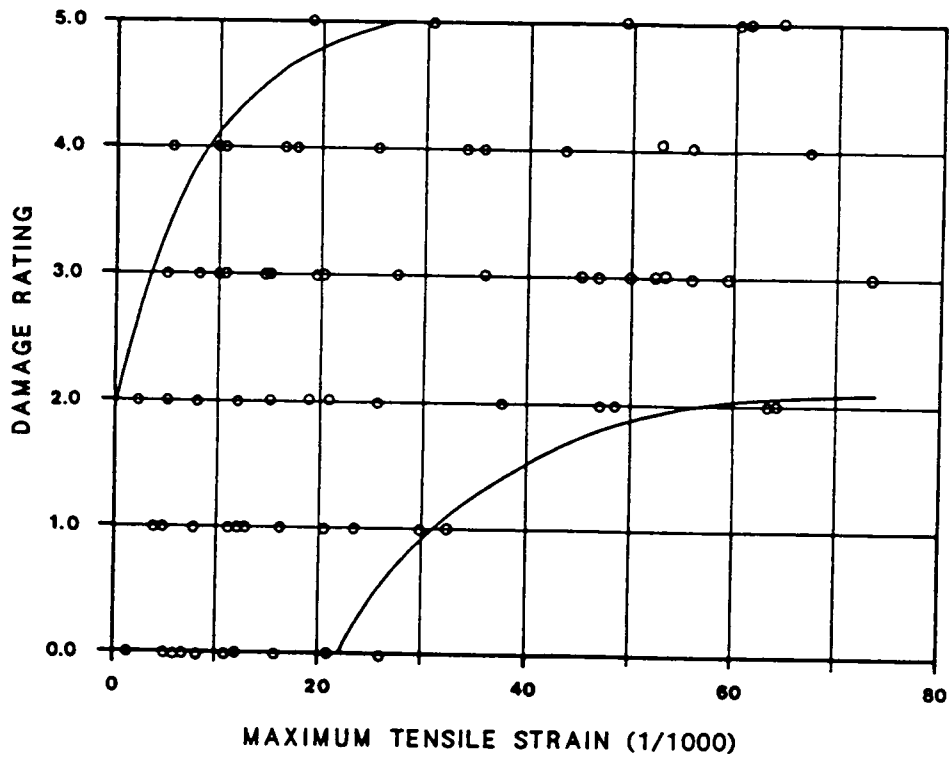

Figure 5.4 Damage Rating vs. Maximum Upper Seam Tensile Strain

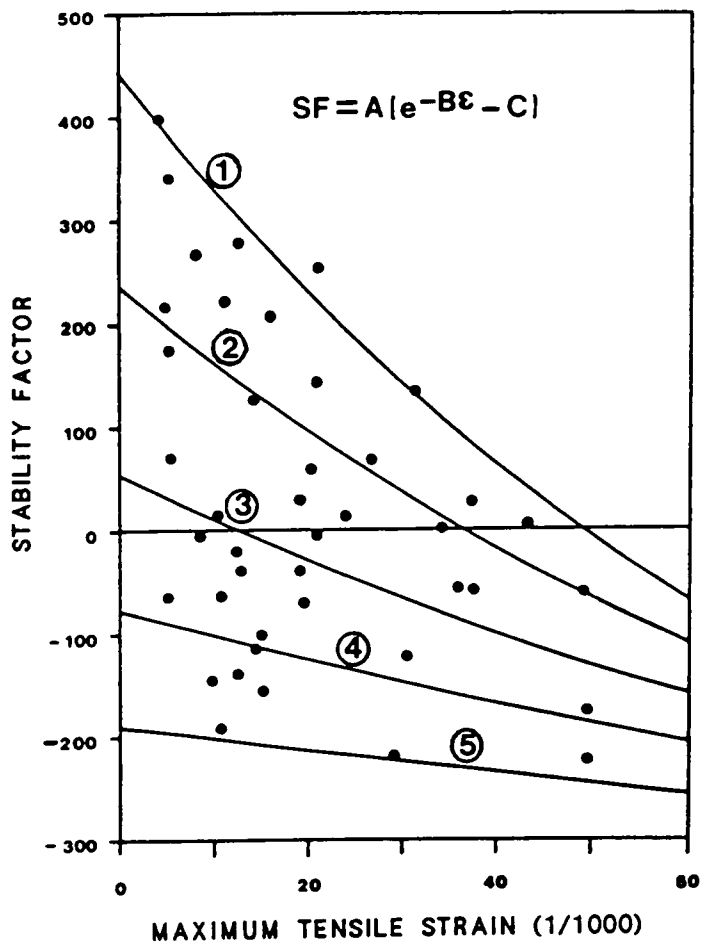

Figure 5.5 Stability Factor vs. Maximum Upper Seam Tensile Strain

$$SF = A(e^{-B\varepsilon}-C) \qquad (5\text{-}7)$$

where SF is the stability factor; ε is the maximum upper seam tensile strain (1/1000); and A, B and C are constants dependent on the roof rating (Table 5.3).

From Figure 5.5, it is readily seen that the stability factor is always negative for roof ratings of four and five. This results from the fact that the roof rating, by incorporating the location and joint factors, is itself an indication of upper seam stability. A roof rating of four or five will usually mean a roof of highly jointed rock, oriented in unfavorable directions, located in the high stress concentration zone or the tension zone, among others.

Table 5.3 Constants for Stability Factor Evaluation

MSRR	A	B	C
1	945	0.0130	0.53
2	740	0.0105	0.68
3	556	0.0081	0.90
4	425	0.0061	1.18
5	313	0.0041	1.80

VI. IMPLEMENTATION OF DESIGN CRITERIA

The ability to combat and control negative interaction effects by designing an effective mining layout and effective measures of strata control is essential to achieving mine safety and productivity. To this end, options for improving upper seam stability are presented in this chapter, along with recommended design procedures for overmining operations. To facilitate the application of the design criteria, a computer program has been developed.

6.1 Upper Seam Mine Layout

6.1.1 General Guidelines

Based on experience and on results from this research effort, guidelines for minimizing interaction effects, in areas where these effects are inevitable, are summarized as follows:

1. Avoid driving entries in the tension zone, as this zone is usually heavily fractured due to the low tensile strength of coal measure rocks.
2. Use the destressed zone over the gob line areas, or within the pressure arch if a pressure arch exists for entries.
3. Use oversized pillars over isolated remnant pillars, or offset entries from those entries bewlow, in the

lower seam.

4. Reduce roof spans and number of entries.
5. Use yield pillars in order to protect entries where long-term stability is essential.
6. Use other stress reduction techniques, such as pillar softening, to shed load onto other areas.

6.1.2 Opening Orientations

Great attention must be given to the orientation of openings in the upper seam with respect to lower seam workings, stress field, and major geological discontinuities. In the case of a single joint set, with its favorable strike/dip combination in the preferred direction based on trough subsidence and/or remnant pillars, the decision is straightforward (Figure 5.2b). If, however, subsidence favors one direction while the joint set favors another, the benefits of each direction must be weighed against the other. For seams with a large M-index and relatively uniform extraction in the lower seam, opening orientation should be determined based on the jointing system. On the other hand, if the two seams are lying in close proximity, it may be more beneficial to base this decision on the lower seam orientations and the subsidence trough. In areas where high stress concentrations are expected in the upper seam with well-defined pillar lines, then it may be best to orient the openings in the direction of the pillar

lines of the lower seam. Over gobline interfaces, if high tension is identified for the upper seam, then openings may best be orientated at an angle to the subsidence trough which offset the effects of the tensile strain (Figure 6.1). In summary, prudent decisions can only be made after all possible direction combinations and their effects on upper seam stability have been evaluated.

6.1.3 Pillar Layouts

Figure 6.2 shows possible layouts of upper seam entries (pillars) over a long remnant pillar. In layout (a), only two pillars support the transferred load, while in layout (b) three pillars support this load. Each layout has its advantages, depending upon load distributions. The two pillars in layout (a) bear equal loads due to symmetry, with higher load probably concentrated towards the two pillar edges facing each other. In layout (b) there are three pillars, with pillar #2 bearing the highest load and pillars #1 and #3 bearing equal loads. It is possible that the load on pillar #2 in layout (b) may exceed that on the pillars in layout (a). This corresponds to a smaller angle of influence in terms of stress transfer to the upper seam, and to a more concentrated peak load towards the center pillar.

An alternative to the two layouts above is to increase the size of the two pillars in layout (a) or the size of

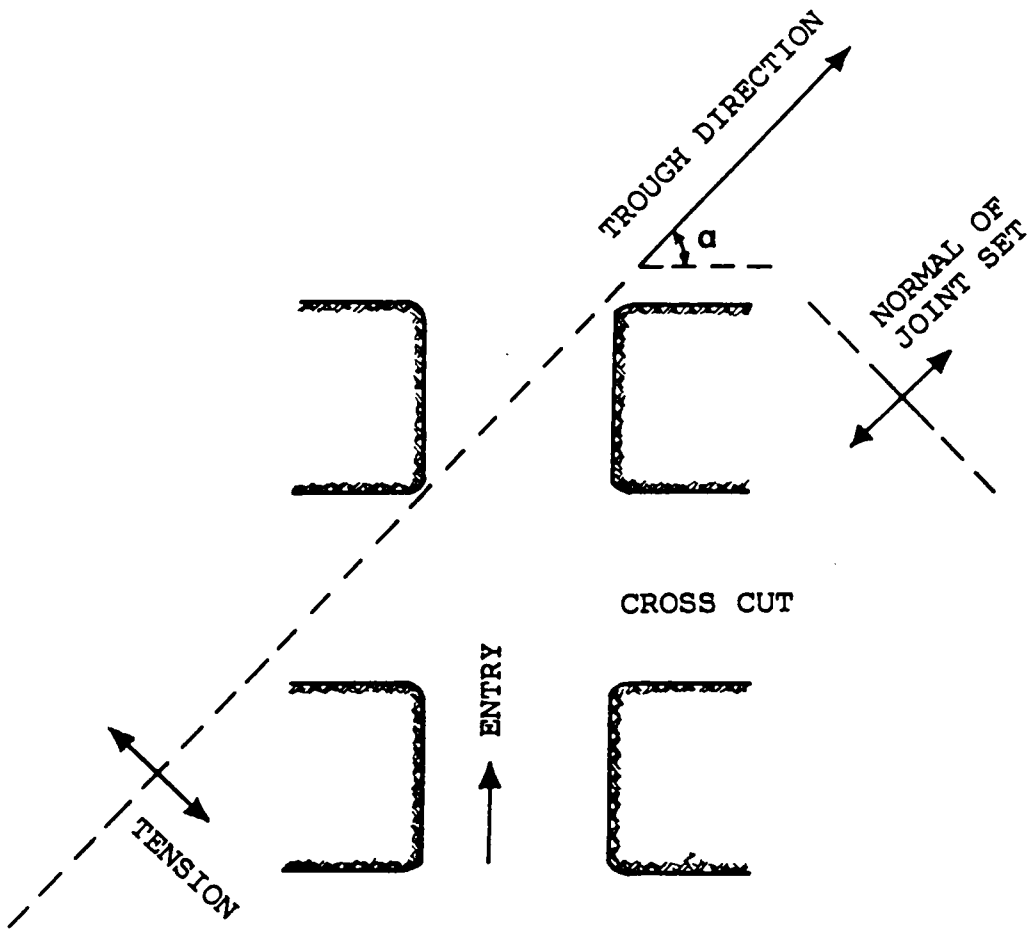

Figure 6.1 Orientation of Upper Seam Entries at an Angle to the Subsidence Trough to Reduce Negative Interaction Effects

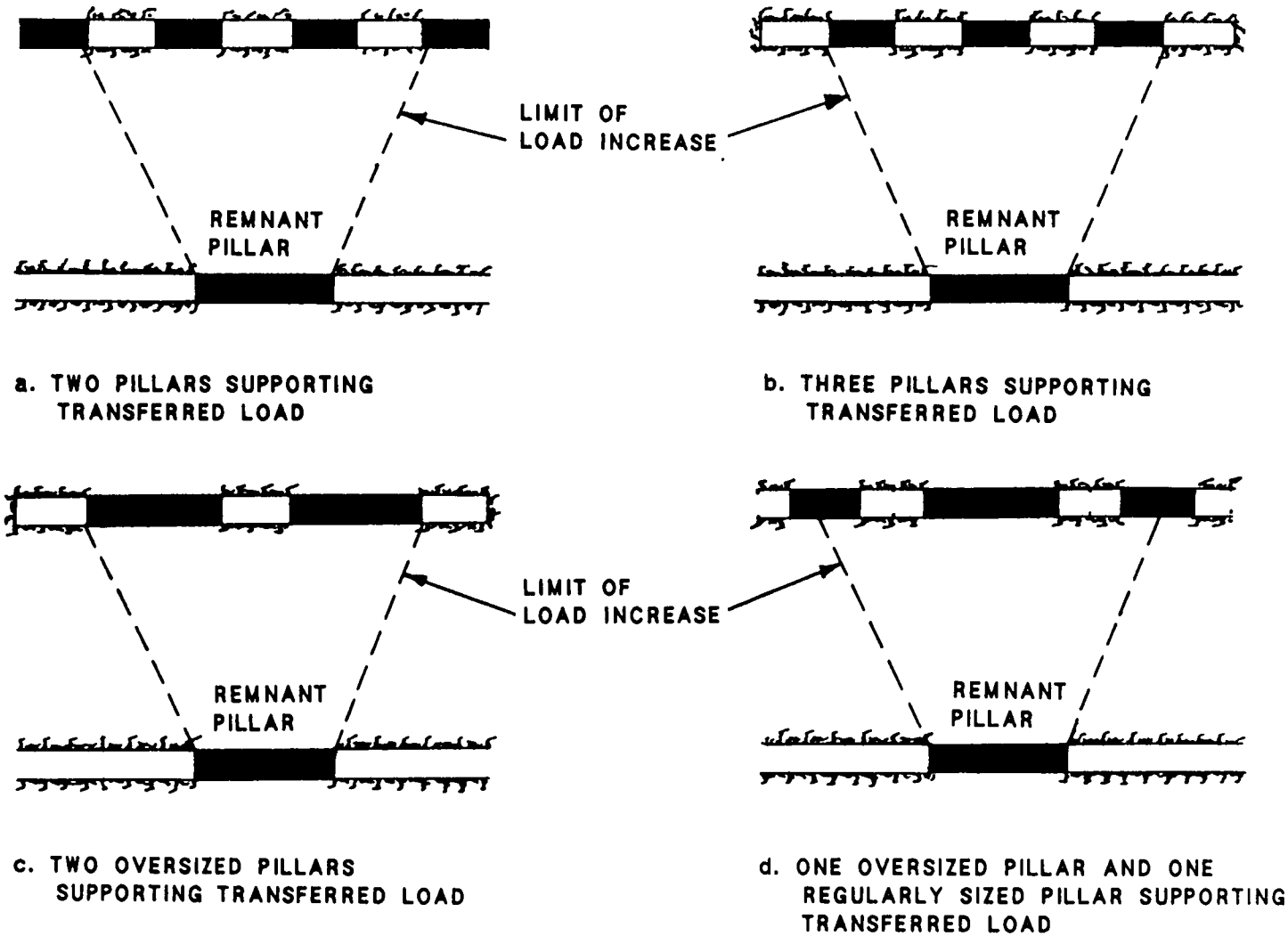

Figure 6.2 Possible Pillar Layouts for Upper Seam Over a Long Remnant Pillar

pillar #2 in layout (b), as shown in layoutc (c) and (d), respectively. This may be necessary when pillar sizes in both layout (a) and (b) are not adequate to support the concentrated load. Simple and mechanically correct, this type of layout may not be easily put into practice, because this would mean varying pillar sizes and possibly room sizes, which makes cutting in actual operations somewhat difficult.

If the remnant pillar is relatively square, then the pillar layout must be considered in three dimensions. Shown in Figure 6.3 are some possible variations of pillar layout with respect to the remnant pillar. As can be seen, the number of pillars supporting the transferred load in layout (a') is nine, while in layout (b') the corresponding number is only four. The difference is proportional to the square of the number of pillars in two dimensions.

It can be seen that the problem is more complicated in three dimensions but the same principles apply. The same argument can be made for and against the alternative lay-outs by altering the sizes of the pillars and rooms.

6.2 Recommended Design Procedures

Simply stated, ground control in multi-seam mining begins with determining the effects of interaction for a given or proposed mining situation. A decision can then be

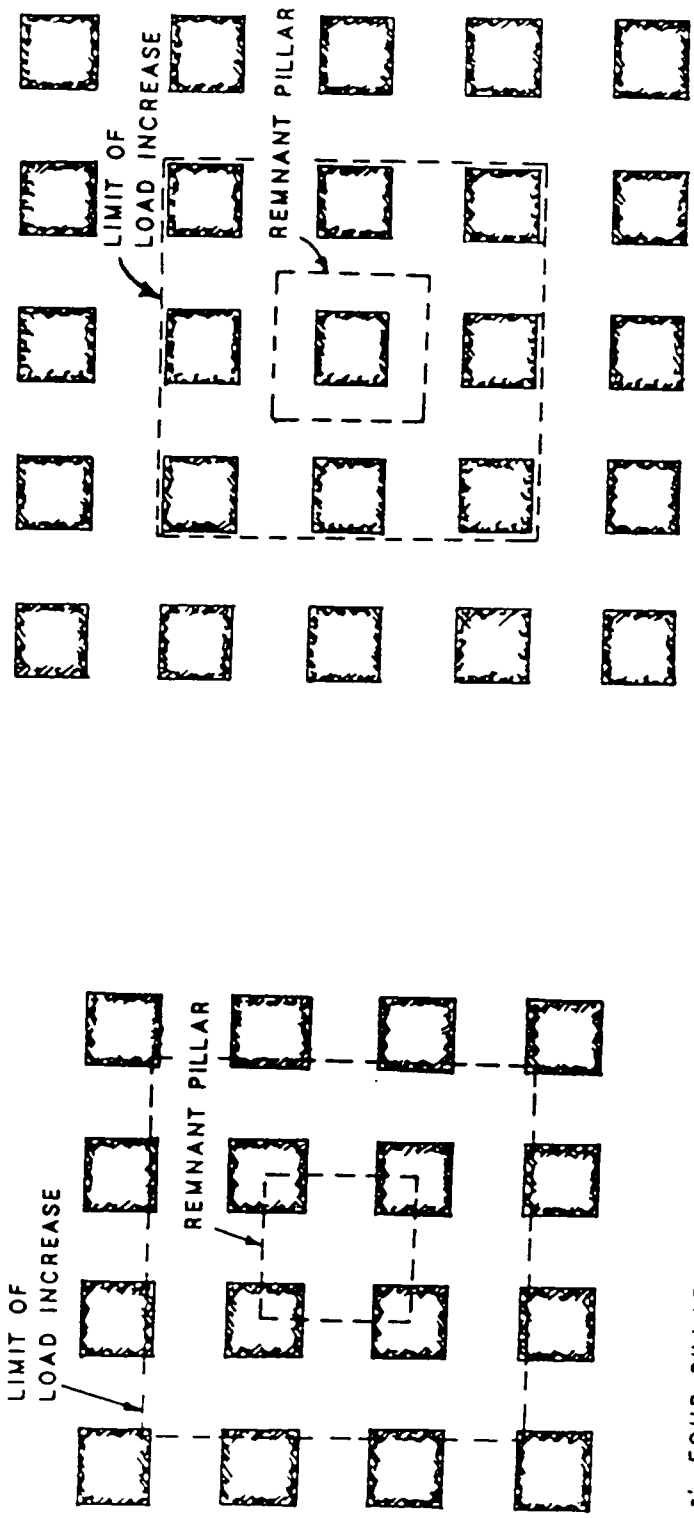

Figure 6.3 Possible Pillar Layouts for Upper Seam Over a Short Remnant Pillar

made either to avoid the troubled area, to support it, or to choose an alternative design. For application purposes, the following procedures are recommended in designing for an upper seam being mined over a previously-mined seam.

1. Collection of Relevant Input Data

Any design in engineering is only as reliable as the input data provided. Therefore, it is of great importance to investigate the geological and mining factors associated with the two seams concerned. Careful mapping of the workings in the lower seam will help to identify locations of possible interaction. Other investigations are necessary in order to detect any geological anomalies, which may be the dominant factors in controlling the interaction mechanism.

2. Classification of Mining Conditions

For design and planning purposes, mining in the upper seam should be divided into the various categories discussed earlier, both vertically and horizontally, once the lower seam workings have been identified. Such classification according to mining location can help to identify the correct mechanism to be used in analyzing interaction effects. To aid in this classification, Table 6.1 summarizes the various zones in which the upper seam can be located and possible situations to be expected.

Table 6.1 Ground Conditions for Various Zones After Mining of Lower Seam

Hori. / Vert.	Remnant Pillar	Lateral Tension	Lateral Compression	No Horizontal Strain	Beyond Trough Boundaries
Caving (Level)*	(Poor, but more due to high pressure than caving)	Very poor	Poor	Poor	Susceptible to damage if too close to gob
Fracturing (Level)* : Heavy : Average : Slight	(Susceptible to damage due to high pressure)	Poor, due to intensification of fracturing	Fair to poor due to fracturing and grade	Difficulty dependent on degree of fracturing	Negligible or no interaction disturbances
Subsidence	(Susceptible to high pressure)	Susceptible to damage due to tension	Fair, but also susceptible to to difficulty due to grading	Usually no negative interaction effects	No interaction disturbances

Notes:

* Refers to the horizontal level.

3. Characterization of Upper Seam Structures

Rock properties required in the design process and stability analysis can be obtained from in-situ and laboratory testing on core samples of typical coal and its surrounding rocks. The geomechanics classification system for multi-seam roof rating (MSRR) developed in Chapter 5 can be used to incorporate and quantify some geological and spatial factors.

4. Preliminary Evaluations

The complexities of multi-seam mining dictates the use of a series of evaluations in order to ensure the most reliable design. The various methods discussed earlier can be used to predict the possibility of any negative interaction effect, as well as its location. Methods for stress calculations can be used both in estimating the magnitude of stress concentrations, and in identifying their locations. The subsidence method is used to delineate tension zones and to calculate strain distributions. Results from this analysis can then be used as a guide during later analysis and design.

5. Stability Analysis

Once the locations of possible interaction are identified, the stability of upper seam structures in these areas must be evaluated, and options for improving ground conditions devised accordingly. Damage in the overlying seam

can affect the pillars, the roof, and the floor, depending upon the location of mining, and on geologic and mechanical properties of the structures involved. Once the stress concentrations and strain distributions are calculated, stability of these structures should be evaluated simultaneously. Sensitivity analysis should be conducted to study the effects of individual factors on stability.

6.3 Computer-Aided Design

6.3.1 General Description of RUMSIM

To aid in the implementation of the design guidelines and to facilitate various design processes, a computer program called RUMSIM (Room-and-pillar Upper seam Mining SIMulator) has been developed for overmining which uses the room-and-pillar method. The program takes a comprehensive approach to the problem of computer-aided mine design by incorporating a series of damage prediction methods, interaction mechanisms, design criteria, and means of minimizing negative interaction effects. Primarily, it is built upon results from this research and previous work, combining the analytical methods, rules of thumb, and empirical relationships which are used in practical designs.

The program is functionally divided into two parts. The first part deals with data manipulation, including data entry, error checking, and data modification. The second

part of the program deals with evaluation of the data. The user has two initial options for evaluation when using the program: either a qualitative (Module A) or a quantitative (Module B) analysis is available. Module A, or qualitative analysis, allows the user to carry out a preliminary evaluation of potential damage and interaction mechanisms, and requires a minimal amount of input information. This module includes such methods as subsidence factor, roof rating (MSRR), stability factor, probability of interaction, M-index, and damage rating. The quantitative analysis involves more detailed stress and strain calculations, and will eventually determine entry sizes and pillar dimensions for any given mining situation. A macro flowchart of the program is shown in Figure 6.4.

Specifically, the program can

- predict the magnitude and location of potential interactive damage;
- calculate stress concentrations and strain distributions;
- design entry and pillar dimensions for a given desired safety factor;
- recommend options for avoiding or minimizing interaction effects and optimum design specifications for a given set of input data; and
- perform sensitivity analysis by allowing the user to interactively modify input data during any phase of

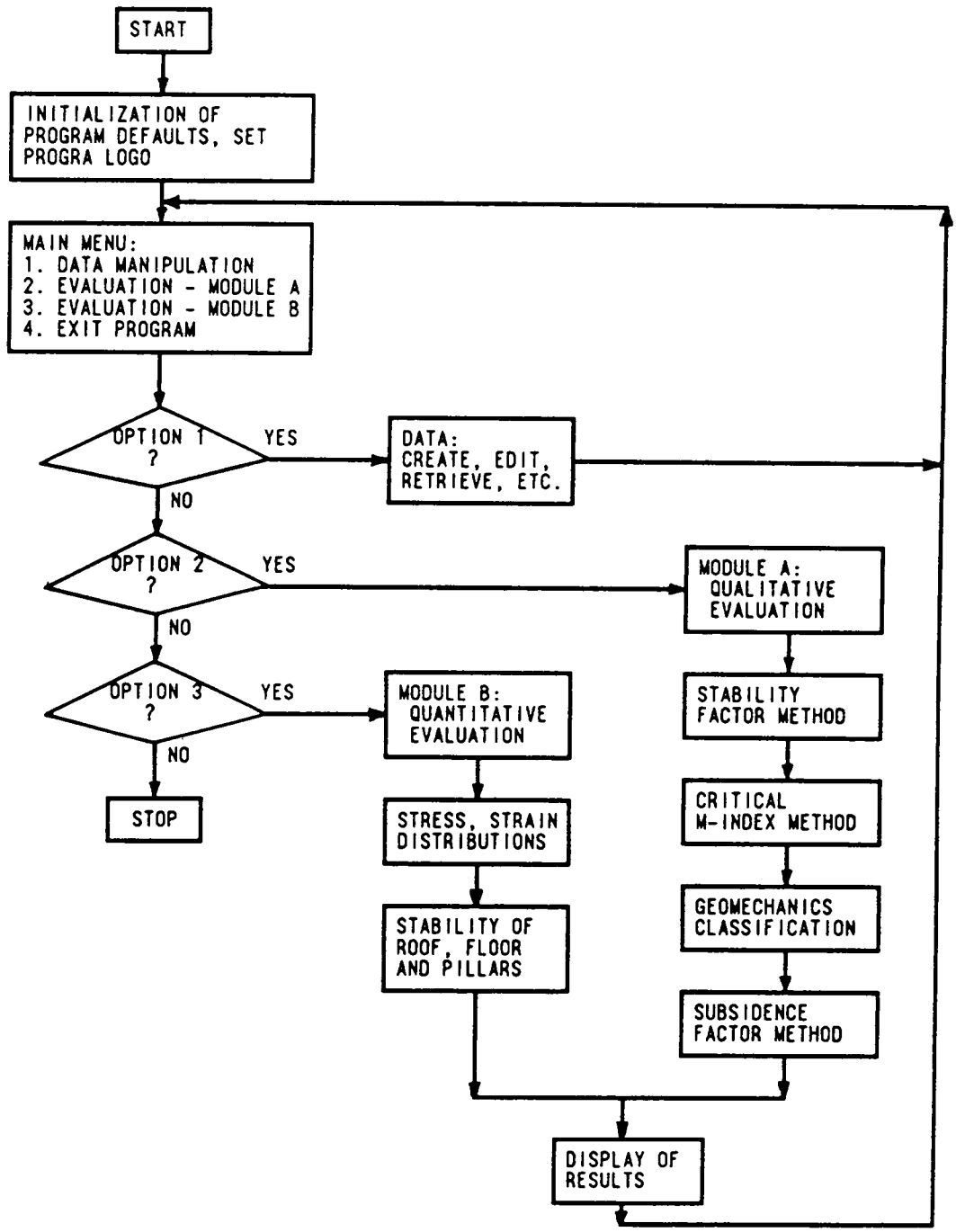

Figure 6.4 Macro Flowchart of Computer Program RUMSIM

program execution.

An important feature of the program, and one which distinguishes it from most other computer programs, is the extensive on-line help it makes available to the user. This includes a definition of variables, suggested values for input data, explanations of empirical relationships and interaction mechanisms. There are altogether 30 help screens which can be accessed from anywhere in the program at any time except during program execution. Figure 6.5 shows a help session focusing on the probability of interaction. This readily available help information not only ensures smooth and accurate execution of the program, but also serves as a technical guide to the user.

The program is written in Turbo Pascal to run on the IBM-PC and compatibles, and is completely menu-driven to provide maximum flexibility in application. Full-screen editing allows data to be easily entered and changed so that sensitivity analyses can be performed until an optimum design is achieved. Output can be in the form of screen display, hardcopy, or disk file. Graphics are used, whenever possible, to provide a better illustration and interpretation of the results.

6.3.2 Data Input and Editing

Data manipulation includes data input, data error checking, data modification and data storage. Full screen

RUMSIM - Help Session Page 11

□ Probability of Interaction

An estimate of the probability of interaction can be obtained using this curve derived from statistical analysis of 93 case studies:

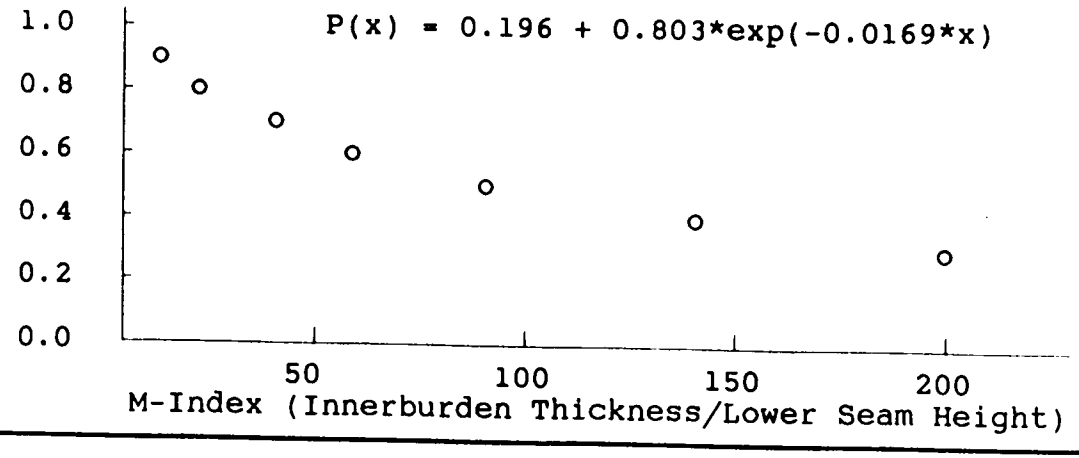

F1 or ESC - Return PgDn - Next Page PgUp - Previous Page

Figure 6.5 Example of a Help Session of RUMSIM

data input is used for fully-interactive data entry and data changes (Figure 6.6). The user can go to any field within a screen or jump to any input page. Extensive data error checking, based on bounds established from field data and theoretical analysis, is provided to assure the best accuracy of input data and reliability of the analysis. Table 6.2 shows typical rock properties compiled for the Appalachian coal fields.

Input to the program includes:

I. General information
- Name and location of property
- Title of analysis
- Date and time of analysis

II. Lower Seam Data
- Seam thickness
- Number of openings (panels)
- Width of each panel
- Width and length of remnant pillars
- Percent of overall extraction
- Time elapsed after mining of lower seam
- Coal properties

III. Upper Seam Data
- Seam thickness
- Coal properties (unit weight, compressive strength, shear strength, angle of internal friction, coal K factor, etc.)

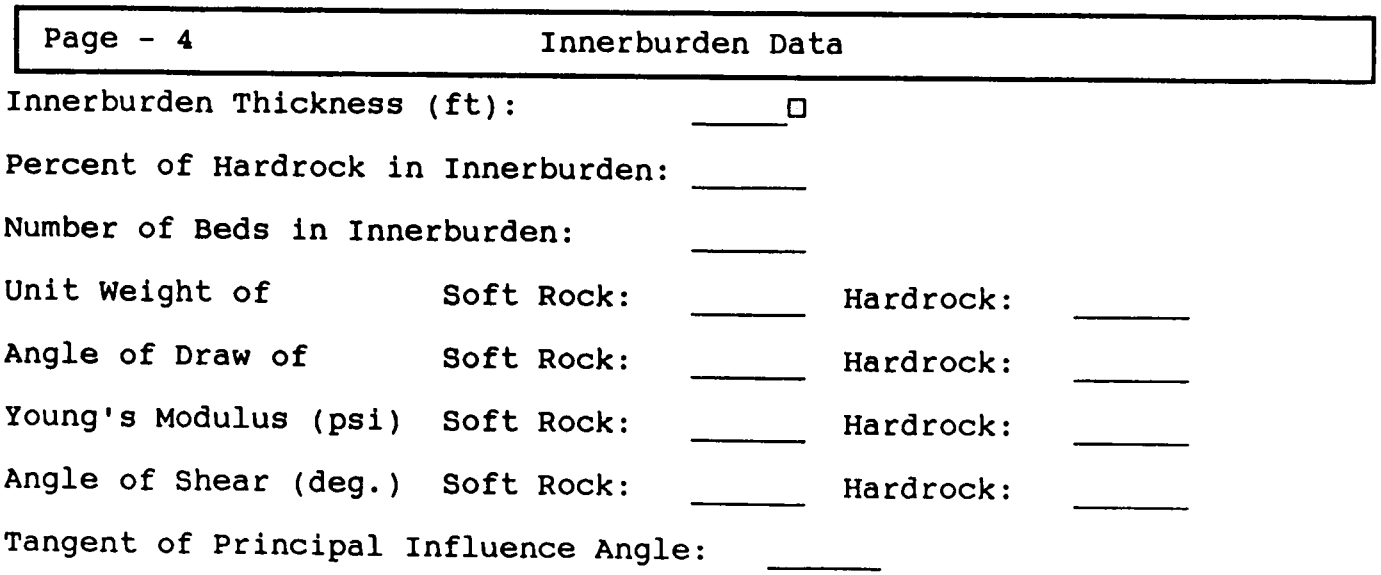

Figure 6.6 Example of an Input Page of RUMSIM for Innerburden Data

Table 6.2 Typical Properties of Coal Measure Rocks for Appalachian Coal Fields

1. Coal k-factor

Coal Seam	k-factor	Average
Pittsburgh	5551-5862	5706
Pocahantas No. 4	4313-4825	4569
Clintwood	4289-5205	4747
Elkhorn No. 4	6000-6250	6125
Harlan	8859-9458	9159
Marker	10120-10600	10360

2. Pillar Loading Angle

Average $\alpha = 21°$

3. Subsidence Parameters

Angle of draw = 28°
Tangent of principal influence angle: $\tan\beta = 2.31 \pm 0.4$
Inflection point = 0.2H
Critical subsidence: W/H = 1.2

4. Elastic Properties

Rock Type	Unit Weight (pcf)	Comp. Strength (psi)	Young's Modulus ($\times 10^6$ psi)	Poison's Ratio	Friction Angle (deg.)
Coal	125	2,000	0.72	0.23	15.0
Shale	160	4,000	1.61	0.10	55.0
Sandstone	145	12,000	3.00	0.15	40.0

5. Rock Strength Classifications

Hard Rock: $\sigma_o = 5688$ psi
Medium Hard Rock: $2844 < \sigma_o < 5688$ psi
Soft Rock: $\sigma_o < 2844$ psi

- Immediate roof-rock type and properties
- Roof-jointing system
- Immediate floor-rock type and properties
- Location of mining in relation to lower workings
- Panel width
- Room-and-pillar size
- Number of entries

VI. Input for Both Seams

- Average overburden thickness (to upper seam)
- Percent of hardrock in overburden
- Average unit weight of rock in overburden
- Innerburden thickness
- Percent of hardrock in innerburden
- Tangent of principal influence angle
- number of beds in innerburden
- thickness of each rock type
- Average unit weight of each rock type
- Angle of draw of each rock type
- Elastic properties
- Ground water

The user has the option of editing any one of the four groups or all input data, and of running a preliminary or a detailed analysis at any stage, provided that the required input information is supplied.

6.3.3 Evaluation and Output

As shown in Table 6.3, the complete output of the program includes the following pages:

0. Title page showing the various phases of program execution.
1. Summary of all relevant input data:
   All major input data are output as a reference for the results of the analysis.
2. Results from empirical analysis (preliminary):
   This includes evaluation by all empirical methods, as listed in Table 6.3. Whether or not interaction is likely or not is predicted based on results from each method. A preliminary analysis will have only the above three output pages.
3. Results from subsidence analysis:
   This page defines the geometry of the lower seam panel and displays the subsidence profile and strain distributions. The number of points calculated depends on the with of the panel.
4. Results from arching and caving analysis:
   First, determination is made whether an arch will be formed. If so, then the arch geometry is computed. The most useful information contained in this page is the height of caving and the width of the pressure arch at upper seam level.
5. Results of roof stability analysis:

Table 6.3 Outputs by Program RUMSIM

Page	Title	Output Parameters
0	RUMSIM Running . . .	Title output showing various evaluation sub-procedures
1	SUMMARY OF INPUT DATA	Summary of relevant input data as a reference for output results
2	EMPIRICAL ANALYSIS	Roof rating (MSRR); damage rating by subsidence factor; damage rating by linear regression model; stability factor; critical M-index and innerburden thickness with and without time effect; probability of interaction; max. subsidence and tensile strain.
3	ARCHING ANALYSIS	Max. upper seam subsidence; Max. width of arch; actual opening width; width of arch at upper seam; height of caving and fracturing zone
4	SUBSIDENCE ANALYSIS	Subsidence and strain distributions as a function of the distance from the left edge of the barrier pillar.
5	PILLAR STABILITY ANALYSIS	Virgin stress; avg. stress concentration; max. stress concentration; pillar sizes; F.S. vs. avg. stress and max. stress; F.S. as a function of pillar sizes.
6	ROOF STABILITY ANALYSIS	Depth of upper seam; virgin stress; avg. stress concentration; max. stress concentration; adjusted density of roof beam; F.S. against comp. failure, shear failure, or buckling.
7	FLOOR STABILITY ANALYSIS	Virgin stress; avg. stress concentration; max. stress concentration; floor config.; upper layer thickness; lower layer thickness; bearing capacity; F.S. vs. avg. load and max. load.; recommended S.F. for stability

The roof stability is evaluated using the beam theory and the voussoir arch theory. The three basic modes of roof failure are all considered: buckling (tension), compressive, and shear.

6. Results of pillar stability analysis:
   Pillar stability is evaluated by computing the factor of safety using the pillar equation developed by Bieniawski. Sensitivity analysis is also automatically carried out, yielding the factor of safety as a function of pillar sizes.
7. Results of floor stability analysis:
   Floor stability is evaluated by comparing the bearing capacity of the floor layer with the bearing load. Both a single-layer and a two-layer configuration can be evaluated.

VII. APPLICATIONS IN DESIGN

Three case studies are presented in this chapter to demonstrate in detail the application of the methods of analysis and of the design guidelines. Although RUMSIM was used for all analyses, emphasis is here given to utilizing the principles and interaction mechanisms involved in multi-seam mine design.

7.1 Case Study No. 1

7.1.1 Description

This case of mining operations in Monogalia County, West Virginia (Table 7.1) was originally documented by Stemple (1956) . The upper seam, the Sewickley, was being mined over the previously-mined Pittsburgh seam, with time lapse between operations ranging from a few months to several years (Figure 2.2). The Pittsburgh seam was mined by driving 20-ft. rooms on 90-ft. centers, with an overall extraction ratio of 60% and of up to 85% where pillar extraction was done. Mining in the Sewickley seam used a similar system, with 20-ft. rooms driven on 70-ft. centers. Pillars were recovered, split, or left in place, depending on ground conditions and on cost of particular sections, with a resulting extraction ratio of approximately 75%.

Experience of the mine showed that upper seam condi-

Table 7.1 Documentation of Case Study No. 1

SOURCE OF INFORMATION:	Stemple, 1956
NAME/LOCATION OF MINE:	Monongalia County, WV.
LOWER SEAM:	
Bed Name:	Pittsburgh
Thickness:	96"
Method of Extraction:	Block system on 90' centers
Extraction Ratio:	85%
Immediate Roof:	6" to 12" drawslate, overlain by about 9' of shales and rider coals
Immediate Floor:	Shale, fairly hard
INNERBURDEN:	
Thickness:	90'.
Percent of Hardrock:	15%
M-Index:	11.2
UPPER SEAM:	
Bed Name:	Sewickley
Thickness:	66"
Immediate Roof:	Sandstone or strong sandy shale
Immediate Floor:	Fireclay or shale, fairly soft
OVERBURDEN:	
Cover thickness:	400'.
Nature of Strata:	Shales, fireclays, thin coals, several limestones, 10' to 25' thick and a sandstone up to 50' thick near the surface
TIME AFTER MINING OF LOWER SEAM:	4.5 years
GROUND WATER:	Not present
ASSESSMENT GROUND CONTROL CONDITIONS:	
Mining Sequence:	Overmining
Location:	Above robbed areas of lower seam
Description:	Fractured roof, coal and floor; mining difficult and expensive
Possible Mechanism:	Pillar supported upper seam
Damage Rating:	3 - Considerable damage
Control Method:	Use of continuous miner reduces blasting effects

tions were generally fair when three to four years had elapsed since lower seam mining while simultaneous mining caused the greatest difficulty. No disturbance was observed where lower seam pillars were left in place. In areas above robbed sections, all upper-seam structures -roof, coal, and floor - had been fractured, making mining difficult and expensive. Most of the damage was recorded in areas over a line between the solid coal and the gob in the lower seam. However, some of the greatest damage did not occur directly above the edge of the remaining coal in the lower seam. Instead, it occurred in areas over the gob and away from the solid coal, usually at a distance of 50 to 200 feet from the edge of the solid coal (Figure 7.1).

7.1.2 Analysis

The analysis of minimum M-index immediately suggested a potentially unstable case in the upper seam, because the actual M-index (innerburden) of 11.3 (90 ft.) was much less than the required minimum M-index of 79, with a 0.86 probability of interaction (Figure 7.2). Figure 7.3 plots the case study against the empirical M-index model. As can be seen, even with a large error margin, the actual innerburden thickness was still considerably less than the stability requirement established by the statistical models. Other results from empirical analyses are also found in Figure 7.2, with all checked critical parameters suggesting

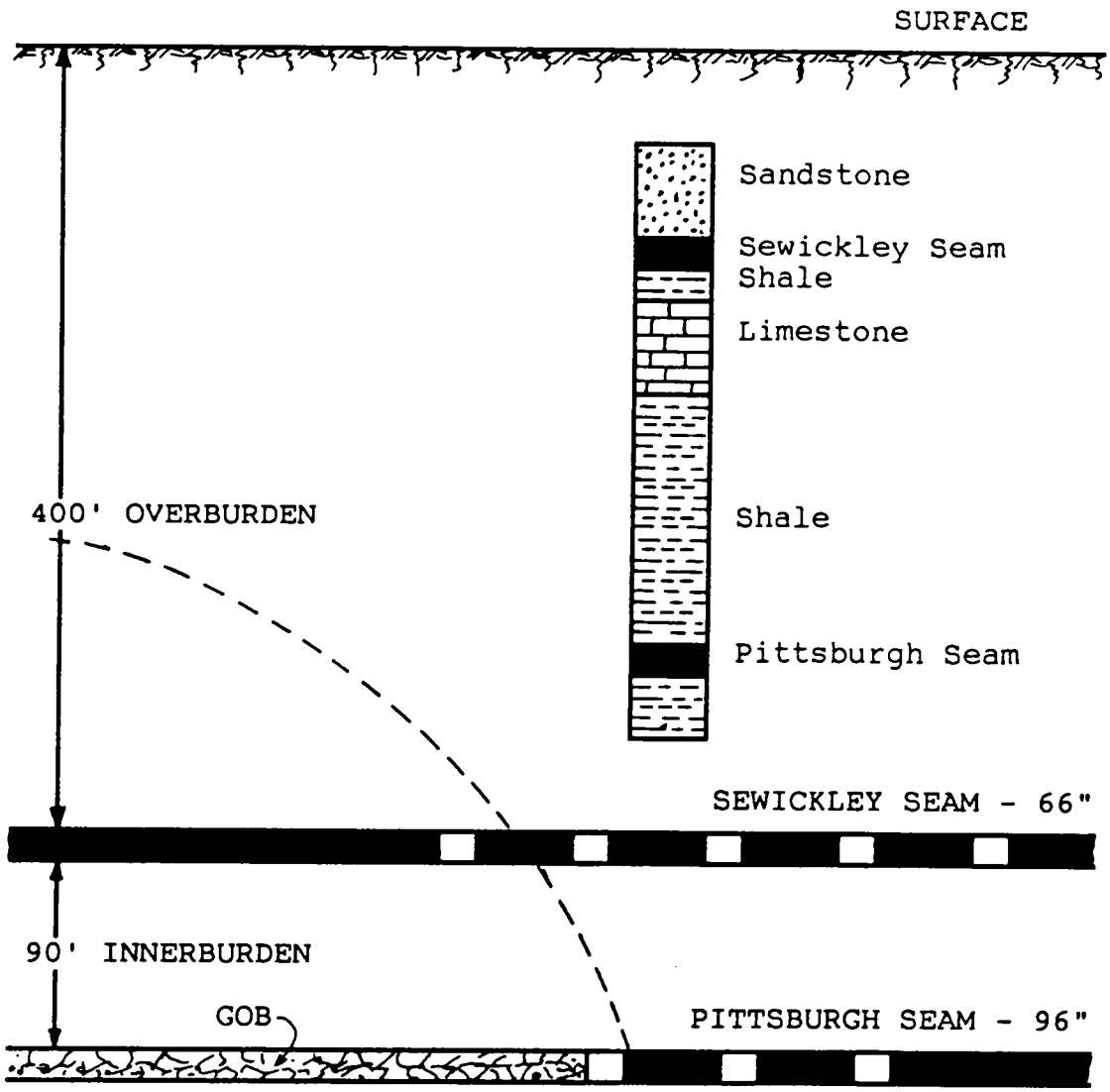

Figure 7.1 Analysis of Upper Seam Failure by Pressure Arch Theory and Load Transference - Case Study No. 1

EMPIRICAL ANALYSIS - Summary Output Page 1/7

The upper seam is located [400] feet below surface.

Roof Rating (MSRR) = [2.1] (on a scale of 1 to 5, with decreasing difficulty)
Stability Factor = -205.4, indicating that interaction [is] likely
Stability Based on Roof Rating = - 180.7, interaction [is] likely

M-index Checking:
Critical Innerburden Thickness:

Time Effect	No Time Effect
Icrit = 588.0 ft.	Icrit = 632.0 ft.

Actual Innerburden Thickness = 90.0 feet
Actual M-index = 11.3
Probability of Interaction = 0.8600
Predicted Average Damage Rating by Linear Regression = 3.7

Subsidence Factor:
Estimated Maximum Subsidence = 5.46 ft.
Estimated Maximum Tensile Strain = 65.3600 (1/1000)
Predicted Damage Rating Based on Subsidence Analysis = 5.0

PgDn - Next Page PgUp - Previous Page ESC - Return to Menu

Figure 7.2 Summary Output of Program RUMSIM of Results from Empirical Analyses - Case Study No. 1

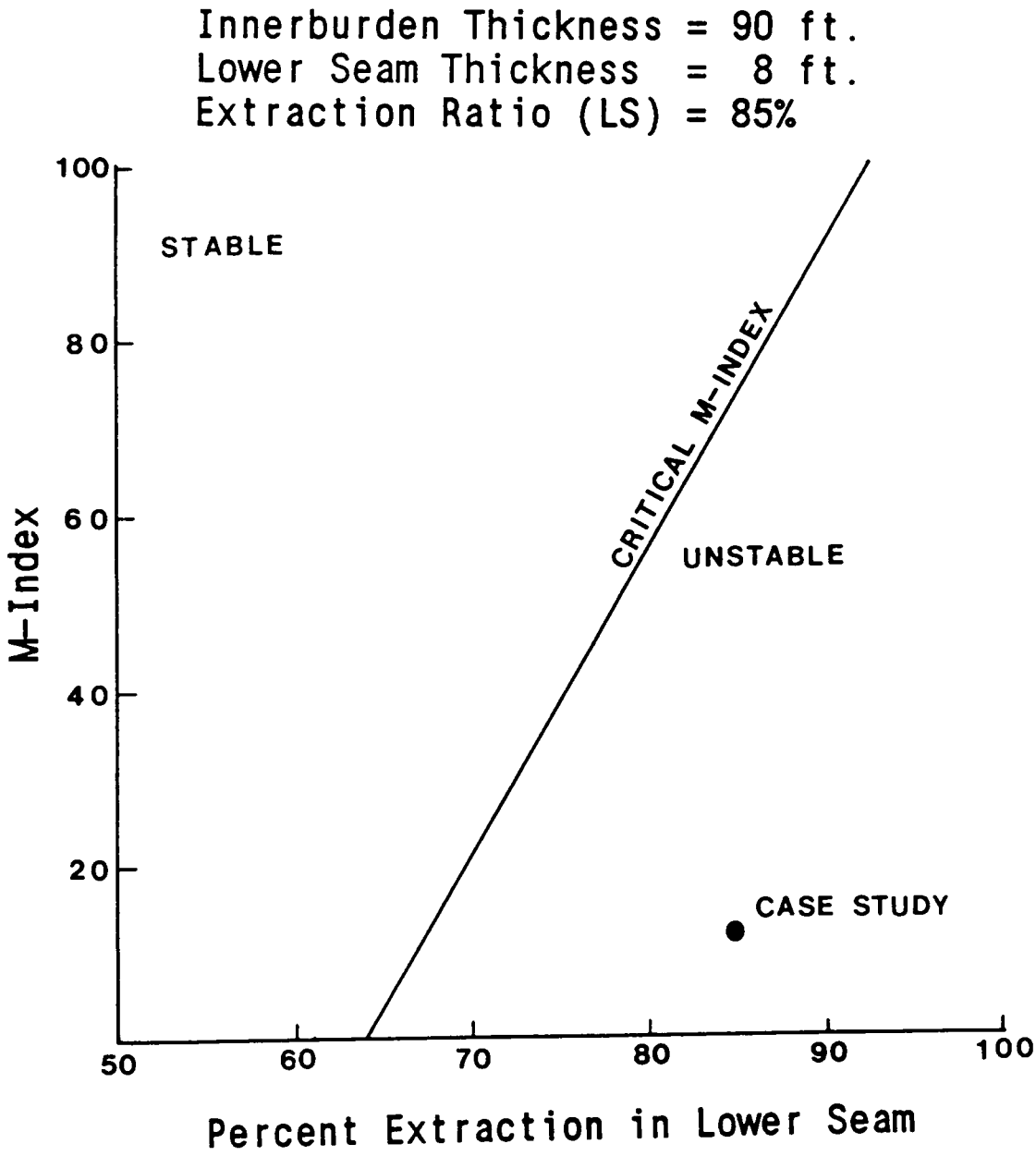

Figure 7.3 Empirical Analysis Using the M-index Method - Case Study No. 1

negative interaction effects.

In view of the fact that the most serious damage occurred at a distance of 50 to 200 feet from the edge of the solid coal, two possible explanations exist although both tend to predict similar locations of damage in the upper seam. The two possible mechanisms are, first, pressure arching, and second, interseam shear failure by the cantilever beam action assumed by the strata overlying the goaf. The shear failure mechanism would predict that the greatest damage would occur 63 feet from the edge, assuming a constant angle of shear of 35 degrees for the predominantly shale innerburden. Since the lower seam panel width exceeds the maximum arch based on the load transfer distance, the compacted waste material in the gob will act as one abutment of an arch. Using the mining depth of 500 feet as the maximum arch height, an arch width of 767 feet is estimated. This would put the load transfer path at 70 feet from the edge of the solid abutment.

The two mechanisms do not necessarily have to be mutually exclusive. In fact, it is not impossible for the layered strata overlying the goaf fail in shear successively further out over the gob with each higher layer of rock. Eventually, in the case above, an arch was formed with one abutment resting on the solid coal and the other on the caved material in the gob. This arching effect then carried the damage in the upper seam out to a point away

from the edge of the solid coal in the lower seam. The fact that the pillars in the upper seam were of substantial size and that all upper seam structures (coal, roof, and floor) had been fractured over robbed areas is also proof that both mechanisms can occur simultaneously.

7.1.3 Options for Improving Conditions

In a situation as described above, interaction is inevitable if a high extraction ratio in the lower seam is desired due to the large thickness of the lower seam, and to the relatively small innerburden thickness. One possible solution is to mine the lower seam in multiple levels and in a descending order, with total extraction of each level. This will minimize the effects of bending and shearing by providing a super-critical subsidence situation with uniform upper-seam displacement. Back-filling of the lower seam gob is another option for improving ground conditions in the upper seam. Mining of the upper seam should be done at least two years after the lower-seam mining has been completed. Mining direction (mains) should be kept parallel to lower seam pillar lines in order to reduce chances of shear failure and to take advantage of stress-relief zones over the gob. Where conditions permit, yield pillars may be used in the upper seam to divert excessive load concentrations to large pillars or to solid coal. In very deep mining situations with heavy ground pressure and

a fractured upper seam, longwall mining may be an alternative.

7.2 Case Study No. 2

7.2.1 Description

This case of mining operations in the Campbell Creek seam (upper seam) and the Eagle seam in West Virginia (Table 7.2) was recorded by Su et al. (1986) . Figure 7.4 shows the mining plans of the mine under study. The upper seam and lower seam are 6.0 feet and 4.5 feet in thickness, respectively. The innerburden between the two seams is about 200 feet thick, and is composed of thick interbedded sandstone and shale beds. The overburden above the upper seam is about 1200 feet thick.

The lower seam was mined more than 20 years ago by the longwall method, with 300-500 foot panels and two rows of 40x40 foot chain pillars. Mining in the upper seam was mainly accomplished by room-and-pillar method except in a few locations. Floor heave was reported as the main problem when the mains of the Campbell Creek seam were developed in the area above the longwall panels in the lower seam. Floor heave developed almost immediately after entries were driven and continued for a period of four to six months. The entry height of the 6-foot seam was reduced to three to four feet. However, the roof remained intact

Table 7.2 Documentation of Case Study No. 2

SOURCE OF INFORMATION:	Su et al., 1986
NAME/LOCATION OF MINE:	Case No. 9, WV
LOWER SEAM:	
Bed Name:	Eagle
Thickness:	54"
Method of Extraction:	Longwall
Extraction Ratio:	Over 90%
Immediate Roof:	Sandstone
Immediate Floor:	Shale
INNERBURDEN:	
Thickness:	200'
Percent of Hardrock:	55%
M-Index:	44.4
UPPER SEAM:	
Bed Name:	Campbell
Thickness:	6.0'
Immediate Roof:	Sandstone
Immediate Floor:	Layered shale
OVERBURDEN:	
Cover thickness:	1200'
Nature of Strata:	Shale, sandstone, etc.
TIME AFTER MINING OF LOWER SEAM:	20 years
GROUND WATER:	Not present
DAMAGE ASSESSMENT:	
Mining Sequence:	Overmining
Location:	Over remnant pillars
Description:	Heavy floor heave of up to 2-3'.
Possible Mechanism:	Load transfer by remnant pillars
Damage Rating:	4 - Severe damage
Control Method:	NA

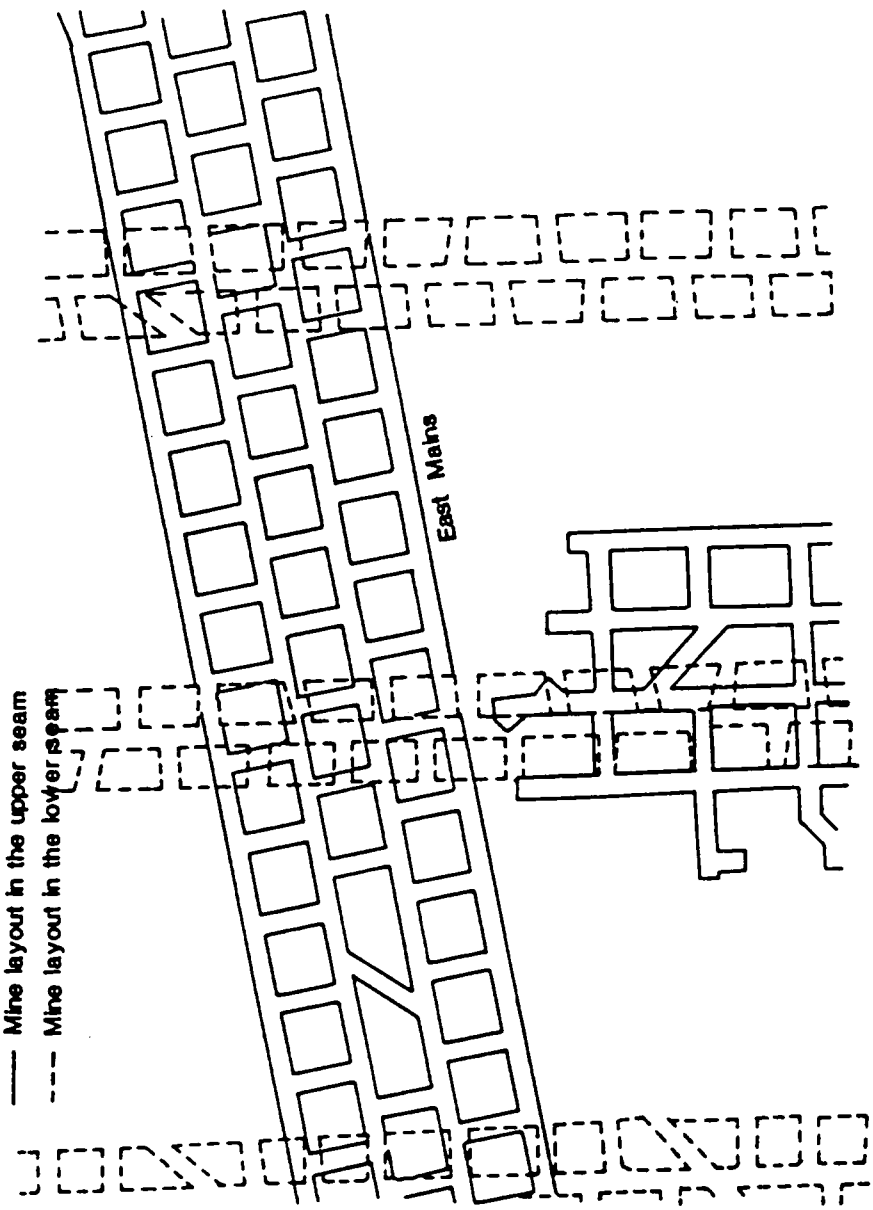

Figure 7.4 Mine Plans and Stratigraphic Sequence of Case Study No. 2 (after Su et al., 1986)

in all cases while the floor heaved, sometimes breaking up in the middle of the entry.

7.2.2 Analysis

As can be seen from Figure 7.5, the mains were being developed almost perpendicular to the lower seam remnant pillar lines. The remnant pillars left in the lower seam in this case served to transfer a tremendous amount of ground pressure to the upper seam floor due to the large overburden thickness and relatively strong innerburden. Analysis by Equations (4-11) and (4-12) puts the estimate of average stress concentration at 2.8, with a maximum of 4.2. This translates into a 5640 psi of ground pressure before entries were driven, while the estimated bearing capacity by RUMSIM was only about 3800 psi (Figure 7.6). The floor, which consisted of thick layers of black to dark shale, apparently failed due to excessive floor pressure. The failure in the form of large convergence helped release much of the transferred pressure, thus leaving the relatively strong roof bed intact.

The extraction ratio in the lower seam was estimated to be over 90%. Based on an average lower-seam mining height of seven feet and an innerburden of 200 feet in thickness, the critical M-index for upper-seam stability is 91 without time effects. Time was not a factor in this case, as the upper seam had been mined more than 20 years ago. The

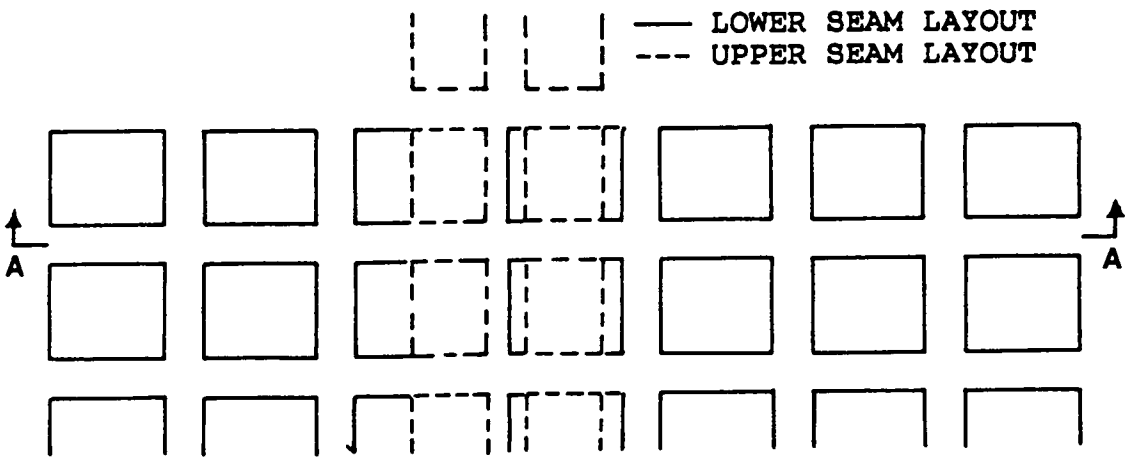

(a) Plan View of Mine Layout

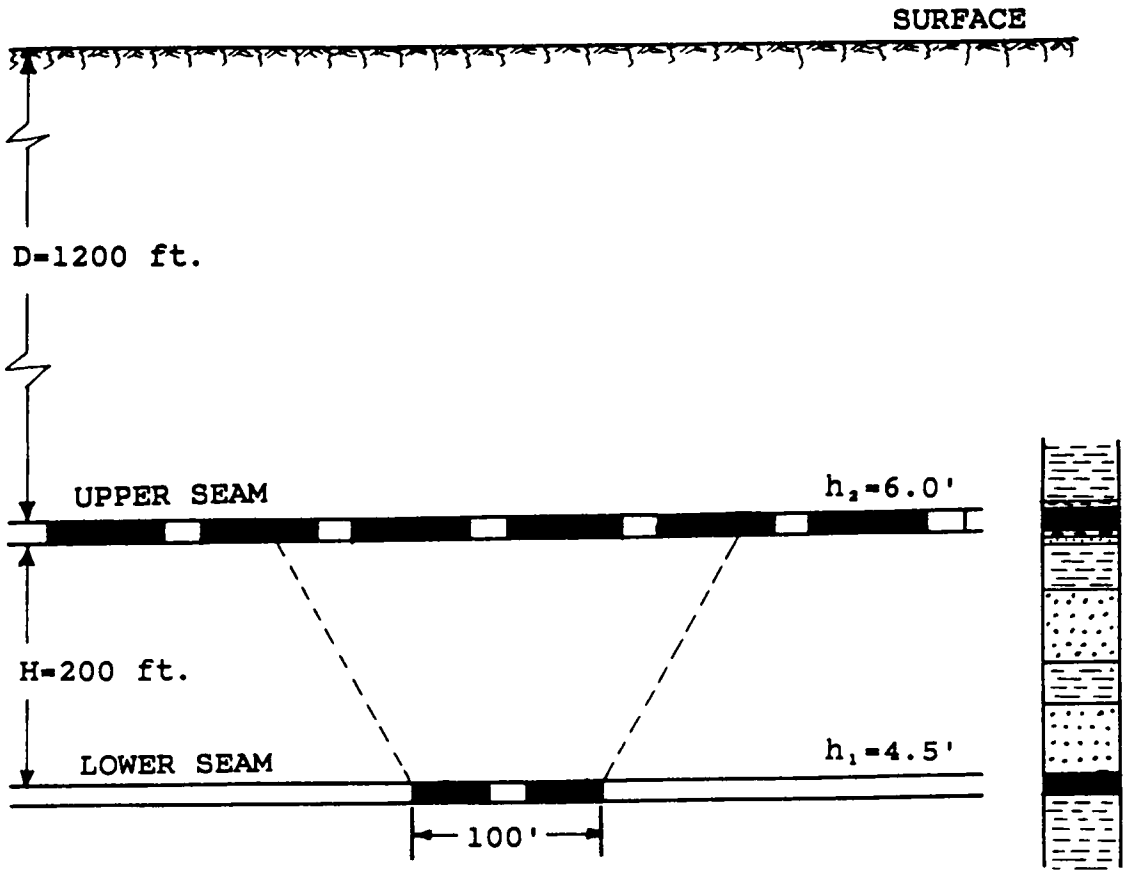

(b) A-A Cross-Section

Figure 7.5 Analysis of Upper Seam Interaction Using the Load Transfer Mechanism - Case Study No. 2

STABILITY ANALYSIS - Floor Stability Output

The upper seam is located [1200] feet below surface.
Upper seam virgin stress is [1333] psi.
Over a remnant pillar of width [100] feet in the lower seam.

Floor Configuration : Single Layer.
Upper Layer Thickness = 20.0 feet; Lower Layer Thickness =

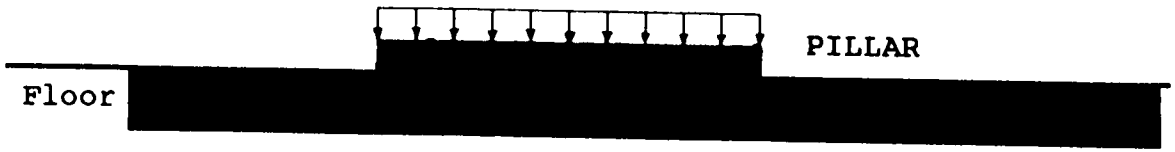

Estimated Bearing Capacity = 3793 psi.
Average Bearing Load = 3600 psi. Factor of Safety = 1.05*
Maximum Bearing Load = 5400 psi. Factor of Safety = 0.70*

* Note: A factor of safety of 2 is recommended against bearing capacity failure.

Figure 7.6 Results of Floor Stability Analysis by RUMSIM - Case Study No. 2

actual M-index was only 44, much less than the required 91 for stability. Results by other empirical methods also indicated similar trends (Figure 7.7)

7.2.3 Options for Improving Conditions

Interaction in this case was inevitable as mining was to proceed into the areas over the remnant pillars in the lower seam. Therefore, if in the future both seams can be designed simultaneously for mining, it is recommended that the upper seam be mined first. Total extraction is most desirable and longwall mining will be able to handle the high ground pressure better than will the room-and-pillar method. In cases where mining must be done over a previously-mined lower seam, upper seam entries should be kept in line with lower-seam pillar lines, placing them over gob areas of the lower seam. Oversized pillars may be necessary in the upper seam since the deep mining conditions will certainly create high ground pressure. Also as described in Chapter 4, an effort should be made to arrange the pillars so that maximum pillar support is achieved (Figures 6.2 and 6.3)

7.3 Case Study No. 3

7.3.1 Description

This case is taken from a report by Su et al. (1986) regarding the same coal seams in West Virginia as examined

EMPIRICAL ANALYSIS - Summary Output

The upper seam is located [1200] feet below surface.

Roof Rating (MSRR) = [2.4] (on a scale of 1 to 5, with decreasing difficulty)
Stability Factor = -77.8, indicating that interaction [is] likely
Stability Based on Roof Rating = - 46.3, interaction [is] likely

M-index Checking:
Critical Innerburden Thickness:
Time Effect
Icrit = 546.0 ft.
No Time Effect
Icrit = 129.0 ft.
Actual Innerburden Thickness = 120.0 feet
Actual M-index = 20
Probability of Interaction = 0.7687
Predicted Average Damage Rating by Linear Regression = 3.6

Subsidence Factor:
Estimated Maximum Subsidence = 2.60 ft.
Estimated Maximum Tensile Strain = 35.0000 (1/1000)
Predicted Damage Rating Based on Subsidence Analysis = 5.0

PgDn - Next Page PgUp - Previous Page ESC - Return to Menu

Figure 7.7 Results of Empirical Analysis by RUMSIM - Case Study No. 2

in Case Study No. 2 (Table 7.3). The upper seam, the Campbell seam, and the Eagle seam are 6.5 feet and 7.0 feet thick, respectively. The two seams are separated by an innerburden of approximately 190 feet, comprised interbedded sandstone, shale, and coal seams. The overburden above the upper seam is 1120 feet in thickness. Figure 7.8 shows the stratigraphic sequence and mining plans of the two seams.

The lower seam has been mined extensively by the longwall method. Mining in the upper seam at the time of the study was relatively new, and was by the room-and-pillar method except in a few locations, where the longwall method had been used. Relatively little problem was encountered when entries were located directly above the gob areas of the lower seam. However, when panel 7A in the upper seam was advanced near the interface line between the gob and solid coal (line AB, Figure 7.8), a major roof control problem occurred in the upper seam. The problem continued even after the face moved beyond the line AB. Eventually the face was stuck and mining had to be abandoned. Later it was found that there were cracks in the roof as high as 20 feet. Several rescue entries were driven in order to reach the troubled face, and a new face was started 225 feet ahead of the old face in the same panel. No major problem was encountered from the new face location onward as mining the rest of the panel progressed.

Table 7.3 Documentation of Case Study No. 3

SOURCE OF INFORMATION:	Su et al., 1984
NAME/LOCATION OF MINE:	Case No. 3, WV
LOWER SEAM:	
Bed Name:	Eagle Seam
Thickness:	84"
Method of Extraction:	Longwall
Extraction Ratio:	Extensively mined, >90%
Immediate Roof:	Shale
Immediate Floor:	Shale
INNERBURDEN:	
Thickness:	190'
Percent of Hardrock:	60%
M-Index:	27
UPPER SEAM:	
Bed Name:	Campbell Creek
Thickness:	78"
Method of Extraction:	Longwall
Immediate Roof:	Shale
Immediate Floor:	Shale
OVERBURDEN:	
Cover thickness:	1120'
Nature of Strata:	Mostly shale and sandstone
TIME AFTER MINING OF LOWER SEAM:	NA
GROUND WATER:	Not present
DAMAGE ASSESSMENT:	
Mining Sequence:	Overmining
Location:	Over gob/solid coal interface areas.
Description:	Cracks in roof as high as 20', Fallen roof; face was finally stuck.
Possible mechanism:	Fractured areas in tension zone of trough subsidence
Damage Rating:	5 - Very severe damage.
Control Method:	NA

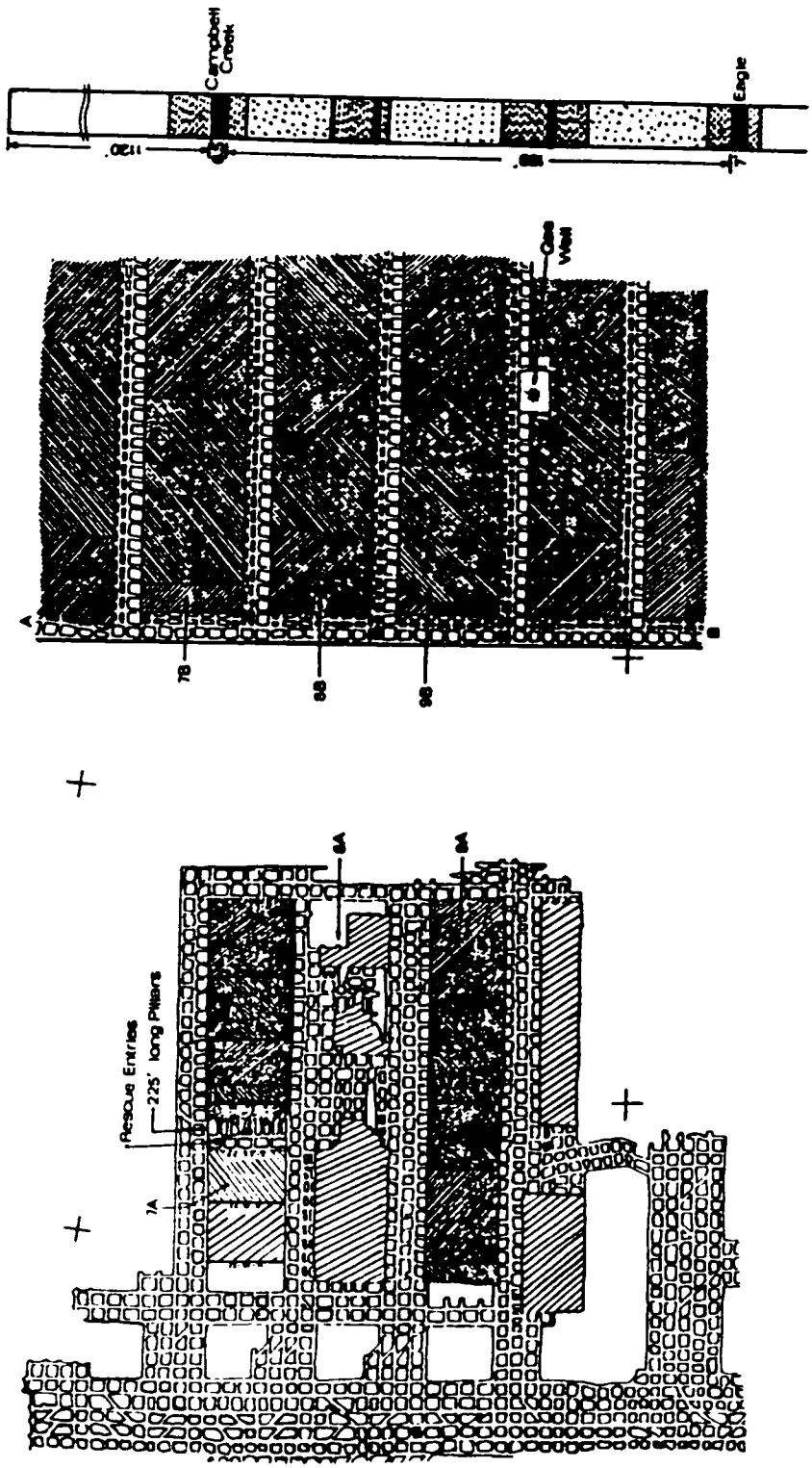

b) Lower Seam Layouts for Case No. 3

a) Upper Seam Layouts for Case No .3

Figure 7.8 Mine Plans and Stratigraphic Sequence of Case Study No. 3 (after Su et al., 1986)

7.3.2 Analysis

This example demonstrates two very important features of overmining operations. First, the protective action of the destressed zone was taken advantage of by driving entries in the stress-relief zone. Second, negative interaction effects were inevitable due to tensile strain created by the trough subsidence when the working face had to cross the areas above the interface line between the lower seam gob and solid coal. The adverse roof conditions in this case were apparently due to dilation, as shown by the fractures in the roof. However, such heavy damage could have been anticipated by a simple analysis of the subsidence trough.

Using the subsidence method described in Chapter 4, a maximum upper seam subsidence of 2.8 feet was found due to the mining of the lower seam, with a corresponding maximum tensile strain of 12/1000 occurring at a distance of 6 feet into the gob. Output of the analysis on subsidence by RUMSIM is shown in Figure 7.9, in which upper seam subsidence and tensile strain distributions are given. Using a tanβ of 2.0 and 60% of sandstone in the innerburden, the tension zone was estimated to be 44 into the gob, with a width of 141 feet (Figure 7.10). This is the area where trouble should be expected for the upper seam. The new face which was started 225 feet from the old face did not erience any problems because it was located outside of the esti-

SUBSIDENCE ANALYSIS - Subsidence and Strain Distributions Page 1/3

Remnant Pillar

Left Edge										Right Edge	
X (ft)			-327	-317	-308	-298	-288	-279	-269	-260	-250	-240
SUBSIDENCE(ft)			0.00	0.00	0.00	0.00	0.00	0.00	0.00	0.00	0.00	0.00
STRAIN(1/1000)			0.0	0.0	0.0	0.0	0.0	0.0	0.0	0.0	0.0	0.0
-231	-221	-212	-202	-192	-183	-173	-163	-154	-144	-135	-125	-115
0.00	0.00	0.00	0.00	0.00	0.00	0.00	0.00	0.00	0.00	0.00	0.00	0.00
0.0	0.0	0.0	0.0	0.0	0.0	0.0	0.0	0.0	0.0	0.0	0.0	0.0
-106	-96	-87	-77	-67	-58	-48	-38	-29	-19	-10	0	10
0.00	0.01	0.01	0.02	0.03	0.04	0.06	0.09	0.14	0.20	0.27	0.37	0.48
0.0	0.0	0.0	0.0	0.0	0.1	0.2	0.6	1.4	2.9	5.4	8.6	12.2
19	29	38	48	58	67	77	87	96	106	115	125	135
0.61	0.76	0.93	1.11	1.29	1.47	1.65	1.82	1.97	2.10	2.21	2.31	2.38
14.9	15.3	12.4	6.3	-1.5	-9.0	-13.9	-15.5	-14.0	-10.8	-7.3	-4.3	-2.3
144	154	163	173	183	192	202	212	221	231	240	250	260
2.44	2.49	2.52	2.54	2.55	2.56	2.57	2.57	2.57	2.57	2.57	2.58	2.58
-1.1	-0.4	-0.2	-0.1	-0.0	-0.0	-0.0	-0.0	-0.0	-0.0	-0.0	-0.0	-0.0

Press a key to continue . . .

Figure 7.9 Results of Subsidence Analysis by RUMSIM - Case Study No. 3

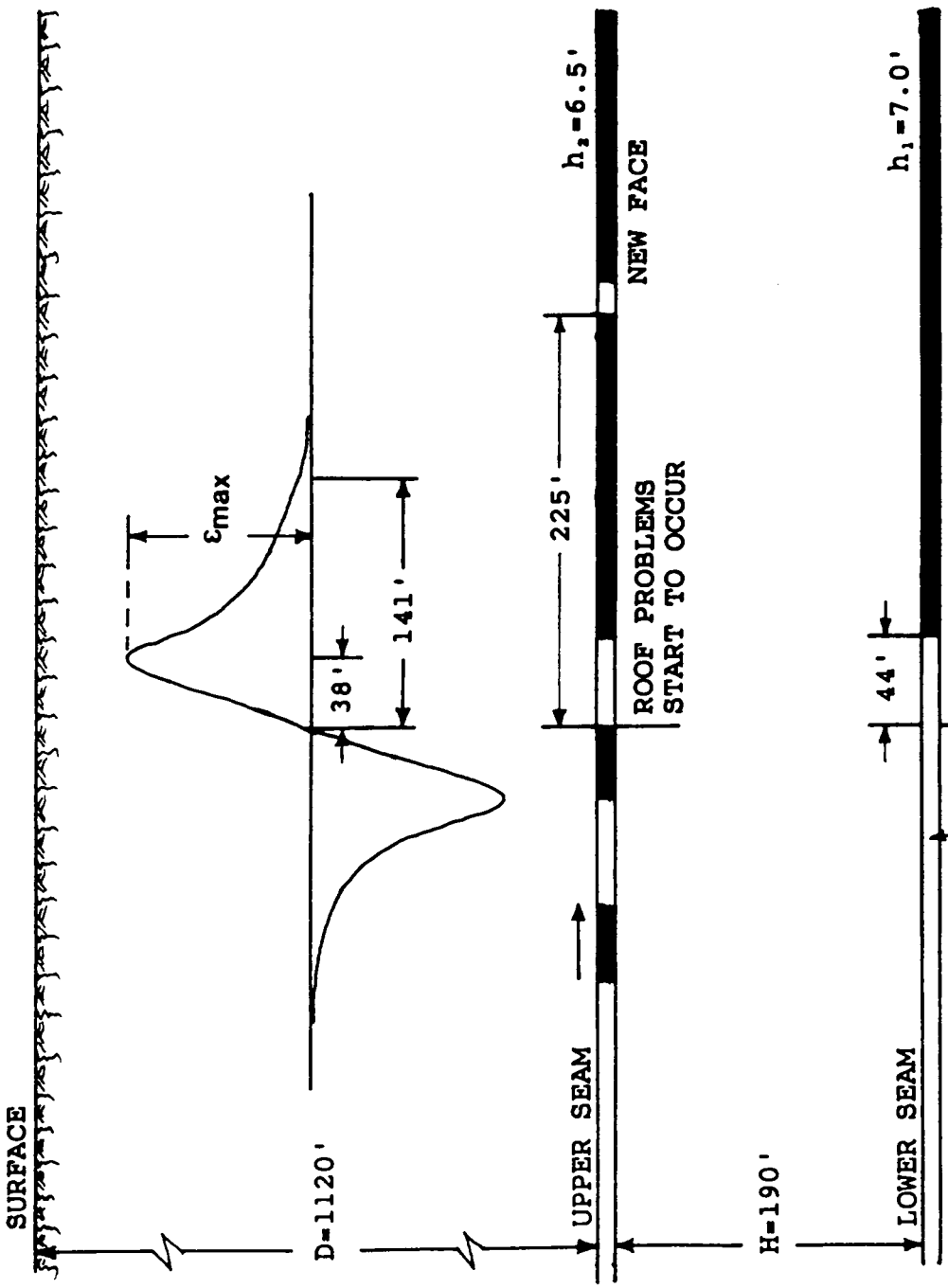

Figure 7.10 Analysis of Upper Seam Interaction Using the Subsidence Mechanism - Case Study No. 3

mated tension zone, even assuming an error margin of 50% for the estimated tension zone width.

7.3.3 Options for Improving Conditions

As pointed out in the preceding discussion, the tension zone could have been anticipated ahead of time if lower seam workings had been mapped and an analysis of the trough subsidence had been conducted. Careful mapping of lower seam workings would allow the mine operator to exercise better judgement so that panels in the upper seam could be placed above the gob in the lower seam. Normally, the driving of entries or advancement of faces in the tension zone should be avoided unless there are particular reasons for these actions. Back-filling of the lower seam gob is another option for improving upper seam conditions. Finally, reversal of the mining sequence of the two seams, with complete extraction in the upper seam, is a desirable alternative if seams are being designed for simultaneous extraction.

VIII. CONCLUSIONS AND RECOMMENDATIONS

8.1 Conclusions

Based on this research, the following conclusions are made for room-and-pillar overmining operations.

1) The critical factors controlling interaction effects are: innerburden thickness and characteristics, overburden, lower seam height, lower seam extraction ratio, and location of mining in the upper seam.

2) Failure modes identified in the upper seam are horizontal dilation (tension/compression) due to trough subsidence waves, stress-induced convergence due to high ground pressure, shearing due to uneven support, and bed separation due to strata sagging and low bonding strengths.

3) The four basic interaction mechanisms associated with overmining identified are: vertical load transfer, trough subsidence, pressure arching, and massive interseam failure. These mechanisms are quantified and used to analyze overmining interactions.

4) A qualitative approach to analyzing interaction effects has been developed based on the results of statistical analyses of case studies, and is used to perform preliminary analyses of potential interaction sites with a minimal amount of input information.

5) For detailed stress and strain analyses of interaction effects, quantitative relationships have been developed. These relationships are employed to determine optimum upper seam pillar sizes, entry dimensions, and floor stability for specified geologic conditions. Based on the degree of predicted damage, a decision can then be made either to avoid the troubled area, to support it, or to choose an alternative design.

6) A roof rating system has been developed for overmining that is used to evaluate the effects of geological factors on upper seam stability. This geological characterization system has made it possible to numerically model the effects of complex geological and structural conditions. As a result, quantitative relationships between upper seam damage and upper seam subsidence and tensile strains have been developed.

7) Quantitative design guidelines have been developed for designing optimum multi-seam mine layouts in overmining using the room-and-pillar method. These include recommended design procedures, guidelines on mine layout and orientations, and options for improving upper seam stability. Optimum mine design can be achieved that will improve mine safety and productivity through advance planning. The most important step is to identify lower seam remnant structures by careful mapping, and to anticipate any potential interactive damage.

8) To facilitate implementation of the interaction mechanisms and design principles, and to aid in the design of overmining operations, an interactive and user-friendly computer program called RUMSIM has been developed. The program incorporates all the results from this research and previous work, and can be used to predict potential interaction and to design an optimum mine layout which will minimize interaction effects. It also includes a detailed technical guide to help the user to understand the mechanisms involved in the analysis. Testing on case studies has demonstrated the effectiveness of the program.

8.2 Recommendations

Ground control problems due to interaction will continue to be a major concern for many coal operators in Appalachia because many coal seams must be worked in multiple horizons. The investigation presented in this dissertation represents the first comprehensive efforts made to address the problem of interaction in overmining operations. For general applications, the methods of analysis and design guidelines presented here will provide the operator with sufficient design information to allow the overmining operations to be carried out.

However, these efforts are by no means exhaustive. Further work is needed in establishing simple but practical

methods for stress analysis on a three-dimensional basis. Finite element and boundary element methods, with capabilities of dealing with bed slipping, joints, non-linear rock properties, and perhaps plastic failure criteria, should be developed. Semi-empirical relationships based on parametric analysis using such methods can then be developed for making stress calculations applicable to practical mine design.

Such analytical work should be accompanied by comprehensive field monitoring and measurements of strata movements in both passive and active modes of the subsidence wave. Correlation should also be made between the geological characteristics and strata behavior.

Yield pillars should be studied as to their effects on multi-seam interaction and as to their effectiveness in alleviating negative interaction effects.

Other areas of future research should include interaction during multi-seam mining by the longwall method, optimum mining sequence when more than two seams are involved, harmonic mining of several seams in order to minimize interaction effects, economic evaluations, and application of expert systems that promise to bring expertise to the fingertips of the mine operator.

REFERENCES

"Report of Sub-committee on Coal Mining to Committee on Ground Movement and Subsidence," (1926) Trans. AIME, Vol. 74, pp. 734-809.

Agapito, J. F. T., Bennet, J. W., and Hunter, J. P., 1978, "Rock Mechanics for Two-seam Mining," Proceedings, 19th U.S. Symposium on Rock Mechanics, Stateline, Nevada, May, pp. 57-64.

Agioutantis, Z. and Karmis, M., 1986, "A Study of Roof Caving in the Eastern U. S. Coalfields," Proceedings 5th Conf. on Ground Control in Mining, A. Wahab Khair, Ed., June 11-13, Morgantown, WV, pp. 134-146.

Barko, E., 1982, "Mechanics of Interseam Failure in Multiple Horizon Mining," M.S. Thesis, Virginia Polytechnic Institute & State University, VA.

Barrientos, G. and Parker, J., 1974, "Use of the Pressure Arch in Mine Design at White Pine," Trans., SME-AIME, Vol. 255, March, pp. 75-82.

Barton, N., Lien, R., and Lunde, J., 1974, "Engineering Classification of Rock Masses for the Design of Tunnel Support," Rock Mechanics, Vol. 6, No. 4, pp. 189-236.

Bieniawski, E. T., 1976, "Rock Mass Classification in Engineering," Proceedings, Symposium on Exploration for Rock Engineering, Johannesburg, Vol. 1, pp. 97-106.

Bieniawski, E. T., 1979, "The Geomechanics Classification in Rock Engineering Applications,", Proceedings 4th International Congress on Rock Mechanics, Montreux, pp. 41-48.

Brauner, G., 1973, "Subsidence Due to Underground Mining," U.S. Bureau of Mines, IC 8571, (Part 1 of Two Parts), 56 pp.

Britton, S. G., 1980, "Mining Multiple Seams," Coal Mining and Processing, Dec., pp. 64-70.

Bruhn, R. W., Magnuson, M. O., and Gray, R. E., 1980, "Subsidence over Abandoned Mines in the Pittsburgh Coalbed," Ground Movements and Structures, Proceedings, 2nd International Conference, J. D. Geddes (Ed.), Univ. of Wales Institute of Science and Technology, John Wiley, New York, pp. 142-156.

Chekan, G. J., Matetic, R. J., and Galek, J. A., 1985, "A Case Study of Ground Control Problems Related to Multiple Seam Mining in the Pittsburgh and Sewickley Coalbeds," SME-AIME Preprint, Albuquerque, NM, Oct. 16-18.

Chekan, G. J, Matetic, R. J. and Galek, J. A., 1986, "Strata Interactions in Multiple-Seam Mining - Two Case Studies in Pennsylvania," RI 9056, U.S. Bureau of Mines.

Coal Mining Research Institute, 1981, Surface Subsidence and Strata Movements in Coal Mining, Coal Mining Publishing Co., 369 pp. (in Chinese).

Denkhaus, H. G., 1964, "Critical Review of Strata Movement - Theories and Their Application to Practical Problems," Journal of the South African Institute of Mining and Merallurgy, Vol. 64, pp. 310-332.

Dunham, R. K. and Stace, R. L., 1978, "Interaction Problems in Multiseam Mining," Proceedings, 19th U.S. Symposium On Rock Mechanics, Mackay School of Mines, Univ. of Nevada, Reno, NV, pp. 174-188.

Ealy, D. L., Mazurak, R. E., and Langrand, E. L., 1979, "A Geological Approach for Predicting Unstable Roof And Floor Conditions in Advance of Mining," Mining Congress Journal, March, pp. 17-22.

Eavenson, H. N., 1923, "Mining an Upper Bituminous Seam after a Lower Seam Has Been Extracted," Trans. AIME, Vol. 69, pp. 398-405.

Ehgartner, B. L., 1982, "Pillar Load Transfer Mechanisms in Multi-Seam Mining," M.S. Thesis, Virginia Polytechnic Institute and State University, Blacksburg, Va., May, 164 pp.

Engineers International, 1981, "Investigation of Problems and Benefits of Underground Multiple Seam Coal Mining," Final Technical Report, Dept. of Energy Contract DE-AC01- 70ET14242, October, 292 pp.

Goodman, G., 1980, "Computer Modelling of Mining Subsidence Using the Zone Area Method," M.S. Thesis, VPI & SU, Blacksburg, VA.

Gray, R. E. and Bruhn, R., 1984, "Coal Mine Subsidence — Eastern United States," Geological Society of Amirica, Reviews in Engineering Geology, Vol. VI, pp. 123-149.

Grenoble, A., Haycocks, C., and Wu, W., 1985, "Computerized

Evaluation of Near-Seam Interaction," Proceedings, 2nd Ann. Conf. on the Application of Computers to the Coal Industry, Tuscaloosa, AL.

Grenoble, A. and Haycocks, C., 1985, "Design Factors in Near Seam Interaction," Proceedings, 4th Conf. on Ground Control in Mining, West Virginia Univ., Morgantown, WV, July.

Hasler, H. H., 1951, "Simultaneous vs. Consecutive Working of Coal Beds," Transactions, AIME, Mining Engineering, May, pp. 436-440.

Haycocks, C., 1980, "Optimizing Extraction for Multi-Seam Mining, Final Report, Allotment Grant, O.S.M., 75 pp.

Haycocks, C., Karmis, M., and Ehgartner, B., 1982, "Ground Control Mechanisms in Multi-Seam Mining," Paper presented at the Fall Meeting, SME of AIME, Hawaii.

Haycocks, C., Ehgartner, B., Karmis, M., and Topuz, E., 1982, "Pillar Load Transfer Mechanisms in Multi-Seam Mining," SME-AIME Preprint No. 82-69.

Haycocks, C., Karmis, M. and Topuz, E., 1981, "Optimizing Productive Potential in Multi-Seam Underground Coal Mining" Proceedings, Coal Conference and Exposition VI, Louisville, KY, National Coal Association, pp. 151-164.

Haycocks, C. and Karmis, M., 1983, "Ground Control Mechanisms in Multi-Seam Mining" Final Report prepared for the Office of Mineral Institutes, Bureau of Mines, U.S. Department of the Interior, Oct., 328 p.

Hedley, D. G. F., 1978, "Design Guidelines for Multi-Seam Mining at Elliot Lake," Canmet Report, Canada Centre for Mineral Energy Technology, 25 pp.

Hladysz, Z., 1985, "Analysis of Risk In Multiple Seam Mining," Preprint 85-357, SME-AIME Fall Meeting, NW, Oct. 16-18,Society of Mining Engineers, AIME, 11 pp.

Holland, C. T., 1949, "Effect on Unmined Seams of Coal by Mining Coal Seams Above or Below," Proceedings, W. Va. Academy of Science, Vol. 19, W.Va. University, pp. 113-132.

Holland, C. T., 1951, "Multiple-seam mining," Coal Age, August, pp. 89-93.

HRB-Singer, Inc., 1976, "The Impact of Overmining on the

Underground Coal Reserve Base," Final Report, Contract No. JO357129, U.S. Bureau of Mines, NTIS, Springfield, VA, PB262518, 302 pp.

Hudock, S. D., 1983, "The effects of the Pressure Arch upon Multiple Seam Mining," M.S. Thesis, Virginia Polytechnic Institute and State University, Blacksburg, VA., Aug., 197 pp.

Johnson, G., 1973, "Rock Mechanics, a Nomogram for the Assessment of Roadway Conditions," Colliery Guardian, Vol. 221, pp. 16-20.

Kane, W. and Karmis, M., 1983, "Prediction and Control of Unstable Ground Conditions in Underground Coal Mines: A Preliminary Report," Proceedings, Annual Workshop, Generic Mineral Technology Center Mine Systems Design and Ground Control, Blacksburg, VA, Nov., pp. 19-34.

Karmis, M. and Jarosz, A., 1985, "Subsidence Control in the Appalachian Coalfields," Proceedings 3rd Annual Workshop, Generic Mineral Technology Center on Mine Systems Design and Ground Control, Univ. of Kentucky, Lexington, KY.

Karmis, M., Jarosz, A., and Schilizzi, P., 1987, "Monitoring and Prediction of Ground Movvements Above Underground Mines in the Eastern United States Coalfields," Proceedings, 6th Int. Conf. on Ground Control in Mining, June 9-11, pp. 184-194.

Karmis, M. and Jarosz, A., 1985, "Subsidence Control in the Appalachian Coalfields," Proceedings, 3rd Annual Workshop, Generic Mineral Technology Center on Mine Systems Design and Ground Control, Univ. of Kentucky, Lexington, KY, pp. 91-120.

Karmis, M., Haycocks, C., and Triplett, T., 1984, "Ground Settlement and Deformation Characteristics above Undermined Areas: Experience from the Eastern U.S. Coalfields," Proceedings, 4th Australia-New Zealand Conference on Geomechanics. Perth, Australia.

Kester, W. M. and Chugh, Y. P., 1980, "Premining Investigations and Their Use in Planning Ground Control in the Illinois Basin Coal Mines," Proceedings, 1st Conf. on Ground Control Problems in the Ill. Coal Basin, Y. P. Chugh and A. Van Besien (eds.), South Ill. Univ., June; pp. 33-43.

King, H. J., Whittaker, B. N. and Batchelor, A. S., 1972,

"The effects of interaction in mine layouts," Proceedings, 5th International Symposium on Minerals and the Environment, Inst. Min. Metallurgy.

King, H. J. and Whittaker, B. N., 1971, "A Review of Current Knowledge on Roadway Behavior, Especially the Problems on Which Further Information IS Required," Proceedings, Symposium on Strata Control in Roadway, London, IME, pp. 73-90.

Kratzsch, H., 1983, Mining Subsidence Engineering, Springer-Verlag, Berlin Heidelberg, New York, 543 pp.

Kripokov, N., 1981, "Analysis of Pillar Stability on Steeply Pitching Seams Using the Finite Element Method," U.S. Bureau of Mines, RI 8579, 33 pp.

Lazer, B., 1965, "Mining Seams above Mined Out Seams," Mining Engineering, Sept., pp. 75-77.

Matetic, R. J., Chekan, G. J., and Galeck, J. A., 1987, "Pillar Load Transfer Associated With Multiple-Seam Mining," U.S. Bureau of Mines, RI 9066, 23 pp.

Marr, J. E., 1975, "The Application of the Zone Area System to the Prediction of Mining Subsidence," The Mining Engineer, Oct., pp. 53-60.

Merril, R. H., 1958, "Roof Span Studies in Limestone," U.S. Bureau of Mines, RI 5406.

Moebs, N. and Ferm, C., 1982, "The Relation of Geology to Mine Roof Conditions in the Pocahontas No. 3 Coalbed," Bureau of Mines, IC 8864, 12 pp.

Moebs, N., and J. L. Ellenberger, 1982, "Geologic Structures in Coal Mine Roof," U.S. Bureau of Mines, IC 8620, 16pp.

NCB - Mining Dept., 1972, "Design of Mine Layout," Working Party Report, London, U.K., 41 pp.

NCB - Production Dept., 1975, Subsidence Engineers' Handbook, London, U.K., 49 pp.

Pariseau, W. G., 1983, "Ground Control in Multi-level Room and Pillar Mines," Final Report prepared for U.S. Bureau of Mines, 111 pp.

Patrick, W. C. and Aughenbaugh, N. B., 1979, "Classification of Roof Falls in Coal Mines," Mining Engineering,

March, pp. 279-283.

Peng, S. S. and Chandra, U., 1980, "Getting the Most from Multiple-Seam Reserves," Coal Mining and Processing, Vol. 17, Nov., pp. 78-84.

Randolph, B. S., 1915, "The Theory of the Arch in Mining," The Colliery Engineer, Vol. 35, pp. 427-29.

Salamon, 1964, "Design of Bord and Pillar Workings," in Rock Mechanics of Underground Coal Mining Systems, Selected Readings, W. Hustrulid, Ed., pp. G.51-G.64.

Schilizzi, P., 1987, "Monitoring and Prediction of Surface Movements above Underground Mines in the Eastern U.S. Coalfields," Ph. D. Dissertation, VPI & SU, Blacksburg, VA, 302 pp.

Scurfield, R. W., 1970, "Staffordshire Mining Layout ofr the Mid-1970's," Mining Engineer, Vol. 130, November, pp 73-84.

Stemple, D. T., 1956, "A Study of Problems Encountered in Multiple-Seam Mining in the Eastern United States," M.S. Thesis, Virginia Polytechnic Institute and State University, Blacksburg, VA., July, 125 pp.

Styler, A. N. and Dunham, R. K., 1980, "Strata deformation above longwall faces," Proceedings, 21st U.S. Symposium on Rock Mechanics, Rolla, MO.

Su, W. H., Peng, S. S., and Hsiung, S. M., 1984, "Optimum Mining Plan for Multiple Seam Mining," Interim Report, Dept. of Mining Eng., College of Mineral and Energy Resources, West Virginia Univ., Morgantown, WV, 71 pp.

Su, W. H., S. S. Peng, and Hsiung, S. M., 1986, "Interaction in Multiple Seam Mining," Proceedings, Engineering Health and Safety Symposium, Ed. A. W. Khair, SME-AIME, pp. 31-44.

Szwilski, A. B., 1979, "Stability of Coal Seam Strata Under Mined by Room and Pillar Operations," Proceedings, 20th U.S. Symposium on Rock Mechanics, pp. 59-65.

Tandanand, S. and Powell, L. R., 1982, "Assessment of Subsidence Data from the Northern Appalachian Basin for Subsidence Prediction," U.S. Bureau of Mines, RI 8630, 14 pp.

Wang, F. D., Ropchan, D. M. and Sun, M. C., 1974, "Proposed

Techniques for Improving Coal Mine Roof Stability by Pillar Softening," Transactions, AIME, v. 255, March, pp. 59.

Webster, S., Haycocks, C., and Karmis, M., 1984, "Subsidence Interaction Effects in Multi-Seam Mining. Proceedings, 2nd Int'l Conference on Stability in Mining, Lexington, KY, Aug., pp. 589-604.

Whittaker, B. N., 1974, "An Appraisal of Strata Control Practice," The Mining Engineer, Oct., pp. 9-24.

Whittaker, B. N. and Pye, J. H., 1975, "Design and Layout Aspects of Longwall Methods of Coal Mining," Proceedings, 16th U.S. Symposium on Rock Mechanics, pp. 303-328.

Whittaker, B. N. and Sighn, R. N., 1979, "Design and Stability of Pillars in Longwall Mining," The Mining Engineer, July, pp. 59-70.

Wilson, A. H., 1972, "An Hypothesis Concerning Pillar Stability," The Mining Engineer, Vol. 131, No. 141, June; pp. 409-417.

Wilson, A. H., 1983, "The Stability of Underground Workings in the Soft Rocks of Coal Measures," Int'l Journal of Mining Engineering, Vol. 1, pp. 91-187.

Wright, R. D., 1973, "Roof Control Through Beam Action and Arching," SME Mining Engineer's Handbook, Vol. 1, pp. 13-80.

Wu, W. and Haycocks, C., 1986, "Statistical Analysis of Interaction Problems in Close-Proximity Multi-Seam Mines," Proceedings, 27th U.S. Symp. on Rock Mech., Tuscaloosa, AL, June, pp. 317-323.

Zachar, R. R., 1952, "Some Effects of Sewickley Seam Mining on Later Pittsburgh Seam Mining," Transactions, AIME Mining Engineering, July, pp. 687-692.

Zhou, Y. and Haycocks, C., 1986, "Designing for Upper Seam Stability in Multiple Seam Mining," Proceedings, 5th Conf. on Ground Control in Mining, Univ. of West Virginia, Morgantown, WV, June, pp. 206-212.

APPENDIX A UPPER SEAM STRESS ANALYSIS FOR DEEP MINING CONDITIONS

When deep mining conditions exist, stress analysis can be conducted using solutions adapted from elastic foundation theories.

Mechanically speaking, lower seam structures can be substituted with stress distributions on the lower seam roof level. Methods of estimating lower seam load distributions have been described in Chapter 4. This appendix presents the basic equations which can be used for upper seam stress analysis in deep mining conditions.

From elasticity, the vertical stress at a distance from a concentrated load in a semi-infinite space (therein deep mining conditions are required) is given by:

$$\sigma_z = \frac{2p}{\pi} \frac{z^3}{(x^2+z^2)^2} \qquad (A.1)$$

where x is the horizontal distance and z the vertical distance from the point of loading.

If stress distribution forms can be simplified into rectangles or triangles, then the stress calculations can be conducted by superimposition of the following three basic forms of stress (Figure A.1). Also, for easier computation, stress increments over the original stress are used. The final stress status is obtained by superimposing

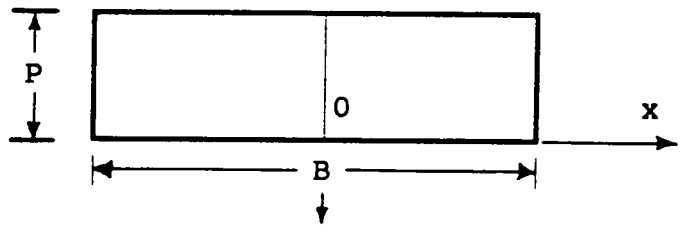

a. Rectangle

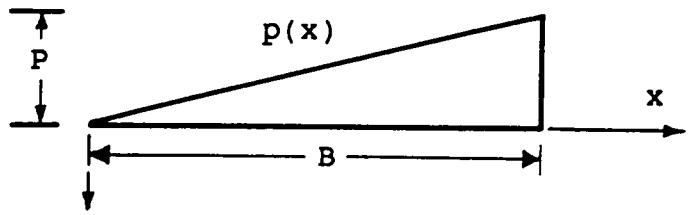

b. Forward Triangle

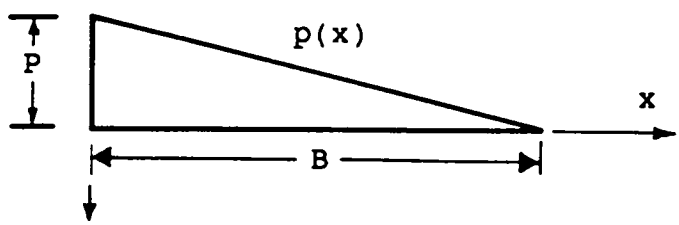

c. Backward Triangle

Figure A.1 Basic Forms of Load Distribution

the original stress and the calculated incremental stress.

Rectangle

Integration of Equation (A.1) over the width of B of the uniformly-distributed incremental load (P) yields the following equation:

$$\sigma_z' = \frac{P}{\pi}\left[\tan^{-1}\left(\frac{B/2-x}{z}\right)+\tan^{-1}\left(\frac{B/2+x}{z}\right)\right]-\frac{BPz(x^2-z^2-B^2/4)}{\pi[(x^2+z^2-B^2/4)+B^2z^2]}. \quad (A.2)$$

Forward Triangle

The incremental load distribution is given by

$$p(x) = (P/B)x \quad (A.3)$$

where p(x) = load increment at x; x = distance from center left of triangle; P = height of stress triangle; and B = base length of stress triangle.

Substituting p(x) for q in Equation (A.1) and integrating, we obtain the following equation:

$$\sigma_z' = -\frac{xP}{\pi B}\left[\tan^{-1}\left(\frac{x-B}{z}\right)-\tan^{-1}\left(\frac{x}{z}\right)\right]-\frac{Pz}{\pi}\,\frac{x-B}{(x-B)^2+z^2}. \quad (A.4)$$

Backward Triangle

The incremental load concentration is given by

$$p(x) = P - (P/B)x \quad (A.5)$$

where the variables are as defined previously.

Again substituting p(x) for q in Equation (A.1) and integrating, we have

$$\sigma_z' = -\frac{(B-x)P}{\pi B}\left[\tan^{-1}\left(\frac{x-B}{z}\right)-\tan^{-1}\left(\frac{x}{z}\right)\right]+\frac{Pz}{\pi}\frac{x-B}{(x-B)^2+z^2} \qquad (A.6)$$

Stress Calculations

Three typical forms of stress distribution most likely to be associated with the remnant structures can be identified, each consisting of rectangles and triangles (Figure A.2):

1. Wide pillar
2. Narrow pillar
3. Gob/coal interface

The vertical stress increment at any point (x,z) can then be calculated by superimposing each individual rectangle and triangle, with proper coordinate transformation.

After the stress increments is calculated, the total stress is determined as follows, taking into account the effect of strata weight:

$$\sigma_z = \sigma_z' + \sigma_o - \frac{\gamma z}{144} \qquad (A.7)$$

The final stress should also be adjusted for the effect

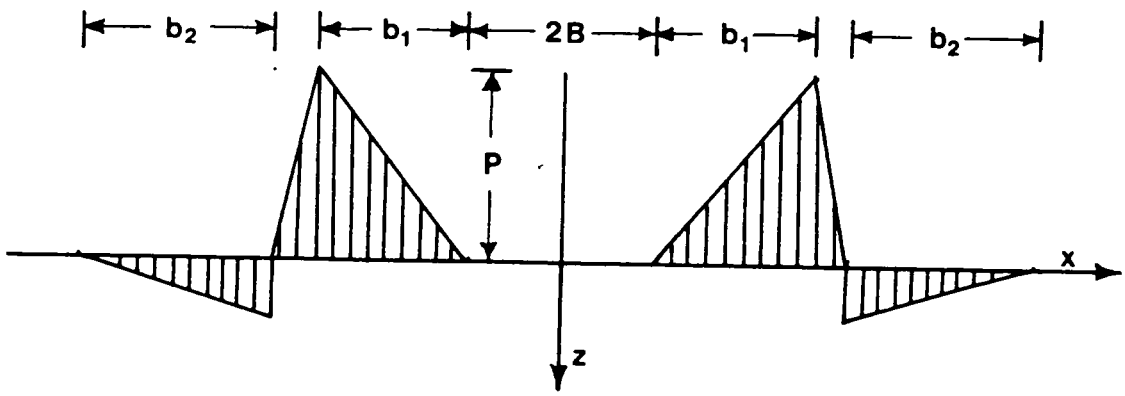

a) Wide Remnant Pillar

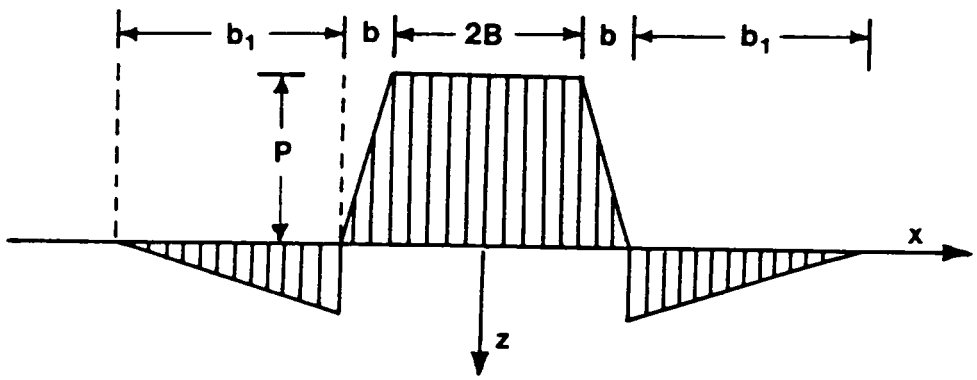

b) Narrow Remnant Pillar

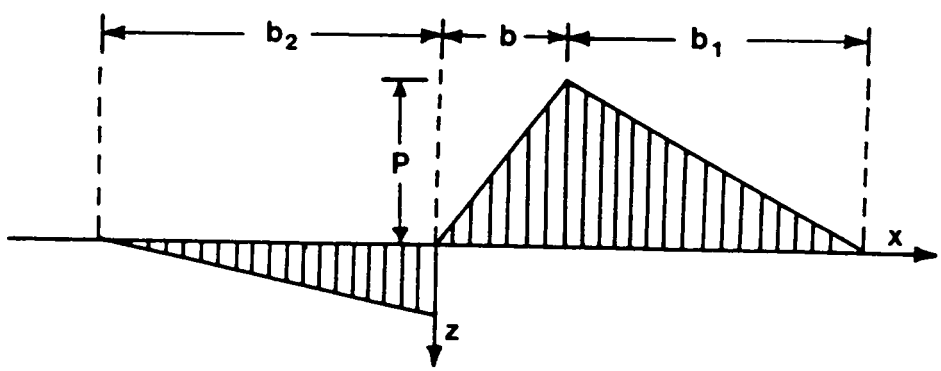

c) Gob/Coal Interface

Figure A.2 Simplified Incremental Load Distributions

of innerburden layering. According to Eghartner (1982), the following factor α is applied to σ_z:

For layers greater than five feet in thickness,

$$\alpha = 0.0172\eta^2 - 0.284\eta + 1.03 \qquad \text{(A.8a)}$$

For layers less than five feet in thickness,

$$\alpha = 0.00956\eta^2 - 0.1977\eta + 0.9889 \qquad \text{(A.8b)}$$

where η = ratio of the vertical distance from the remnant pillar to the width of the remnant pillar. For the gob/coal interface, the distance into the solid coal at which stress reaches primitive stress can be taken as equal to the pillar width.

Therefore, the final stress at a point (x,z) above a remnant structure is given by:

$$\sigma_z^* = \alpha\sigma_z \qquad \text{(A.9)}$$

where σ^* = final stress at (x,z) after modifications to compensate for the effects of innerburden weight and innerburden stratification.

The vita has been removed from the scanned document